PNNL-11621
UC-2030

**Pacific Northwest National Laboratory**

Operated by Battelle for the U.S. Department of Energy

# Gas Release During Salt-Well Pumping: Model Predictions and Laboratory Validation Studies for Soluble and Insoluble Gases

L. M. Peurrung
S. M. Caley
P. A. Gauglitz



August 1997

Prepared for the U.S. Department of Energy
under Contract DE-AC06-76RLO 1830

PNNL-11621

PACIFIC NORTHWEST NATIONAL LABORATORY
*operated by*
BATTELLE
*for the*
UNITED STATES DEPARTMENT OF ENERGY
*under Contract DE-AC06-76RLO 1830*

**Printed in the United States of America**

**Available to DOE and DOE contractors from the Office of Scientific and Technical Information, P.O. Box 62, Oak Ridge, TN 37831; prices available from (615) 576-8401.**

**Available to the public from the National Technical Information Service, U.S. Department of Commerce, 5285 Port Royal Rd., Springfield, VA 22161**


This document was printed on recycled paper.

PNNL-11621
UC-2030

# Gas Release During Salt-Well Pumping: Model Predictions and Laboratory Validation Studies for Soluble and Insoluble Gases

L. M. Peurrung
S. M. Caley
P. A. Gauglitz

August 1997

Prepared for
the U.S. Department of Energy
under Contract DE-AC06-76RLO 1830

Pacific Northwest National Laboratory
Richland, Washington 99352

# Executive Summary

The Hanford Site has 149 single-shell tanks (SSTs) containing radioactive wastes that are complex mixes of radioactive and chemical products. Of these, 67 are known or suspected to have leaked liquid from the tanks into the surrounding soil, while 82 are considered sound (Hanlon 1996). To minimize the amount of material that could potentially leak into the surrounding soil, all of the SSTs are scheduled to have drainable liquid removed and to be designated as interim stabilized. Of the SSTs, 117 have been declared stabilized while only 32 require further processing (Hanlon 1996). The Tri-Party Agreement (Ecology 1996) has set a series of milestones for completing interim stabilization with completion set for September 2000. While process equipment exists for removing drainable liquid, and its operation is well known from previous pumping campaigns, a number of safety issues associated with the release and potential ignition of flammable gases within the tanks is interrupting progress on completing the removal of drainable liquid.

The safety concerns associated with flammable gases stem from the observation that some of the wastes in the SSTs generate and retain hazardous amounts of flammable gases, including hydrogen, nitrous oxide, and ammonia. Of the 32 SSTs remaining to be declared interim stabilized, 31 need to have drainable liquid removed by salt-well pumping, and 17 of these are on the Flammable Gas Watch List (FGWL) (Hopkins 1995; Hanlon 1996). Salt-well pumping to remove the interstitial liquid from SSTs is expected to cause the release of much of the retained gas, both soluble (principally hydrogen) and insoluble (principally ammonia), posing a number of safety concerns. Research at Pacific Northwest National Laboratory (PNNL)[(a)] has sought to quantify the release of flammable gases during salt-well pumping and post-pumping operations. This study is being conducted for the Project Hanford Management Contract Team as part of the PNNL Flammable Gas Project. Understanding and quantifying the physical mechanisms and waste properties that govern gas release during salt-well pumping will help to resolve the associated safety issues both during the pumping operation and after, during storage of waste.

The overall purpose of this ongoing study of salt-well pumping is to develop a quantitative understanding of the release rates and cumulative releases of flammable gases from SSTs as a result of salt-well pumping. The current study is an extension of the previous work reported by Peurrung et al. (1996), which showed that draining liquid from a simple waste simulant released essentially all of the retained gas in a controlled manner. Model predictions for actual tank behavior also showed controlled release of insoluble gas (hydrogen) and a very prolonged release of the dissolved gas (ammonia). While this study helped elucidate gas release behavior and provided a model for actual tank behavior that has been verified against laboratory studies, the laboratory studies did not investigate the release of soluble gases, and both the experiments and modeling were limited to homogeneous waste configurations.

---

(a) Pacific Northwest National Laboratory is operated by Battelle for the U.S. Department of Energy under Contract DE-AC06-76RLO 1830.

The first objective of the current study was to conduct laboratory experiments to quantify the release of soluble and insoluble gases. These studies were conducted with glass bead packs and surrogate gases rather than with actual tank waste and retained gases. The second objective was to determine experimentally the role of characteristic waste heterogeneities on the gas release rates. The third objective was to adapt and evaluate the computer model STOMP (Subsurface Transport over Multiple Phases) (White and Oostrom 1996) used by Peurrung et al. (1996) to predict the release of both soluble and insoluble gases during and after salt-well pumping. To evaluate and verify the STOMP model, one-dimensional (1-D) simulations were compared to the series of experimental results for soluble and insoluble gas releases for both homogeneous and heterogeneous waste simulants. The fourth and final objective of the current study was to predict the gas release behavior for a range of typical tank conditions and actual tank geometry. In these models, we seek to include all the pertinent salt-well pumping operational parameters and a realistic range of physical properties of the SST wastes.

All four project objectives were met. Comparisons of the laboratory experiments with the 1-D STOMP model predictions generally show good agreement for homogeneous packings, particularly for the larger (1-mm diameter) beads. The agreement between laboratory results and model predictions for heterogeneous packings is only fair quantitatively but still good qualitatively. A continuing issue with the laboratory studies is the incomplete recovery of the insoluble gas ($SF_6$), which we attribute to leaks in the system and losses during draining. However, these losses amount to no more than a two-fold uncertainty in gas release rates.

An analysis of the laboratory and modeling work completed to date provides insight into the mechanisms of gas release during salt-well pumping and lays the foundation of a technical basis for conducting operations safely. However, the studies with heterogeneous media suggest that some additional work is needed to complete the overall picture. The discussion below summarizes findings to date. Moreover, the model has not been validated using actual tank waste.

**Mechanisms of Gas Release**

The results of these studies clearly show very different gas release mechanisms for the two types of gas. The distinction arises because the insoluble gas (hydrogen) chiefly resides in trapped gas bubbles, while the majority of the soluble gas (ammonia) inventory is dissolved in the liquid phase. Insoluble gas is primarily released as the retreating liquid exposes trapped gas bubbles, which then diffuse through connected gas channels to the surface of the saltcake. As expected, essentially all of the insoluble gas in the exposed bubbles is released, although the release rate depends on several parameters. Some insoluble gas release can also occur as the liquid head is reduced during the draining process, causing the trapped gas bubbles to expand. Depending on the parameter range, these expanded bubbles may connect and allow gas flow or may remain trapped until exposed to the invading gas by the retreating liquid. For either mechanism, if draining ceases, the release of further trapped gas stops, and the relatively small amount of released gas in the drained portion of the saltcake quickly dissipates.

The behavior of the soluble gas (ammonia) is quite different. Much of it is withdrawn with the pumped liquid; however, capillary forces hold some residual liquid in the pores after draining, including a substantial inventory of dissolved gas. This gas volatilizes into adjacent

air-filled pores and then diffuses into the dome space like the insoluble gas. Thus, the amount of soluble gas ultimately released to the dome space is roughly equal to the initial concentration of dissolved gas times the amount of nonpumpable liquid. Because of the affinity of the soluble gas for the liquid phase, many pore volumes of air are required to deplete the liquid of dissolved gas. Soluble gas release thus takes longer than insoluble gas release. Moreover, if draining ceases, soluble gas release continues until the residual liquid is depleted. This implies that while the liquid pump rate could be used to control the rate of hydrogen release and accumulation in the tank dome space, the ammonia release could not be controlled in this manner.

**The Effect of Heterogeneity**

The laboratory and the one- and two-dimensional (2-D) modeling results all show that heterogeneities can have a profound effect on gas release. Low-permeability layers, particularly near the top of the saltcake, displayed an ability to retard the release of both soluble and insoluble gases. In one experiment with several layers of graded sands, draining did not release any of the insoluble gas. This result challenges the assumption that salt-well pumping will cause retained gases to be released. An assessment of the degree and size of heterogeneities in the tank waste is needed to settle this issue.

**Predictions of Gas Release Rate and Cumulative Release**

The 2-D model results include predictions of the amount of pumpable liquid and the rate and cumulative amount of gas released. Conditions for a base case were selected to represent a 6.1-m (20-ft) thick saltcake with a permeability of 22 darcies and an initial gas saturation of 10%.[a] Approximately 84% of the liquid drained from the saltcake, while 16% remained trapped in the interstitial pores by capillary forces. In the simulation, the liquid pumping rate was initially limited to 19 L (5 gal)/min and fell to less than 0.2 L (0.05 gal)/min after about 400 days of continuous pumping. In 430 days, 90% of the drainable liquid had been pumped. At that time, 98.6% of the hydrogen was released to the dome space. Assuming a total inventory of 100 standard cubic meters (SCM) of hydrogen, the initial release rate was as high as 12 SCM/day (0.3 standard cubic feet per minute [scfm]); however, a more typical release rate was 1 to 0.1 SCM/day.

Assuming the same saltcake characteristics, 12.3% of the ammonia was released as gas to the dome space over the course of 430 days in the simulations. Ultimately, 20.9% of the initial ammonia inventory was released to the dome, but only after several years. The other 79.1% was removed with the liquid phase. Assuming a total inventory of 100 SCM of ammonia, the initial release rate was 0.6 SCM (20 $ft^3$)/day, while a more typical rate was 0.1 to 0.01 SCM/day.

Active ventilation of tanks appears to be necessary to prevent dome space concentrations of flammable gas from exceeding the 25% lower flammability limit (LFL), but only during the early part of draining. Hydrogen is the primary concern. However, this conclusion assumes a relatively homogeneous waste.

---

(a) 10% gas saturation is equivalent to 5% void fraction. The gas saturation is defined as the fraction of the porosity (taken here as 50%) occupied by gas.

## The Effect of Changing Waste Properties

Decreasing the permeability of the saltcake in the simulations increased the time required to complete draining and decreased the amount of pumpable liquid. These effects combined to slow the release rates of both hydrogen and ammonia but increased the total amount of ammonia ultimately released to the dome space.

Increasing the initial gas saturation (void fraction) from 10% (5% void) to nearly 20% (10% void) did not have a strong effect on release rates beyond the expected factor of two. The relative fraction of the initial ammonia inventory ultimately released as gas to the dome space was about the same because it depends primarily on the amount of residual liquid, which is roughly equal for the two cases.

The thickness of the saltcake affected its initial drain rate, with thick wastes exerting more pressure on their liquids to drain. The hydrogen release rate in the early part of draining was therefore somewhat higher for thick wastes. However, the effect on ammonia release was the opposite, with fluxes slightly higher for thinner wastes because of the decreased influx of invading air and the larger amount of liquid retained in the waste at the end of draining.

## The SCOPE Model

Finally, a simple, lumped-parameter model of the soluble gas release rate was developed for the Safety Controls Optimization by Performance Evaluation (SCOPE) elicitation:

$$R_{NH_3} = \alpha\,(y_{eq} - y_{dome})\,e^{-0.67t/t_{1/2}},$$

where $R_{NH3}$ is the flux of ammonia into the dome space in scfm, $\alpha$ is a global constant in scfm $NH_3$/mole fraction $NH_3$, $y_{eq}$ is the mole fraction of ammonia in the gas phase in equilibrium with the dissolved ammonia in the waste, $y_{dome}$ is the dome-space ammonia mole fraction, $t$ is time, and $t_{1/2}$ is a characteristic decay constant (in the form of a half-life) that depends on the physical properties of the waste. STOMP predicted that the global constant $\alpha$ was equal to 1.2 scfm/mole fraction. For our best estimate of saltcake consistency, $t_{1/2}$ was equal to 540 days. At early times (roughly the first third to half of the overall draining time), STOMP predicts a higher release rate than this approximation. To estimate a bounding gas release rate, a simple correction consistent with the STOMP results is to multiply the estimate by a factor of 10 during draining.

## Executive Summary References

Ecology, EPA, and DOE. 1996. *Hanford Federal Facility Agreement and Consent Order*. Washington State Department of Ecology, U.S. Environmental Protection Agency, and U.S. Department of Energy, Olympia, Washington, as amended.

Hopkins JD. 1995. *Methodology for Flammable Gas Evaluations.* WHC-SD-WM-TI-724, Westinghouse Hanford Company, Richland, Washington.

Hanlon BM. 1996. *Waste Tank Summary Report for Month Ending September 26, 1996.* WHC-EP-0182-102, Westinghouse Hanford Company, Richland, Washington.

Peurrung LM, SM Caley, EY Bian, and PA Gauglitz. 1996. *Gas Release During Salt Well Pumping: Model Predictions and Comparisons to Laboratory Experiments*. PNNL-11310, Pacific Northwest National Laboratory, Richland, Washington.

White MD and M Oostrom. 1996. *STOMP Subsurface Transport Over Multiple Phases, Theory Guide*. PNNL-11217, Pacific Northwest Laboratory, Richland, Washington.

# Acknowledgments

The authors wish to thank Mark D. White of Pacific Northwest National Laboratory for his important contributions to this work. Mark, who is the primary developer of the STOMP code, made a number of modifications that allowed STOMP to model gas release during salt-well pumping, checked the code results for consistency in this application, helped resolve a number of numerical difficulties, and generally provided valuable expert counsel. The authors would also like to thank Steve Barker of Lockheed Martin Hanford Company for providing much of the information on the estimates of retained gas in tanks yet to be pumped.

# Contents

# Figures

# Tables

# 1.0 Introduction

The Hanford Site has 149 single-shell tanks (SSTs) containing radioactive wastes that are complex mixes of radioactive and chemical products. Of these, 67 are known or suspected to have leaked liquid from the tanks into the surrounding soil, while 82 are considered sound (Hanlon 1996). To minimize the amount of material that could potentially leak into the surrounding soil, all of the SSTs are scheduled to have drainable liquid removed and to be designated as interim stabilized.[a] Of the SSTs, 117 have been declared stabilized, and only 32 require further processing (Hanlon 1996).[b] Many of the tanks have been declared stabilized administratively, with only 44 tanks having had drainable liquid removed. The Tri-Party Agreement (Ecology 1996) has set a series of milestones for completing interim stabilization by September 2000. While process equipment exists for removing drainable liquid, and its operation is well known from previous pumping campaigns, a number of safety issues associated with the release and potential ignition of flammable gases within the tanks is interrupting progress on completing the removal of drainable liquid.

The safety concerns associated with flammable gases stem from the observation that some of the wastes in the SSTs generate and retain hazardous quantities of flammable gases, including hydrogen, nitrous oxide, and ammonia. Of the 32 SSTs remaining to be declared interim stabilized, 31 need to have drainable liquid removed by salt-well pumping (241-C-106 [C-106] does not need salt-well pumping because its waste will be removed), and 17 of these are on the Flammable Gas Watch List (FGWL) (Hopkins 1995; Hanlon 1996). Salt-well pumping to remove the interstitial liquid from SSTs is expected to cause the release of much of the retained gas, both insoluble (principally hydrogen) and soluble (principally ammonia), posing a number of safety concerns. Research at Pacific Northwest National Laboratory (PNNL)[c] has sought to quantify the release of flammable gases during salt-well pumping and post-pumping operations. This study is being conducted for the Project Hanford Management Contract Team as part of the PNNL Flammable Gas Project. Understanding and quantifying the physical mechanisms and waste properties that govern gas release during salt-well pumping will help to resolve the associated safety issues both during the pumping operation and after, during storage of waste.

Salt-well pumping, or interim stabilization, is a well-established operation for removing drainable interstitial liquid from SSTs that began in the mid-1970s (Grimes 1978). Of the 149 SSTs at Hanford, 44 have had drainable liquid removed by salt-well pumping (Caley et al. 1996).

---

(a) While essentially all of the drainable liquid must be removed, specific criteria are used to determine when liquid removal is sufficiently thorough to allow the SSTs to be designated as interim stabilized (Hanlon 1996).

(b) Two additional tanks have been declared stabilized since Hanlon (1996).

(c) Pacific Northwest National Laboratory is operated by Battelle for the U.S. Department of Energy under Contract DE-AC06-76RLO 1830.

While salt-well pumping has been conducted in many tanks for years, only recently have studies focused on understanding how it releases retained flammable gases. The first quantitative studies of gas release during salt-well pumping were associated with the safety assessment for salt-well pumping FGWL tanks conducted by Los Alamos National Laboratory (WHC 1996). As part of this safety assessment, the release rate of gas initially trapped in bubbles as a result of draining liquid from an SST (the model neglected the release of soluble gases such as ammonia) was estimated.[a] In this model, it was assumed that, as the waste was drained, all of the trapped gas bubbles in the drained region were released. The consequence of this assumption is that the release rate is proportional to the salt-well pumping rate.

More recently, Peurrung et al. (1996) conducted both modeling and laboratory studies of how draining liquid releases retained gas. The experiments focused on the release of insoluble gas from homogeneous simulants that mimicked coarse saltcake. The model was used to elucidate the dominant gas release mechanisms in the laboratory experiments and to predict the gas release behavior from a typical tank during pumping (both soluble and insoluble gases were included in the model). This study showed that draining liquid from a simple simulant released essentially all of the retained gas in a controlled manner. The model predictions for the actual tank behavior also showed controlled release of insoluble gas (hydrogen) and a very prolonged release of the dissolved gas (ammonia). While this study has helped elucidate gas release behavior and has provided a model for actual tank behavior that has been verified against laboratory studies, the laboratory studies have not investigated the release of soluble gases, and both the experiments and modeling have been limited to homogeneous waste configurations.

Caley et al. (1996) summarized waste tank information that was considered potentially useful in characterizing the release of flammable gases during salt-well pumping. Of the 44 tanks that have been salt-well pumped, only six have been monitored for flammable gases during pumping operations. Table 1.1 summarizes some data for these tanks. While these tanks were monitored for flammable gas accumulation in the tank dome space, the results in the last column indicate that the flammable gas concentrations were ten-fold less than the action limit of 25% of the lower flammability limit (LFL). These six tanks are not on the FGWL, as noted in the table, and are probably not representative of the more hazardous tanks. They are included for comparison with Table 1.2, which includes the FGWL tanks. The third column shows estimates of the void fraction retained in the waste for which good data are available; these void fractions are all zero. In the fourth column, results from the flammable gas screening of Hodgson et al. (1997) are shown. The % LFL values represent the potential dome space concentration if a bounding volume of the retained gas were released rapidly compared with the mixing and dilution within the tanks (Hodgson et al. 1997). While two of these tanks have amounts above 25% of the LFL, these values are derived from very uncertain data and are included here for completeness. The fifth column shows an estimate of the ammonia concentration in the waste from Agnew (1997). The sixth column gives the fraction of waste solids that are saltcake.

---

(a) Spore JW. 1996. *Conservative Gas Releases for Tank 241-A-101.* Los Alamos National Laboratory Calc-Note, TSA10-CN-WT-SA-GR-046.

**Table 1.1** Recently Salt Well Pumped Tanks with Gas Monitoring

| Tank [a] | FGWL[b] | Void Fraction (%)[c] | Hydrogen (% LFL)[d] | Ammonia (moles/L)[e] | Saltcake (%)[f] | Peak FG (% of LFL)[g] |
|---|---|---|---|---|---|---|
| BY-103 | no | | 26 | 0.01 | 99 | 3 |
| BY-106 | no | | 123 | 0.05 | 85 | 1 |
| BY-109 | no | 0 | 10 | 0.01 | 80 | 3 |
| S-108 | no | 0 | 0.04 | 0.08 | 99 | 2 |
| S-110 | no | 0 | 0.32 | 0.1 | 66 | 2 |
| T-104 | no | | 0.14 | 0.07 | 0 | 2 |

(a) Full tank designations are 241- followed by tank farm designation (BY, S, T) and tank number. Common usage omits the 241, using just the tank farm designation and tank number.

(b) Designated as on the Flammable Gas Watch List (Hanlon 1996).

(c) Void fraction determined from estimates of retained gas volume and volume of wet solids. The retained gas is the 50th percentile barometric pressure estimate from data reported in Hodgson et al. (1997) and supporting spreadsheets; we include here only those void fractions based on FIC or Enraf level data.

(d) Values represent the potential flammable gas concentrations in the tank dome spaces as described by Hodgson et al. (1997); the values given are the largest entries for each tank in Table 2-1. Many of these estimates have large uncertainties and overestimate retained gas.

(e) Values from Appendix E, "Total Inventory Estimate" (Agnew 1997).

(f) Fraction of waste classified as saltcake by Hanlon (1996).

(g) Peak flammable gas concentration during pumping as reported by Caley et al. (1996) (for BY-106, only data following relocation of sampling point [after 9/19/ 95] are considered).

Liquid should drain more completely from saltcake waste; sludge drains poorly. Accordingly, Tank 241-T-104 (T-104) should behave much differently than tanks with a majority of saltcake.

Although gas release during salt-well pumping is normally associated with draining liquid, a number of other gas release mechanisms can occur, and these may potentially be triggered by salt-well pumping. Stewart et al. (1996) reported a comprehensive analysis of potential gas release mechanisms from SSTs with typical waste configurations.

The release of retained gas during the pumping operation causes a number of safety concerns, but the expected reduction in retained gas also reduces the flammable gas hazard during subsequent waste storage. Recently, a risk evaluation methodology (Safety Controls Optimization by Performance Evaluation [SCOPE]) has been initiated that provides a relatively complete representation of the flammable gas hazard (Sandia 1997). Within this analysis is a simple model of the release of both insoluble and soluble gases during salt-well pumping and the degree that the flammable gas hazard is thereby reduced.

Salt-well pumping of the SSTs on the FGWL and of other tanks thought to retain potentially hazardous volumes of flammable gases is expected to begin soon. Table 1.2 lists the tanks remaining to be salt-well pumped and several of their distinguishing features. To understand how gas is released during salt-well pumping, it is important to have reasonable estimates for the volume of trapped gas in the waste.

**Table 1.2** Tanks Remaining To Be Salt-Well Pumped

| Tank[a] | Anticipated Start Date[b] | FGWL[c] | Void Fraction (%)[d] | Hydrogen (% LFL)[e] | Ammonia (moles/L)[f] | Saltcake (%)[g] |
|---|---|---|---|---|---|---|
| T-104 | ongoing | - | | 0.14 | 0.07 | 0 |
| BY-109 | ongoing | - | 0 | 27 | 0.01 | 80 |
| T-110 | 05/97 | yes | 0 | 32 | 5E-6 | 0 |
| SX-104 | 07/97 | yes | 0 | 10 | 0.1 | 78 |
| BY-103 | 07/97 | - | | 26 | 0.01 | 99 |
| A-101 | 09/97 | yes | | 379 | 0.05 | 100 |
| AX-101 | 09/97 | yes | | 0.5 | 0.06 | 100 |
| SX-103 | 10/97 | yes | 18 | 216 | 0.09 | 82 |
| S-109 | 11/97 | - | | 145 | 0.07 | 98 |
| BY-105 | 11/97 | - | | 144 | 0.09 | 69 |
| BY-106 | 12/97 | - | | 123 | 0.05 | 85 |
| S-102 | 12/97 | yes | 19 | 226 | 0.04 | 99 |
| SX-102 | 01/98 | yes | 12 | 93 | 0.1 | 78 |
| S-101 | 01/98 | - | 6 | 109 | 0.1 | 41 |
| SX-106 | 02/98 | yes | 9 | 78 | 0.09 | 86 |
| SX-105 | 02/98 | yes | | 87 | 0.1 | 89 |
| C-103 | 03/98 | - | | 2 | 0.030 | 0 |
| U-107 | 04/98 | yes | 8 | 87 | 0.08 | 89 |
| U-108 | 05/98 | yes | | 300 | 0.09 | 89 |
| U-111 | 06/98 | - | 0 | 97 | 0.07 | 92 |
| U-109 | 07/98 | yes | 8 | 118 | 0.1 | 86 |
| S-107 | 08/98 | - | 4 | 138 | 0.1 | 19 |
| U-105 | 09/98 | yes | 9 | 270 | 0.1 | 83 |
| U-103 | 10/98 | yes | 10 | 161 | 0.9 | 90 |
| U-102 | 11/98 | - | | 203 | 0.9 | 84 |
| S-111 | 12/98 | yes | 14 | 181 | 0.1 | 75 |
| S-106 | 01/99 | - | 33 | 223 | 0.06 | 94 |
| U-106 | 02/99 | - | 3 | 37 | 0.1 | 82 |
| SX-101 | 04/99 | yes | 3 | 28 | 0.1 | 75 |
| S-112 | 06/99 | yes | 0 | 30 | 0.08 | 99 |
| S-103 | 10/99 | - | 20 | 72 | 0.1 | 96 |

(a) Full tank designations are 241- followed by tank farm designation (BY, S, T) and tank number. Common usage omits the 241, using just the tank farm designation and tank number.

(b) Personal communication from DT Vladimiroff (June 1997).

(c) Designated as on the FGWL (Hanlon 1996).

(d) Void fraction determined from estimates of retained gas volume and volume of wet solids. The retained gas is the 50$^{th}$ percentile barometric pressure estimate from data reported in Hodgson et al. (1997) and supporting spreadsheets; we included only those void fractions based on FIC or Enraf level data.

(e) Values represent the potential flammable gas concentrations in the tank dome spaces as described by Hodgson et al. (1997), and the values given are the largest entries for each tank in Table 2-1; many of these estimates have large uncertainties and are overestimates of retained gas.

(f) Values from Appendix E, "Total Inventory Estimate" Agnew (1997).

(g) Fraction of solids classified as saltcake by Hanlon (1996).

Unfortunately, direct information on the quantity or fraction of gas retained in SSTs is only available for two SSTs. Shekarriz et al. (1996) report 14.2 ± 1.4% void for A-101 and about 16% on average for U-103.[a] Although these are the only direct measurements existing for the void fraction in SSTs, several studies have estimated retained gas volumes. Whitney (1995) screened Hanford tanks for trapped gas by correlating the changes in waste level with barometric pressure fluctuations due to gas bubbles compressing and expanding. Hopkins (1995) presented a methodology for evaluating trapped gas in Hanford waste tanks that includes both the barometric pressure evaluation and level increases in the waste. Hodgson et al. (1997) presented an evaluation of a number of tanks based on the methodology described by Hopkins (1995). The evaluation by Hodgson et al. (1997) focused on determining the largest potential flammable gas concentration in the dome space of the tanks. While retained void fractions are not directly reported in the evaluation, the results can be used to directly calculate the void fraction in the settled solids layer. The fourth column shows estimates of the void fraction retained in the waste, for which good data are available. While these data are limited, they show that the void fractions are not negligible and that they represent a substantial volume of retained gas in many tanks. In the fifth column, results from the flammable gas screening of Hodgson et al. (1997) are shown. It should be emphasized that the method of Hopkins (1995) and the evaluation of Hodgson et al. (1997) used data and tank parameters that had a large uncertainty and some very conservative assumptions. Still, it is evident that the potential concentration of flammable gases in the remaining tanks is much higher than in the tanks previously pumped and listed in Table 1.1.

The sixth column shows an estimate of the ammonia concentration in the waste from Agnew (1997). Essentially all of these estimates show high enough ammonia concentrations to raise concern. The measured ammonia concentration reported by Shekarriz et al. (1997) for A-101 ranged from 0.003 to 0.03 moles/L, which is somewhat less than the estimates given by Agnew (1997).

The seventh column gives the fraction of the waste that is saltcake. SST waste has a range of physical properties and is typically classified as sludge, saltcake, or supernatant liquid (Hanlon 1996). Hanlon describes saltcake as waste that resulted from crystallization and precipitation after the liquid waste was concentrated and that is composed of precipitated salt crystals, while it describes sludges as wet solids (insoluble) that were formed (precipitated) during sodium hydroxide additions to the waste. The % saltcake is shown in Table 1.2 because liquid should drain more completely from saltcake waste while sludge drains poorly. (This expectation is confirmed in this study with model results for different permeability waste.) Of the 30 tanks remaining to be pumped, 25 contain more than 75% saltcake. Accordingly, understanding the gas release behavior of saltcake waste will be much more important than addressing gas release from sludge tanks.

---

(a) Average void fractions from four samples from a recent presentation by LA Mahoney, ZI Antoniak, JM Bates, and A Shekarriz entitled, *Preliminary Retained Gas Sampler Measurement Results for Hanford Waste Tank 241-U-103.* May 1997. TWSFG97.40, PNNL, presented to the SCOPE expert panel.

## 1.1 Objectives

The overall objective of this ongoing study is to develop a quantitative understanding of the release rates and cumulative releases of flammable gases from SSTs as a result of salt-well pumping. The current study is an extension of the previous work reported by Peurrung et al. (1996). The first objective of this current study was to conduct laboratory experiments to quantify the release of soluble and insoluble gases. The second was to determine experimentally the role of characteristic waste heterogeneities on the gas release rates. The third objective was to evaluate and validate the computer model STOMP (Subsurface Transport over Multiple Phases) (White and Oostrom 1996) used by Peurrung et al. (1996) to predict the release of both soluble (typically ammonia) and insoluble gases (typically hydrogen) during and after salt-well pumping. The fourth and final objective of the current study was to predict the gas release behavior for a range of typical tank conditions and actual tank geometry. In these models, we seek to include all the pertinent salt-well pumping operational parameters and a realistic range of physical properties of the SST wastes. For predicting actual tank behavior, two-dimensional (2-D) simulations were performed with a representative 2-D tank geometry.

## 1.2 Mechanisms of Gas Release During Salt-Well Pumping

Flammable gases are retained in tank waste both as gas bubbles and as dissolved gas (primarily ammonia). The principal mechanisms of bubble retention and details of specific bubble retention mechanisms have been discussed previously (Gauglitz et al. 1994, 1995, 1996; Rassat and Gauglitz 1995; Stewart et al. 1996). Observations of bubble retention in actual SST and double-shell tank (DST) wastes have also been reported (Gauglitz et al. 1996; Bredt et al. 1995; Bredt and Tingey 1996). For bubbles retained in particulate simulated waste (saltcake with coarse particles), the previous work showed that the morphology of the retained bubbles depends on a Bond number, which is a ratio of gravitational forces to surface tension. Where the waste has relatively coarse particles typical of saltcake (on the order of 10 to 100 microns) (Rynolds 1992; Herting et al. 1992), it is expected that the dominant bubble retention mechanism will be capillary force, that the bubbles will finger between the particles constituting the particulate medium, and that the bubble behavior during draining can be represented by a classical porous media approach.

Figure 1.1 depicts salt-well pumping in an SST that contains a drainable saltcake. Interstitial liquid drains through the screened interval of the salt well, where a pump removes it. In the vicinity of the salt-well screen the fluid level is reduced most quickly, while the fluid level away from the well decreases more slowly. Draining the fluid draws air into the pores between the salt crystals. Once the air has invaded the pores and exposed previously trapped bubbles, the gas within these bubbles can be released from the waste by diffusing into the tank dome against the invading air. Also shown in the figure is the expansion of bubbles caused by the reduced hydrostatic head on the bubbles as the liquid is drained from the waste. When the gas void fraction is low, these bubbles will simply expand. In contrast, if the gas fraction is high enough, the expanding bubbles will connect and flow upward. In general, the gas fraction that defines the

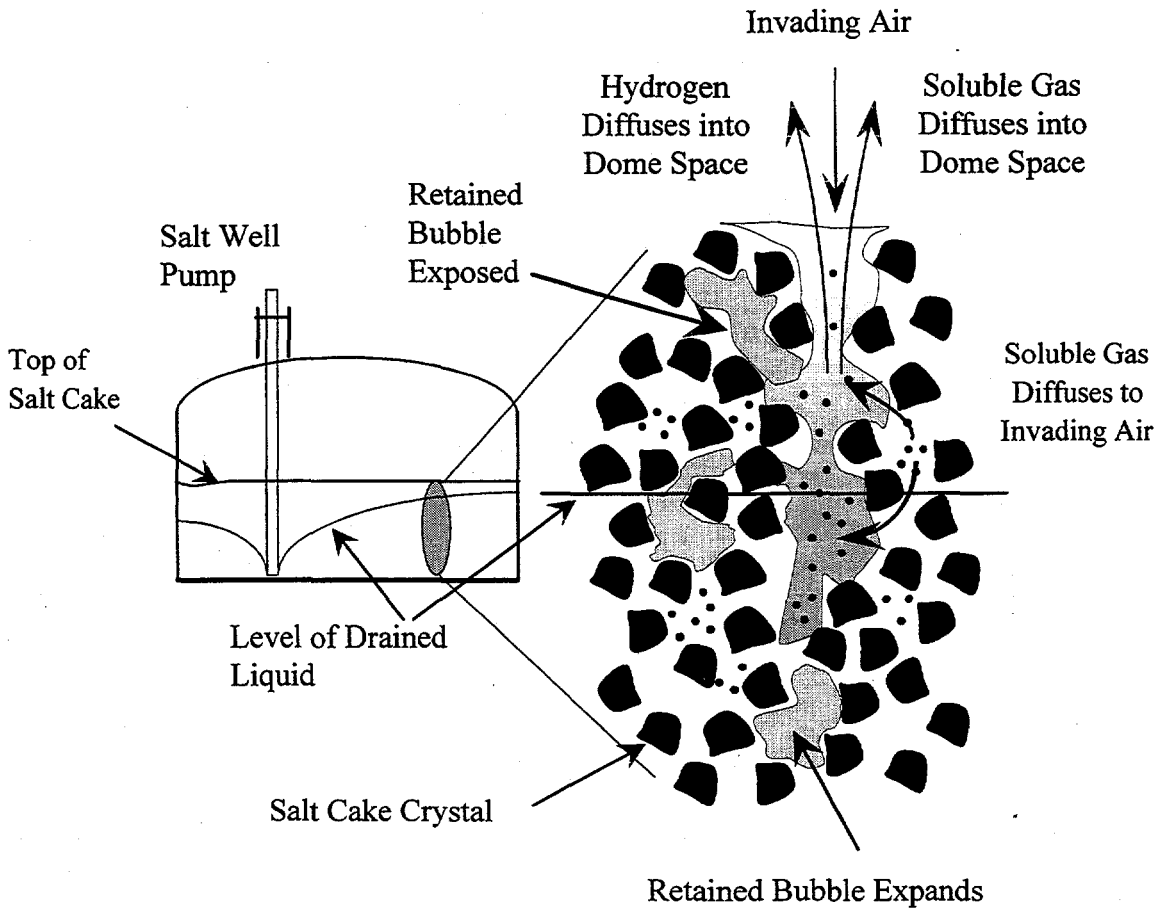


**Figure 1.1.** Draining Interstitial Liquid by Salt-Well Pumping Causes Invading Air to Expose Retained Bubbles and Retained Bubbles to Expand as Fluid Head Decreases (dissolved soluble gas [small dots] diffuses and partitions into invading air; both gas species then diffuse into tank dome against invading air)

transition at which bubbles connect depends on the porosity and connectedness of the pores and the distribution of the retained bubbles. While this transition depends on many things that are difficult to measure, it is an easy parameter to vary in models.

This figure also depicts the movement of dissolved soluble gas (primarily ammonia), which is shown as small dots. The dissolved soluble gas vapors diffuse through the aqueous phase and partition into the invading air. Once within the invading air, these vapors diffuse through the gas phase into the tank dome. Naturally, the dissolved gases can also diffuse through the aqueous phase to the tank dome, but diffusion through the aqueous phase is much slower than diffusion through the gas phase.

Previous studies by Peurrung et al. (1996) evaluated the interplay between a number of mechanisms controlling the release of gas during draining. A series of experiments and computer simulations was conducted to explore a range of draining rates and column lengths,

and both nitrogen and helium were used to represent the invading air. The draining rate studies were used to investigate the relative rates of upward diffusion and the downward velocity of the invading gas. Studies were conducted in which the downward velocity of the invading air dominated (fast draining), where these rates were equivalent, and where the downward velocity was negligible compared with the upward diffusion (slow draining). As depicted in Figure 1.1, the draining rate depends on the distance from the salt well. The different column lengths and switching between nitrogen and helium (larger gas phase diffusions coefficient) enabled us to verify the dominant role of gas-phase diffusion on the release rates.

Peurrung et al. (1996) also reviewed the available data for porous media properties that should be expected for the actual SST waste. They concluded that it is reasonable to assume that saltcake waste in SSTs will behave as a typical porous media in terms of how gases and fluids migrate. Simmons (1995) reviewed the liquid retention behavior of tank waste and has been successful in understanding many aspects of tank draining by treating the waste as a permeable medium. Accordingly, our approach will build upon the traditional porous media concepts that have so far been successful.

# 2.0 Modeling Approach

The STOMP computer code simulates flow and transport through porous media. It was developed at PNNL and has been used primarily for modeling soil hydrology. STOMP solves differential equations representing mass balances in air, water, and other phases (e.g., oil or ice) using the integral volume finite difference technique. Flows are Darcy-type based on the intrinsic and relative permeability of the porous medium and its liquid and gas phases. STOMP can also calculate an energy balance to solve nonisothermal problems, but this capability was not used for this study.

This section of the report describes the physics included in the model and how it was applied to salt-well pumping. For further details on the mathematics and solution technique, see the STOMP manuals (White and Oostrom 1996).[(a)]

STOMP models gas and liquid flow through an immobile, porous, solid phase. It is thus well suited for studying liquid draining and gas release during salt-well pumping. However, saltcake "slumping," or subsidence, will not be considered in this report, nor will yielding of material. As discussed in Section 1, the validity of applying this model to tank waste depends on the degree to which saltcake behaves like a typical permeable material. However, we believe that description is appropriate.

## 2.1 Modeling the Gas Phase

Because STOMP is a finite difference model, the solution domain is discretized on a grid to form "elements," or "nodes." For example, to simulate draining a tank in the vertical dimension only, a 10-m-high column of waste might be discretized into forty 25-cm-tall elements. Each element is assumed to be homogeneous; that is, physical properties, saturations, concentrations, and pressures are assumed to be uniform within the element. Thus there are no details of phenomena occurring on length scales shorter than an element width. Instead, microscopic behavior is accounted for by the governing equations on macroscopic variables, which is a well-established method of modeling multiple phases in porous media (Dullien 1992).

For this reason, STOMP does not model individual bubbles, which are too small to be resolved by discretization. Instead, each element has a homogeneous gas phase volume fraction. The bubble-like behavior of the gas is incorporated through the constitutive equations used to relate gas and liquid phase pressures to gas saturation. The constitutive model used for this report is a relation based on the work of Parker and Lenhard (1987; Lenhard and Parker 1987) that allows gas to be trapped during imbibition. By using this form, a static initial condition is possible with a certain volume fraction of gas immobilized or "trapped" in the otherwise saturated saltcake. The model also allows the element to contain, simultaneously, some gas that

(a) MD White and M Oostrom. 1995. *STOMP User's Guide* (draft). WE Nichols, NJ Aimo, M Oostrom, and MD White. 1995. *STOMP Application Guide* (draft). Pacific Northwest National Laboratory, Richland, Washington.

is not trapped and is connected to gas spaces in adjacent elements. While there are no "round" or "dendritic" bubbles in STOMP (since they are too small to be resolved), the flavor of the model is of dendritic bubbles of two length scales:

1. smaller than the width of the element; participate in intra-element transport only

2. span the width of the element; participate in inter- and intra-element transport.

The model limits the amount of gas that can be kept in a trapped state to a specified value, above which the trapped gas begins to interconnect over distances larger than a single element. The user sets this "maximum trapped gas saturation" at a fixed, global value that applies to the whole porous medium. However, the *local* maximum trapped gas fraction at a particular point may be less than the *global* value due to that point's drainage/imbibition history. That is, if the element has been only partially drained and reimbibed, some of the locations where trapped gas could be held are assumed to be lost.

To illustrate the nature of the trapped and free gas, consider the trapped gas fraction in an otherwise liquid-saturated element as the liquid level slowly falls. Initially, only trapped gas is present—in this example, a 5% gas saturation out of a 10% maximum before bubbles connect and flow occurs. There are no gas fluxes since all gas is fixed in place and does not contribute to transport between elements. As liquid drains and the liquid level falls, gas saturation increases due to the decrease in pressure. If the absolute pressure were to fall by a factor of two, the trapped gas would swell until it exceeds the maximum saturation. The fraction in excess of 10% would then become free gas, interlinked with the free gas above it, and would flow upward. (Potentially, the flow could decrease the gas saturation until it falls below the maximum, resulting in pulses of gas up through the medium. This bubble-like gas release was what we originally expected the model to show. In STOMP, however, the gas release tends to be more steady. Gas fluxes out of these bubbles are kept small because the gas relative permeability is strongly dependent on the free gas saturation. As the free gas saturation starts to increase, the relative permeability tends to increase just enough to release it.)

As downward flow of liquid brings the liquid level down to a new element, the gas saturation in that element rises sharply as air begins to flow into it from above. In addition to this new free gas, the trapped gas is gradually freed. When the liquid level falls past the element to the one below it, opening it to gas flow, air begins to flow down through the element. Some of the air influx contributes to desaturating the element itself, while the rest flows through and desaturates lower elements.

If the liquid draining stopped, some of the trapped gas remaining in elements in the capillary fringe would remain trapped. Re-imbibing the elements would trap gas again (now composed of air as well as ammonia, hydrogen, etc.), but not necessarily the maximum amount.

## 2.2 Modeling the Bubble Gases as Solutes

STOMP includes solutes that can partition into the gas, liquid, or solid phases. It also calculates the amount of air dissolved in the liquid phase and water vapor in the gas phase. In

STOMP, all components within an element are at thermodynamic equilibrium, so there are no kinetics of evaporation or partitioning. Solutes are assumed to be passive tracers. They do not affect the physical properties of the gas or liquid phases, and when they volatilize, they do not contribute any new volume. Solutes instantaneously partition between gas and liquid phases according to a partition coefficient that relates their gas and liquid phase concentrations. Hence the gas phase in an element is always saturated with the solute in the sense that the concentration in the gas is in equilibrium with that currently in the liquid. Note that this assumption would be in error if there were significant mass transfer limitations due to slow diffusion in the liquid.

STOMP handles solute transport by first solving mass and energy balances on the gas and liquid phases, then calculating the resulting convective and diffusive fluxes of solutes in those phases. (Note that solutes in trapped gas phases do not participate in either type of flux.)

In this study, the gas bubbles released during salt-well pumping were modeled as air bubbles containing passive tracer gases. The drawback to this approach is that when a water-soluble gas such as ammonia partitions into the gas phase, there is no increase in gas volume. The model may therefore underpredict the gas saturation somewhat, which would result in small underestimates of gas release rates. This effect would be more important when the gas content of the tank is near the percolation threshold. However, it becomes negligible when the concentration of insoluble gases (e.g., hydrogen or air) in bubbles or drained pores is much higher than that of soluble gas, which is generally the case in salt well pumping. This issue was discussed in Peurrung et al. (1996, Appendix A), which included an estimate of the effect of the assumption on the model's gas release predictions.

## 2.3 Modeling the Tanks

Modeling the tanks requires specification of geometry, discretization scheme, pumping duration, physical properties and constitutive relations, and initial and boundary conditions. Typically the one-dimensional (1-D) simulations discretize a 1-m (3-ft) column packed with beads into 160 nodes, while the tank simulations discretize a 610-cm- (20-ft)-high waste into 40 elements vertically. Both cases assume azimuthal symmetry. For the 1-D modeling results, no radial variations are included. For the 2-D results, the domain has a diameter of 23 m (75 ft) with 10 radial elements. Simulations vary in duration from 10 days to thousands of years of (simulated) time, including pumping time and time for released gas to dissipate from the porous medium. While actual pumping activity will never extend beyond a few years, the simulations were allowed to continue to demonstrate the physical response of a tank.

The physical properties for the 1-D model results are based on the materials used in the laboratory experiments. These properties include the permeability of the bead pack, its saturation properties, the density and viscosity of water, and the diffusivities and solubilities of the insoluble gas ($SF_6$) and the soluble gas (isopropyl alcohol).

The permeability and saturation properties of the waste in the 2-D tank modeling correspond to those for a poorly graded sand (Metz 1976). The saturation function values have been revised somewhat from those used in previous work (Peurrung et al. 1996). The fluid viscosity and density are 24 cP and 1.4 g/cm$^3$, respectively, as measured for Tank A-101 liquid

waste. Two solute gases are included, one representing hydrogen and one representing ammonia. The partition coefficient for the ammonia is specified to be $5\times10^{-3}$ (moles of solute/$m^3$ of gas)/(moles of solute/$m^3$ of aqueous phase). This partition coefficient corresponds to a Henry's Law constant of six moles of ammonia/kg water/atm ammonia measured for simulants (Norton and Pederson 1994). Other values of physical properties and their sources are listed in Table 2.1.

The initial condition for all simulations is static with the liquid level at the top of the porous medium. Trapped gas is distributed uniformly throughout the waste; gas and aqueous pressures are equilibrated at all positions.

No flux boundary conditions are imposed on the sides of the column or tank. Gas phase and solute phase fluxes are permitted through the top surface, but no gas flux is allowed through the bottom surface. A constant gas-phase pressure is specified on the top surface. Accumulation of solute gas in the space above the upper surface is neglected, so a zero solute gas concentration is imposed there. For the 1-D model, the liquid level was lowered at a constant rate by enforcing a pressure boundary condition on the bottom surface that decreased linearly in time until the end of draining.

For the 2-D simulations, a hydraulic gradient boundary condition is imposed at the salt-well screen (i.e., the inner radial surface). Such a boundary condition creates a linear pressure gradient in the vertical direction in both the liquid and gas phases, resulting in an equilibrated saturation profile above the saturated liquid level. To simulate pumping, the base liquid- and gas-phase pressures are decreased linearly in time and then held constant at a head corresponding to a small amount of liquid left in the bottom of the tank. The rate at which the pressure is reduced (and hence the liquid level is lowered) is controlled so that the apparent pumping rate does not exceed 5 gpm, the operational limit in the field (WHC 1996).

**Table 2.1.** Typical Values of Physical Parameters Used in the STOMP Simulations[a]

| Parameter | Typical Values | | Units | Source/Basis |
|---|---|---|---|---|
| | 1-D (beads) | 2-D (waste) | | |
| *Dimensions* | 3 ft high x 1 in. diameter | 20 ft high x 75 ft diameter | | 2D: typical of tanks remaining to be salt-well pumped |
| Porosity of solid phase | 0.4 - 0.5 (used lab value) | 0.5 | unitless | Typical of porous solids without large heterogeneities |
| Hydraulic conductivity | 30 m/hr | 22 darcy (base case) | | 2D: Handy 1975, Metz 1976 |
| van Genuchten alpha parameter | Drainage/ Imbibition: 1-mm beads: 22/33 0.2-mm beads: 4.4/6.6 | 2/3 (base case) | 1/m | 1D: fit observations of drainable liquid 2D: Corresponds to poorly graded sand, has holdup height about 1 ft (Simmons) steepness fits intuition for this permeability and observations of drainable porosity |
| van Genuchten n parameter | 8 | 4 | unitless | |
| Residual liquid saturation | 0.08 | 0.10 | unitless | Typical of beads and soils, respectively |
| Maximum entrapped air saturation (void fraction) | 0.18 (0.072) | 0.20 (0.10) | unitless | 1D: based on observations 2D: higher based on RGS measurements (Shekarriz et al. 1997) |
| Gas phase diffusivity | $SF_6$: 0.397 IPA[b]: 0.440 | hydrogen: 0.75; ammonia: 0.25 | $cm^2/s$ | |
| Initial gas-phase concentration | used lab values | hydrogen: 80% ammonia: 0.044% inert gas: 20% (equates to 100 SCM each for $H_2$, $NH_3$) | | 2D: Typical total gas inventory of 100 SCM (Shekarriz et al. 1997) |
| Initial liquid-phase concentration | used lab values | hydrogen: ~ 0 ammonia: $3.9\times10^{-3}$ | mol/liter | Fixed by initial gas-phase concentration and gas-aqueous partition coefficient |
| Liquid phase diffusivity | $1\times10^{-5}$ | $0.04\times10^{-5}$ | $cm^2/s$ | Typical of aqueous diffusion at the corresponding liquid viscosity |
| Gas-aqueous partition coefficient | $SF_6$: $10^{10}$ IPA: $1.13\times10^{-3}$ | hydrogen: $10^{10}$ ammonia: $5\times10^{-3}$ | $m^3$ aq/$m^3$ gas | $SF_6$/hydrogen treated as essentially insoluble; ammonia value based on Norton and Pederson (1994) for tank waste |
| Initial trapped gas saturation (void fraction) | used lab value | 0.10 (0.05) | unitless | Typical of nonconvective layers (Shekarriz et al. 1997) |
| Air density | 1.20 | | $kg/m^3$ | Welty et al. (1984); T = 25°C of assumption |
| Liquid density | 999.3 | 1400 | $kg/m^3$ | Handy (1975) |
| Liquid viscosity | 1 | 24 | cP | 24 cP based on SA[c] |

(a) For input parameter definitions, see *STOMP User's Guide* (draft), MD White and M Oostrom, PNNL.
(b) Isopropyl alcohol
(c) WHC-SD-WM-SAD-036 Rev. 0, *A Safety Assessment for Salt-Well Jet Pumping Operations in Tank 241-A-101: Hanford Site, Richland, Washington* (1996). This viscosity value is cited in Appendix G as conservative.

# 3.0 Experimental Approach: Model Validation Using One-Dimensional Column Experiments

STOMP is a general porous media modeling tool that includes most of the relevant physics for salt-well pumping (except for increases in void fraction caused by volatilization of soluble gas). To confirm the validity of the model for salt-well pumping applications, it would be best to compare its predictions with actual in-tank measurements during pumping operations. However, neither the release rate data for tanks with substantial retained gas nor the physical characteristics of the waste are readily available. Moreover, pumping tends to occur in a start-stop manner that does not facilitate model validation. However, model validity can also be tested in the laboratory, where the operating conditions and materials can be kept simple and well understood.

To study the gas release phenomena typical of salt-well pumping, 1-D column experiments were designed to mimic salt-well pumping by draining liquid from a bead pack containing bubbles. The bubbles were spiked with an insoluble gas, sulfur hexafluoride ($SF_6$), and the liquid was a solution of isopropyl alcohol (IPA) in water. The amount of each gas released into the head space of the column was then measured. Several experiments were used to investigate the effects of parameters such as packing height, packing permeability, and soluble gas content. The reader is also referred to our previous report (Peurrung et al. 1996) for validation studies using only an insoluble gas. These experiments included studies of the effect of depressurizing the column to cause bubble coalescence.

## Experimental Method and Materials

Figure 3.1 is a schematic of the experimental apparatus, which, in most experiments, consisted of a 2.54-cm (1-in.)-diameter, 1.2-m (4-ft)-tall polycarbonate column filled to a height of 0.91 m (3 ft) with 1-mm glass beads to represent the permeable saltcake. Some experiments used a 0.41-m (16-in.) column filled to a height of 0.3 m (12 in.) with glass beads to investigate the effect of packing height. In addition, some experiments used 0.2-mm glass beads or a combination of 1- and 0.2-mm glass beads to investigate the effects of packing permeability and heterogeneity. The column was also filled with a known concentration of IPA in water to just above the glass beads, and any trapped air bubbles were released with gentle agitation, giving a fully liquid-saturated bead pack. IPA was chosen to represent the soluble gas, ammonia ($NH_3$), present in the actual waste tanks. IPA is non-toxic, much less flammable than ammonia, and is detected by the available analytical instrument with a greater degree of sensitivity. Its Henry's Law Constant is only about 10 times less than that of ammonia (i.e., $NH_3$ is 10 times more volatile than IPA). Most experiments used a 0.624-M IPA solution that has an equilibrium vapor concentration of 0.73% IPA, and so its release behavior should reflect that of highly soluble ammonia. Other experiments used lower (0.365%) and higher (2%) IPA equilibrium vapor concentrations to investigate the effect of varying soluble gas content. (Laboratory operations were limited to the 2% value due to flammability concerns.)

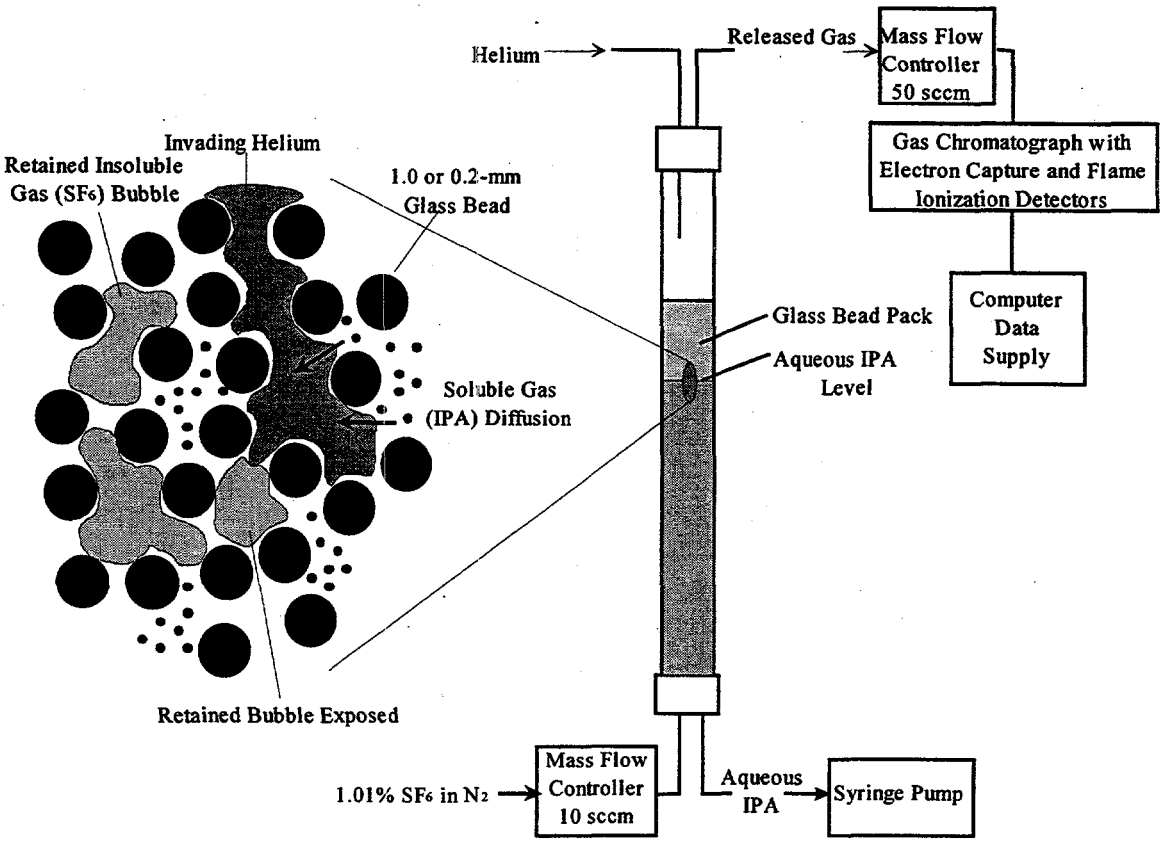


**Figure 3.1.** Schematic of Experimental Apparatus

Insoluble gas bubbles were introduced to the column by bubbling nitrogen containing a tracer gas, $SF_6$, at a concentration of 10,000 ppmv (1.01 mol%) through the bottom of the column. $SF_6$ was chosen to represent the hydrogen present in the actual waste tanks because it is insoluble, is detectable at very low concentrations by the available instrumentation, and raises no safety concerns in the laboratory. Because both $SF_6$ and $H_2$ are essentially insoluble, the release behavior of $SF_6$ should reflect that of hydrogen. The flow rate of the gas addition was controlled at 10 standard cubic centimeters per minute (sccm) with a Brooks Instrument Division 5850E flow controller. Gas addition was stopped just as bubbles could be seen flowing through the liquid above the bead pack so that minimal IPA was stripped from solution. A liquid-level indicator was used to measure the liquid volume increase as a result of the gas addition and hence the volume of retained gas bubbles in the bead pack. The volume added varied from 1 to 5% of the bead pack volume. This measured initial amount of gas was used in subsequent mass balance calculations to determine how much of the retained $SF_6$ was released during the experiments.

After gas bubbles were introduced into the bead pack, the column was pressurized to $2.4 \times 10^5$ Pa (20 psig) to compress the gas bubbles. A continuous purge stream of helium swept the head space of the column and passed to a Hewlett Packard 5890 gas chromatograph (GC) with an electron capture detector (ECD) calibrated for $SF_6$ and a flame ionization detector (FID)

calibrated for IPA. The IPA solution was drained from the bottom of the column until the liquid was level with the bead pack so that minimal IPA was stripped from solution during the head-space purge. Once the head space of the column was purged of any trace $SF_6$ (indicated by a negligible measurement on the ECD), most of the remaining IPA solution was drained from the bead pack via the bottom of the column to simulate salt-well pumping. The liquid drain rate was controlled and kept constant during all experiments using an ISCO model 500D syringe pump. Typical drain time was about 5.5 hours. A residual amount of IPA solution (about 10–25 mL) was purposely left in the bottom of the column so that no trapped gas bubbles escaped. In addition, some residual IPA solution is held in the drained glass beads by capillary forces. The amount of IPA in the residual solution was assumed to be the initial amount of IPA present and was used in mass balance calculations to determine how much of the retained IPA was released during the experiments.

The continuous purge stream of helium through the column head space carried any released $SF_6$ bubbles and IPA vapor to the GC, which was set up to automatically inject a sample every 10 to 20 minutes and measure the concentration of $SF_6$ and IPA in the sample. The continuous purge stream was controlled at 50 sccm with a second Brooks Instrument Division 5850E flow controller so that the measured concentration of $SF_6$ on the ECD and IPA on the FID was directly proportional to the $SF_6$ bubble and IPA vapor release rates. Draining experiments typically concluded when the measured amount of $SF_6$ was negligible (less than 1 ppbv) indicating that the majority of the $SF_6$ had been released. The IPA vapor release rates were longer than the $SF_6$ release rates, and typically only about 5–25% of the IPA was released during the experiment.

# 4.0 Results

The discussion of results is divided into two sections. In the first, the model predictions and the data from the column experiments are presented. The discussion is focused on the agreement between experiments and model. This section also illustrates some of the key physical phenomena as well as qualitative results and trends. In the second section, the full 2-D solution is applied to simulate salt-well pumping, using physical properties more like those of tank waste, hydrogen, and ammonia. The focus of the 2-D results is on providing a "best estimate" of the amount of hydrogen and ammonia that will be released during salt-well pumping. In addition, this section also evaluates parametric sensitivity by showing how the gas release predictions change when some of the key physical properties are varied.

## 4.1 Column Experiment Results and Model Predictions

As described in Section 3, all of the experiments involved draining columns packed with glass beads. The primary parameters that were varied in the experiments were the initial IPA concentration (equilibrium vapor concentration of 0.365, 0.73, or 2%), the height of the packing (3 or 1 ft), and the size of the beads (1- or 0.2-mm diameter). Other parameters such as the initial gas saturation or porosity differ somewhat from test to test simply due to experimental variability. The last two cases (subsections 4.1.5 and 4.1.6) show results for layered columns in which a thin layer of 0.2-mm beads is placed either in the middle or on top of a packing of 1-mm beads.

### 4.1.1 Three Feet of 1.0-mm Beads

For this experiment, the 1.2-m (4-ft) polycarbonate column was filled to a 0.91-m (3-ft) height with 1.0-mm glass beads. A 0.624-**M** solution of IPA in water (0.73% IPA equilibrium vapor concentration) was then added to the column to a level just above the bead pack. $SF_6$ gas was bubbled through the bottom of the column at ambient pressure, and the column was pressurized to $2.4 \times 10^5$ Pa (20 psig), resulting in an initial trapped gas saturation of 11% (4.1% void). The column head space was purged of $SF_6$. Then 191 mL of IPA solution was drained from the column at a constant rate of 0.51 mL/min for 5.5 hours until the water level fell to the bottom of the column, leaving approximately 25 mL of solution held up in the column by capillary forces. IPA and $SF_6$ fluxes emanating from the top of the column were measured for about 200 hours.

At the conclusion of the experiment, the calculated experimental mass balances gave 67% $SF_6$ removal and 6.6% IPA removal. However, 100% release of the $SF_6$ can be expected under these conditions of nearly complete draining. There are several possible explanations for the difference of 33%. A small, but non-negligible fraction of the $SF_6$ (less than 4%) could have partitioned into the aqueous phase and exited the column with the drained liquid. A small amount of $SF_6$ may have been retained as trapped bubbles at the bottom of the column if draining was not entirely complete. If draining continued for too long, however, some gas may have been pulled out in bubbles through the liquid draining line. Some $SF_6$ may also have been trapped in fittings below the bead pack when $SF_6$ was bubbled into the column and subsequently expelled during draining. Finally, some $SF_6$ may have adsorbed to surfaces in the column (including beads and fittings).

Each of these mechanisms would affect only the mass balance on $SF_6$, our insoluble gas. However, we feel that none of these mechanisms could account for the roughly 9 mL of gas missing from the mass balance. Instead we suggest that the most likely source of the bulk of the losses is leaks in the system. Since these losses would affect measurements of both gases, the data reported for both $SF_6$ and IPA may be somewhat lower than expected. Since the cause of the losses has not been determined, however, we have refrained from normalizing the data to account for them and to improve the fit of the model to the data.

The experimental data and model predictions for the instantaneous gas fluxes are shown in Figure 4.1. The fit between the data and the model prediction for this case is excellent. The $SF_6$ flux in both cases shows an initial peak during draining (the first 5.5 hours, or the left-most part of the figure) as bubbles near the top of the column are released. Even though the falling liquid level draws a flow of gas into the column, the gas in the bubbles released initially can diffuse out of the column relatively quickly because the path for diffusion is short. However, the flux decreases somewhat toward the end of draining as the diffusion path becomes longer and released gas diffuses against the counterflow less effectively. Once draining stops at 5.5 hours, however, there is a rebound in the $SF_6$ flux because the counterflow ceases. A long tail follows this peak as released gas slowly dissipates from the column.

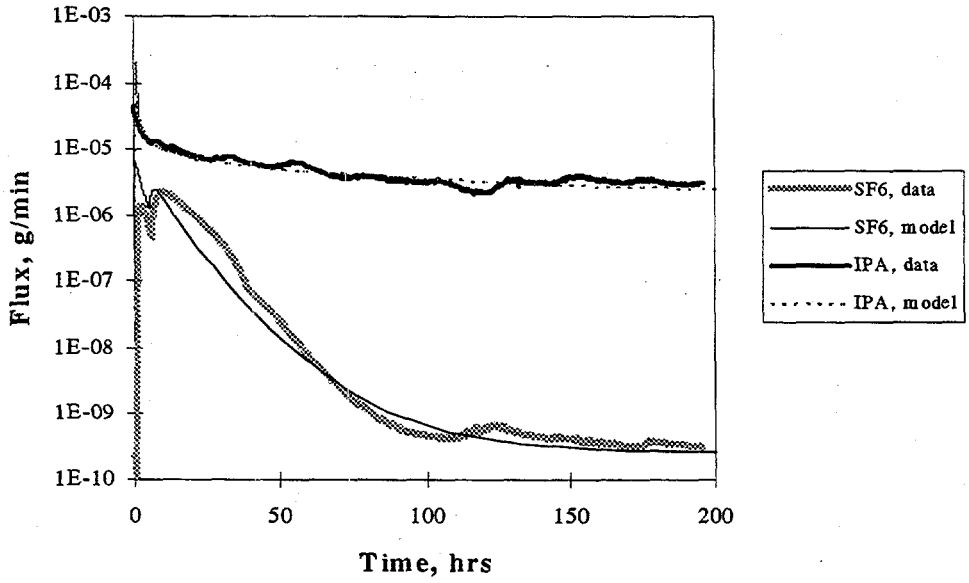


**Figure 4.1.** Experimental and Predicted Gas Release, 3-ft Column of 1.0-mm Beads

IPA, the soluble gas, displays a different flux behavior. The beads, once drained, still retain a significant amount of liquid held by capillary forces between the beads. This liquid has a large inventory of dissolved gas that can quickly volatilize into the invading air in adjacent large pores. Therefore, as soon as drained beads are exposed to the invading air, a large IPA flux is seen. The first IPA to volatilize is that at the very top of the column, and depletion is slow because of the large inventory of dissolved gas. The diffusive flux is therefore large and unimpeded by the invading air because the path length for diffusion is very short. Thus no significant dip in the peak is seen at the end of draining. The IPA flux is far more prolonged than the $SF_6$ flux, because while draining exposes and releases the $SF_6$ immediately, volatilization of the IPA in the residual moisture continues long after draining ends.

Figure 4.2 shows the cumulative fluxes for the two gases. Ultimately, for a well-drained column such as this in which all the bubbles were exposed, one would expect 100% release of the $SF_6$. As discussed above, the data shows a cumulative $SF_6$ release of only 67%, which we attribute primarily to leaks. The results show that the released $SF_6$ has essentially completely dissipated after about 50 hours.

For the IPA, the expected total release would be approximately equal to the initial concentration of IPA in the liquid times the amount of residual liquid held in the column. With 25 mL of 0.624-**M** IPA solution remaining (at a molecular weight of 60 g/mol), the ultimate cumulative flux would be about 0.9 grams (corresponding to 100% on Figure 4.2). However, the model shows that it would take roughly 50,000 hours (140 days) to completely dissipate the IPA. As Figure 4.2 shows, the data do not predict as large a cumulative IPA flux as the model after 200 hours; the data show 6.6% release, while the model shows 16%. Even if the flux values were normalized by a factor of 1/0.67 to account for potential leaks, the cumulative IPA release would be only 9% – still less than that predicted by the model.

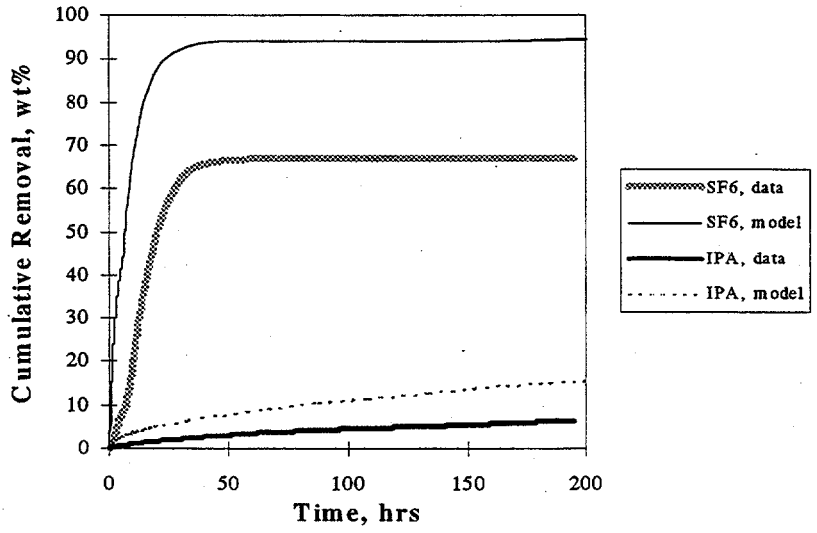


**Figure 4.2.** Experimental and Predicted Cumulative Release, 3-ft Column of 1.0-mm Beads

### 4.1.2 Effect of Varying Initial IPA Concentration

Volatilization of dissolved gas can create new bubbles or expand existing ones, increasing the potential pathways for gas release. However, because STOMP handles the retained gases as infinitely dilute solutes in a fixed number of moles of trapped gas (see Section 2), it does not account for new bubble volume generated by volatilization. The assumption that the retained gases occupy no volume is a reasonably good one when they are dilute, but the assumption must be questioned as their concentrations increase, particularly that of the soluble gas. Different initial IPA concentrations were therefore used in the next two tests to assess their effect on gas release rates and the agreement between model and data.

In the first of two tests with higher IPA concentrations, a 1.71-**M** solution of IPA in water was added to the 1.2-m (4-ft) column to just above the 0.91-m (3-ft)-tall bead pack. This more concentrated IPA solution resulted in a higher equilibrium vapor concentration of 2% (compared with the 0.73% IPA used in other experiments). The initial trapped gas saturation for this test was 8.8% (3.5% void). The IPA solution was drained from the bottom of the column at 0.44 mL/min for 5.5 hours, leaving approximately 22 of the initial 168 mL of solution. IPA and $SF_6$ fluxes were measured for 140 hours. At the conclusion of the experiment, the calculated experimental mass balances gave 32% $SF_6$ removal and 7% IPA removal.

The second test used a reduced concentration of IPA, a 0.31-**M** solution water. This less-concentrated IPA solution resulted in a lower equilibrium vapor concentration of 0.365%. The initial trapped gas saturation for this test was 7.1% (2.7% void). The IPA solution was drained at 0.42 mL/min for 5.5 hours, leaving approximately 26 of the initial 165 mL of solution in the column. IPA and $SF_6$ fluxes were measured for 165 hours. At the conclusion of the experiment, the calculated experimental mass balances gave 67% $SF_6$ removal and 4.6% IPA removal.

In addition, data from a test conducted last year by Peurrung et al. (1996) are included in this discussion to show the case in which the initial IPA concentration was zero. Experimental conditions (packing length and bead diameter) were the same for all the tests; the only difference other than small variations in initial void fraction was the initial IPA concentration.

The experimental data for these tests are presented in Figures 4.3 through 4.6 along with model predictions. The model simply predicts in Figure 4.3 that the flux of IPA is proportional to the initial IPA concentration, and the data show flux ratios that are in reasonably good agreement with the concentration ratios.

Because the cumulative flux is plotted as a weight percent, the model predictions for each case in Figures 4.4 are exactly the same, and the data should also collapse to the same curve under the assumption of infinite dilution. While the IPA cumulative flux data are similar, they fall considerably below the model prediction. The IPA removal amounts for each of the tests after approximately 140 hours were 7% for the 2% IPA case, 5.4% for the 0.73% IPA case, and 4% for the 0.365% IPA case. The model prediction at 140 hours is 11% IPA removal. A trend is present between the three model cases, but the failure of the assumption of infinite dilution would tend to increase the IPA release rate beyond that predicted by the model. Looking more closely at the instantaneous fluxes in Figure 4.3, the model predicts a very high initial flux that

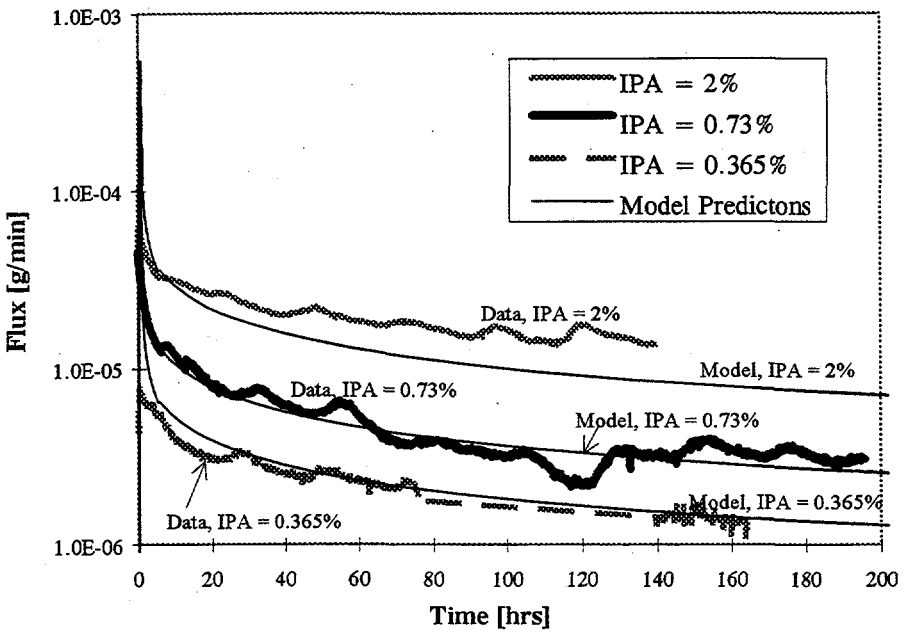


**Figure 4.3.** IPA Flux Data for Tests with Varying Initial IPA Concentration

does not seem to be reproduced in the data and that causes a substantial offset between the predicted and actual cumulative release early in the experiment. This early peak could be a numerical artifact of the model, or its absence could represent some depletion of the IPA near the surface of the packing.

Figure 4.5 shows that higher or lower initial IPA concentrations have no apparent effect on the $SF_6$ release rate. While there are small changes in the relative peak heights from case to case, the lack of a systematic trend suggests simple test-to-test variability. The STOMP model, based on the assumption of infinite dilution, predicts no change in the $SF_6$ flux. For completeness, data from a test conducted last year with the same operating conditions but no IPA is also presented. The similarity in behavior shows good qualitative agreement between experiments conducted from one year to the next.

Figure 4.6 shows cumulative $SF_6$ removal and illustrates the large variability in $SF_6$ recovery from experiment to experiment. The $SF_6$ mass balance was only 32% for the test with 2% IPA, while 122% was recovered in last year's test (0% IPA). A 68% loss is somewhat atypical. Of the nine homogenous bead pack tests conducted this year and the nine conducted last year, the average $SF_6$ mass percent removed was about 70% (i.e., 30% unaccountable losses). The large, unaccountable loss seen in the test with 2% IPA could be attributed to the accidental withdrawal of gas bubbles from the bottom of the column during draining. Because the IPA content of these gas bubbles is small, any bubbles lost in this manner would not contribute significantly to IPA losses. Thus, this explanation would be consistent with the relatively good agreement between the predicted and measured IPA flux.

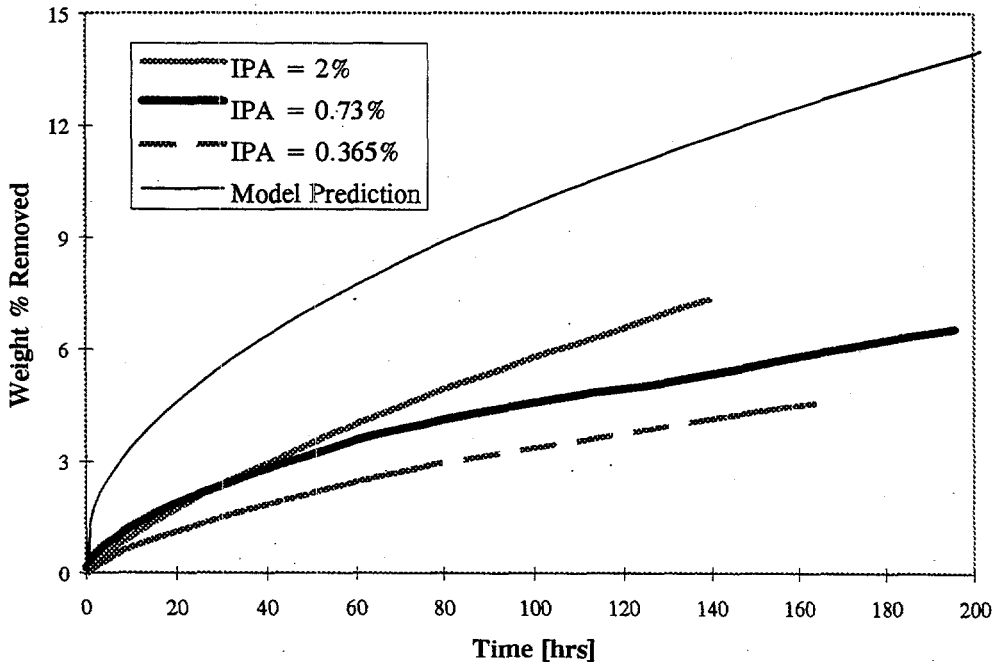


**Figure 4.4.** IPA Cumulative Removal Data with Varying Initial IPA Concentration

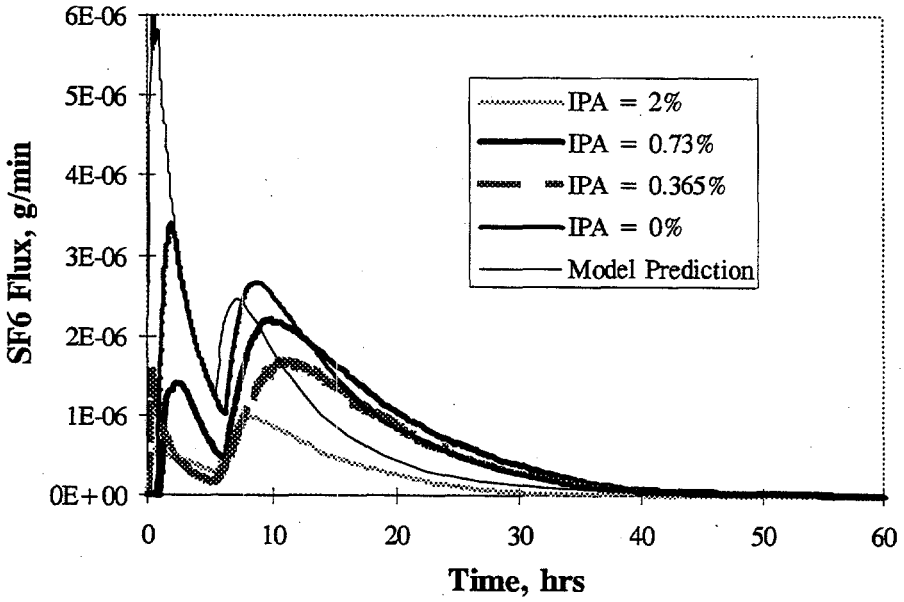


**Figure 4.5.** $SF_6$ Flux Data for Tests with Varying Initial IPA Concentration

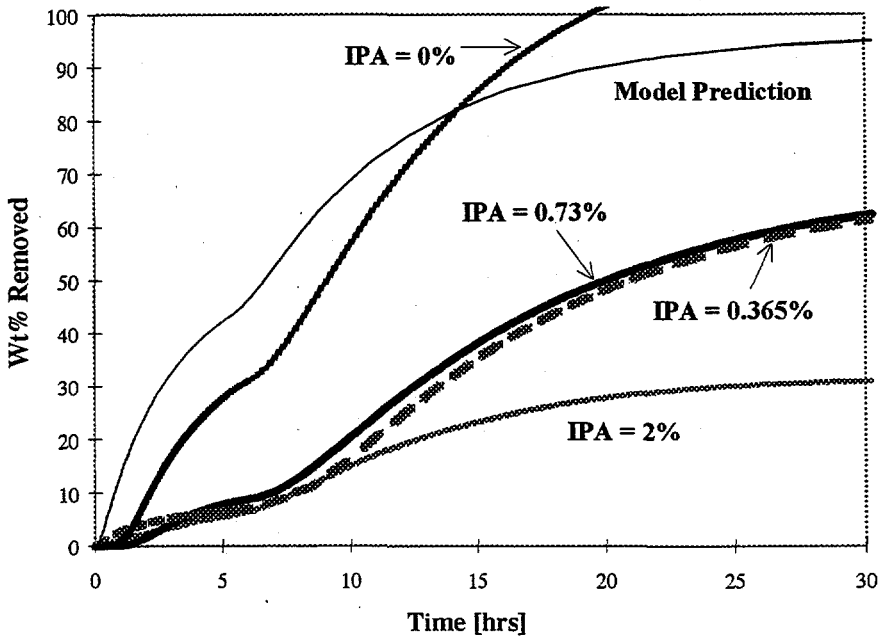


**Figure 4.6**. $SF_6$ Cumulative Removal Data for Tests with Varying Initial IPA Concentration

### 4.1.3 Three Feet of 0.2-mm Beads

In this test, the 1.2-m (4-ft) column was filled with 0.2-mm glass beads. Somewhat less gas was bubbled into the column, resulting in an initial trapped gas saturation of 3.9% (1.4% void). The 0.624-**M** IPA solution was drained at a constant rate of 0.42 mL/min for 5.4 hours, leaving approximately 37 mL of residual solution in the column. (The smaller beads exert higher capillary forces on the liquid, so more liquid remains at the end of draining.) Fluxes from the top of the column were measured for approximately 150 hours. At the conclusion of the test, the experimental mass balances gave 70% $SF_6$ removal and 5% IPA removal.

The flux data are shown in Figure 4.7. The results are qualitatively similar to those for the 1-mm beads, but the fit between the data and model is not as good for $SF_6$ release. The data show the $SF_6$ flux tailing off more rapidly than predicted by the model. As before, a large initial spike in the IPA flux is predicted but not seen in the experiment. Figure 4.8 shows the normalized cumulative fluxes. Both the experiment and the model show virtually no $SF_6$ released after 150 hours and 5% of the IPA released within that time. For this test, the cumulative IPA flux observed after 150 hours is almost exactly the same as that predicted.

Why does the model fit the $SF_6$ data for the 1.0-mm beads well but is not as accurate for the 0.2-mm beads? For the predictions of flux during draining, we suspect that the answer lies in how the model handles the tortuosity of partially drained beads. For our purposes, the primary difference in behavior between the 1.0- and the 0.2-mm beads is the height of the capillary fringe

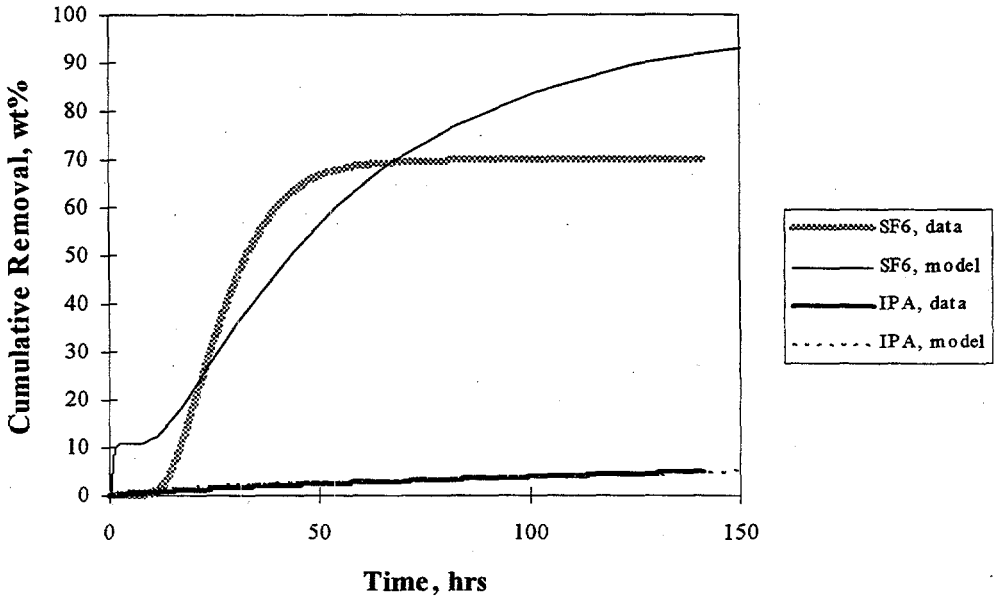


**Figure 4.7.** Experimental and Predicted Gas Release, 3-ft Column of 0.2-mm Beads

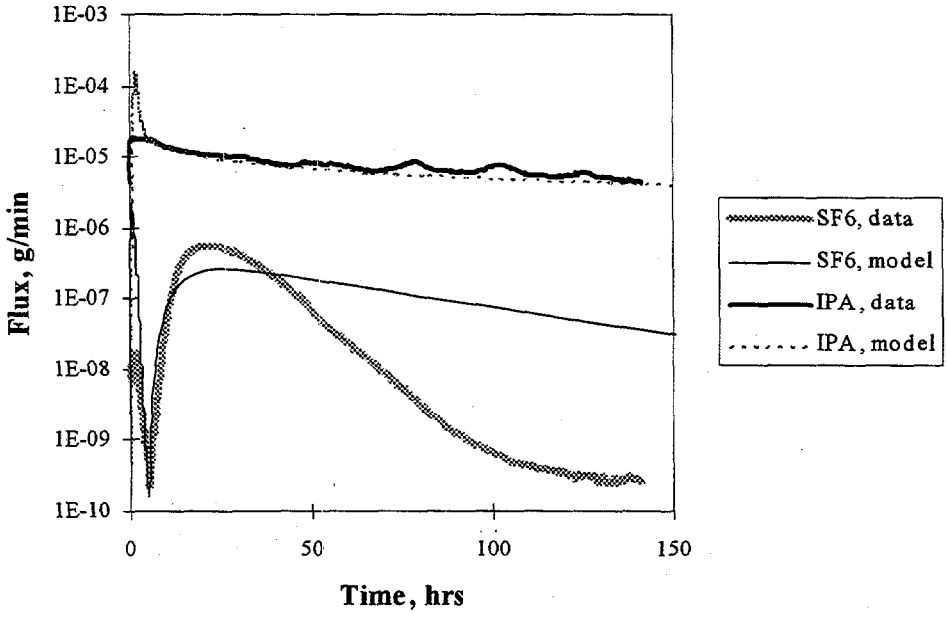


**Figure 4.8.** Experimental and Predicted Cumulative Release, 3-ft Column of 0.2-mm Beads

above the liquid level. The height of this fringe affects how rapidly the beads drain completely. That is, as the liquid level recedes in a packing of large beads, the beads go from being saturated to holding only residual liquid between them in a relatively short period of time. With small beads the capillary fringe is larger, so the draining process takes longer for a given region.

As currently implemented, the model assumes a constant pore tortuosity, a multiplier that accounts for the longer effective path length for diffusion through tortuous gas-filled pores. However, the tortuosity of a nearly saturated pore is generally higher than it is when fully drained, so the tortuosity ought to depend on gas saturation. STOMP includes a model based on the work of Millington and Quirk (1959) for calculating the tortuosity based on the local gas saturation. However, applying that particular model did not give completely satisfactory results, either. While it retarded both fluxes during draining and thus improved the predictions for early times, it tended to make the rates at which the fluxes tailed off even slower.

The long tail-off times (particularly for $SF_6$), may be due to another artifact in the model. While the model traps gas bubbles, solute gases are not effectively trapped because of the equilibrium assumption in the vapor-liquid partitioning. Once any free gas is present in a particular element in the model, the solute concentration in the free gas and the solute concentration in the trapped bubbles in that element are always the same. In effect, $SF_6$ in the trapped bubbles can instantaneously tunnel through the liquid phase to the free gas. This artificial phenomenon occurs because of the assumption of local equilibrium in the model.

We hope to address both of these problems with the model in future work. A new scheme has been developed for treating trapped phases and adding mass transfer limitations to STOMP for other applications. A better agreement between experiment and model may be possible by combining the new approach to trapping gas with the Millington and Quirk treatment of saturation-dependent tortuosity.

### 4.1.4 One Foot of 1.0-mm Beads

A shorter, 0.41-m (1.3-ft) column was used for the next two experiments to study the effect of changing the packing length. In the first of these tests, the column was filled to a height of 0.30 m (1 ft) with 1.0-mm glass beads. The initial trapped gas saturation was 10% (4.7% void). The IPA draining rate was 0.42 mL/min for 2 hours, leaving approximately 15 of the initial 65 mL of solution in the column. IPA and $SF_6$ fluxes were measured for 115 hours. At the conclusion of the experiment, the calculated experimental mass balances gave only 40% $SF_6$ removal and 11% IPA removal.

Figures 4.9 and 4.10 show the instantaneous and cumulative fluxes for this test. With the 1.0-mm beads, the qualitative agreement between data and model is again very good, though the poor recovery of both gases hurts the overall quantitative agreement. With the shorter packing height and hence the reduced path length for diffusion, both fluxes are initially larger and decay more rapidly after draining than for the 1-m (3-ft) packing. The cumulative amount of IPA released at the end of the test, 11%, would be raised to 28% if both sets of data were normalized to 100% $SF_6$ removal. The model predicts 35% IPA release.

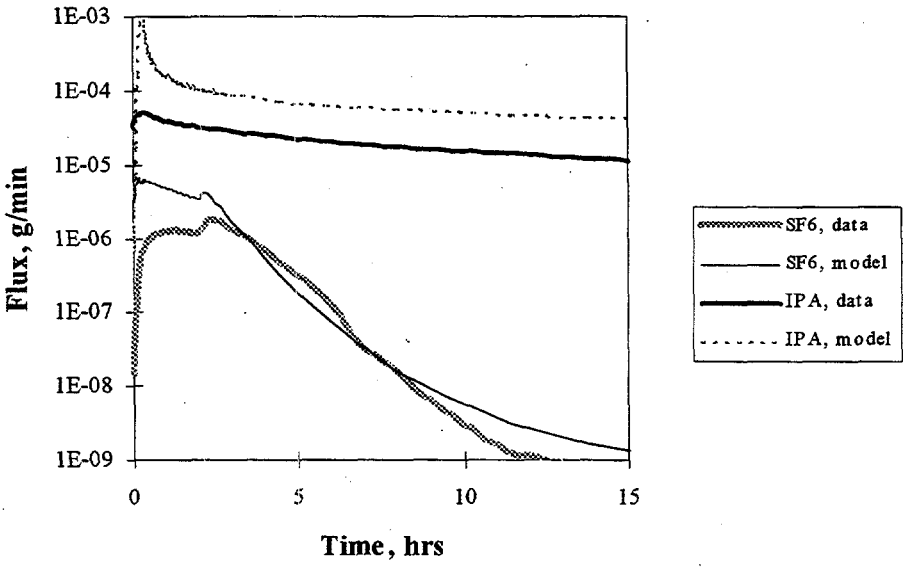


**Figure 4.9**. Experimental and Predicted Gas Release, 1-ft Column of 1.0-mm Beads

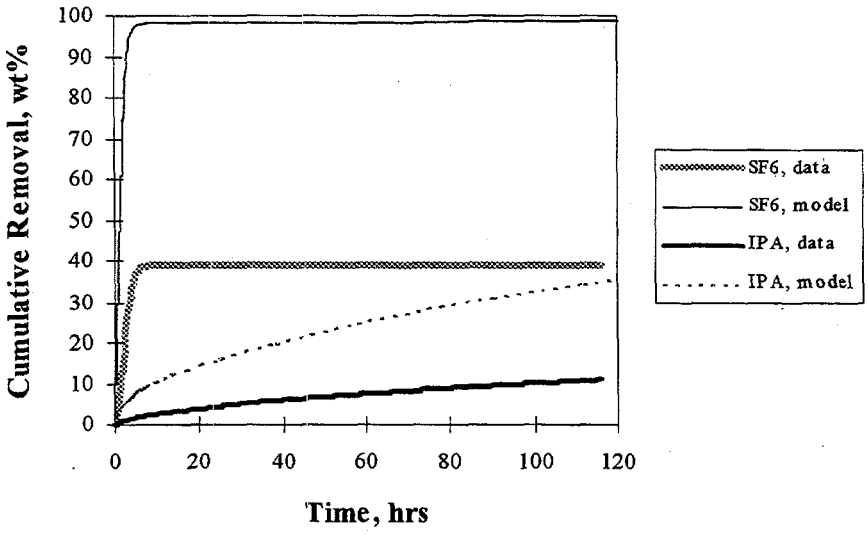


**Figure 4.10.** Experimental and Predicted Cumulative Release, 1-ft Column of 1.0-mm Beads

### 4.1.5 One Foot of 0.2-mm Beads

The second of the tests with the shorter column used 0.2-mm beads. The initial trapped gas saturation was 7.8% (3.2% void). The IPA solution was drained out the bottom of the column at 0.42 mL/min for 1.7 hours, leaving approximately 18 of the initial 60 mL. IPA and $SF_6$ fluxes were again measured for approximately 115 hours. At the conclusion of the experiment, the calculated experimental mass balances gave 55% $SF_6$ removal and 15% IPA removal.

Figures 4.11 and 4.12 show the resulting instantaneous and cumulative fluxes. The agreement between data and model prediction is fairly reasonable. Despite an apparent 45% loss of the $SF_6$, the cumulative amount of IPA released after 115 hours (15%) is nearly twice the 8% predicted.

### 4.1.6 Middle Layer of 0.2-mm Beads

The next two experiments explored the effect of heterogeneity in the medium by adding a horizontal layer of 0.2-mm beads to packings of 1.0-mm beads. Both tests used the 1.2-m (4-ft) column to give an overall packing height of about 1 m (3 ft). In the first, the layer was placed in the middle of the packing. To form the layered packing, 0.66 m (2.2 ft) of 1.0-mm beads were added followed by 3.8 cm (1.5 in) of 0.2-mm beads and 0.30 m (1 ft) of 1.0-mm beads. The

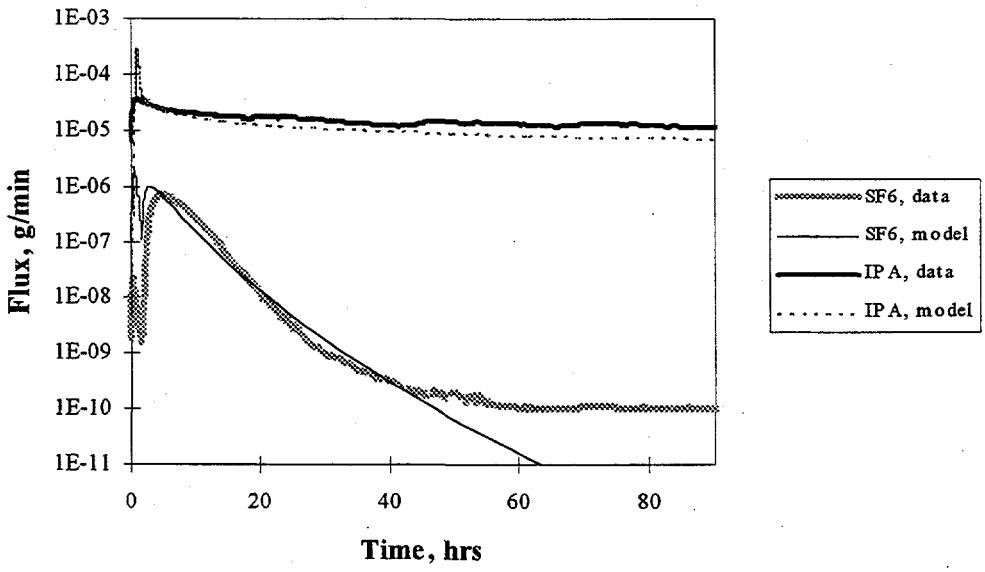


**Figure 4.11.** Experimental and Predicted Gas Release, 1-ft Column of 0.2-mm Beads

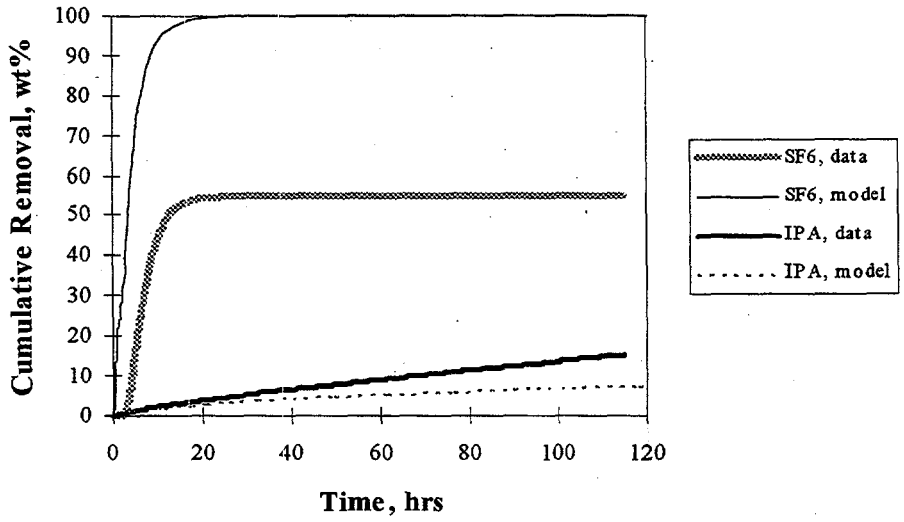


**Figure 4.12.** Experimental and Predicted Cumulative Release, 1-ft Column of 0.2-mm Beads

initial trapped gas saturation was 13% (5% void). (When modeled, the distribution of gas among the three layers was specified as 13/1/13% because the gas is expected to lodge mainly in the larger pores of the large beads.) IPA solution was drained out the bottom of the column at 0.42 mL/min for 5.6 hours, leaving about 30 of the initial 215 mL of solution in the column. IPA and $SF_6$ fluxes were measured for 300 hours. At the conclusion of the experiment, the calculated experimental mass balances gave 63% $SF_6$ removal and 10% IPA removal. For this test and the next, the $SF_6$ was still being released at a significant rate at the end of the experiment. Therefore, 100% removal will not be assumed within that time.

Figures 4.13 and 4.14 show the resulting instantaneous and cumulative fluxes. We expected the layer of small beads to provide a region of low gas permeability in terms of both absolute and relative permeability since the small beads retain more liquid after draining. The layer should therefore retard the fluxes of gases from the lower half of the column. Both the data and the model show this behavior, which is easiest to see in the $SF_6$ flux. Instead of an immediate and rapid exponential decay after draining, a prolonged release is seen. In the data, this tail shows an interesting oscillatory behavior with a telltale period of about 24 hours. We attribute this daily expulsion of gas to 5–10°C daily temperature swings in the laboratory. As the room heats up in the afternoon, bubbles coalesce below the layer of small beads and release some gas. This gas then dissipates overnight.

Aside from this daily variation in the flux data, the overall agreement between the data and model is again very good. Both $SF_6$ flux curves exhibit an initial peak, a minimum at the end of draining, a slowly developing secondary peak, and a long decay tail. The IPA curves show the same sort of behavior as in the other tests. Because the IPA flux is largely controlled by the material near the top of the column (at least for the first hundreds of hours), little difference is seen when a layer is added in the middle.

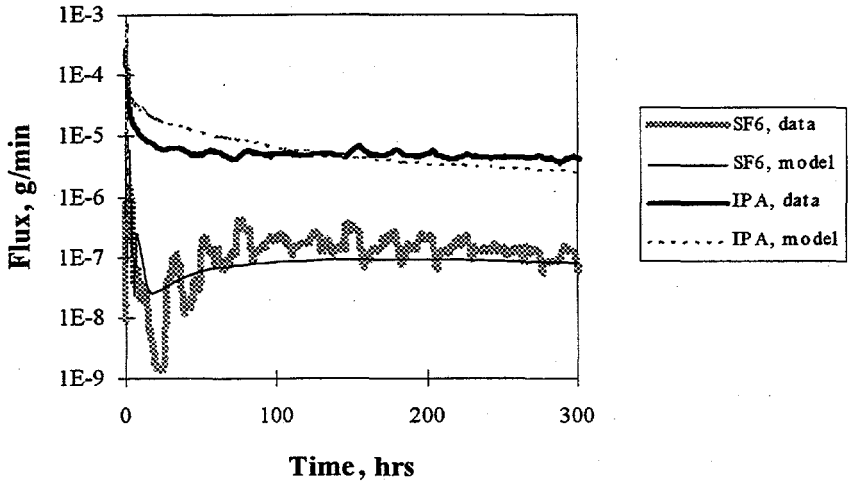


**Figure 4.13.** Experimental and Predicted Gas Release, 3-ft Column of 1.0-mm Beads with a Middle Layer of 0.2-mm Beads

The observed and predicted cumulative fluxes were both 63% for $SF_6$ (somewhat fortuitously, as you can see from Figure 4.14) and 10 and 13%, respectively, for IPA.

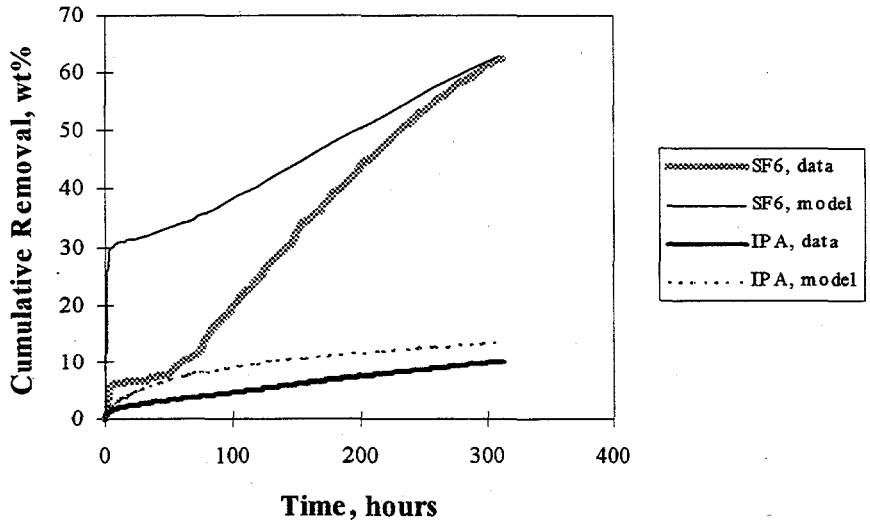


**Figure 4.14.** Experimental and Predicted Cumulative Release, 3-ft Column of 1.0-mm Beads with a Middle Layer of 0.2-mm Beads

### 4.1.7 Top Layer of 0.2-mm Beads

In the second experiment with layered beads, 3.3 cm (1.3 in) of 0.2-mm beads were placed on top of 0.91 m (3 ft) of 1.0-mm beads. Total bead height was thus 0.94 m (3.1 ft). The initial trapped gas saturation was 13% (4.9% void). The IPA solution was drained at 0.42 mL/min for 5.2 hours until approximately 24 of the initial 200 mL of solution remained in the column. IPA and $SF_6$ fluxes were measured for 240 hours. At the conclusion of the experiment, the calculated experimental mass balances gave 68% $SF_6$ removal and 25% IPA removal.

Figures 4.15 and 4.16 show the resulting instantaneous and cumulative fluxes. The effect of the layer of small beads on top is to reduce the flux of $SF_6$, especially during draining. Once drained, the flux does rebound to somewhat lower levels than without the layer (see Figure 4.1). Likewise, the IPA release rate is somewhat reduced. The predicted cumulative releases are 93% and 5% for $SF_6$ and IPA, respectively. As was seen in the data for the packing with the layer in the middle, some daily release of gas is seen.

### 4.1.8 Multiple Layers of Four Sizes of Ottawa Sand

A final experiment, using four different sieve fractions of sand, was conducted to explore the effect of complex heterogeneity in the medium. The purpose of this test was to determine whether the gas release behavior was significantly different for an extremely complicated packing using a distribution of particle sizes, including some smaller than the 0.2-mm beads used previously. While methods exist to model complex heterogeneities, we have not yet adapted these techniques to STOMP, and no attempt was made to model this experiment.

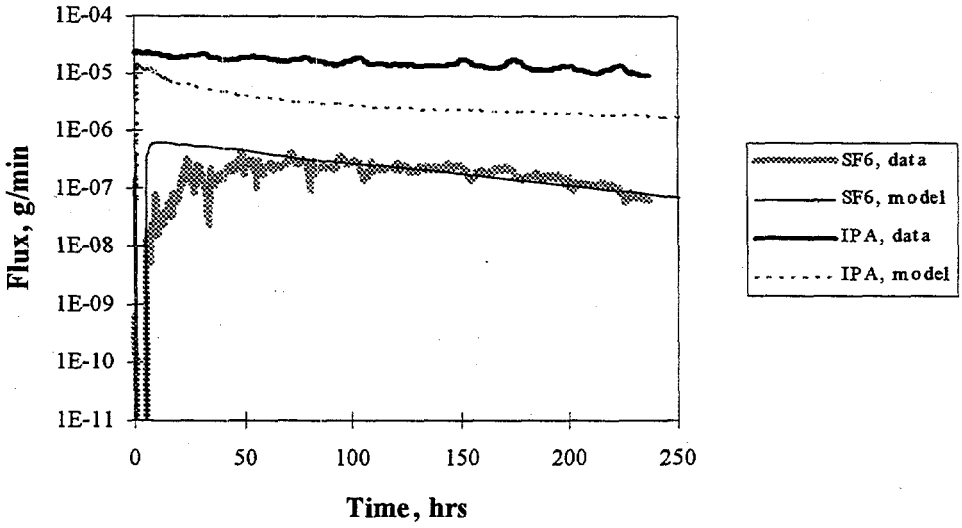


**Figure 4.15.** Experimental and Predicted Gas Release, 3-ft Column of 1.0-mm Beads with a Top Layer of 0.2-mm Beads

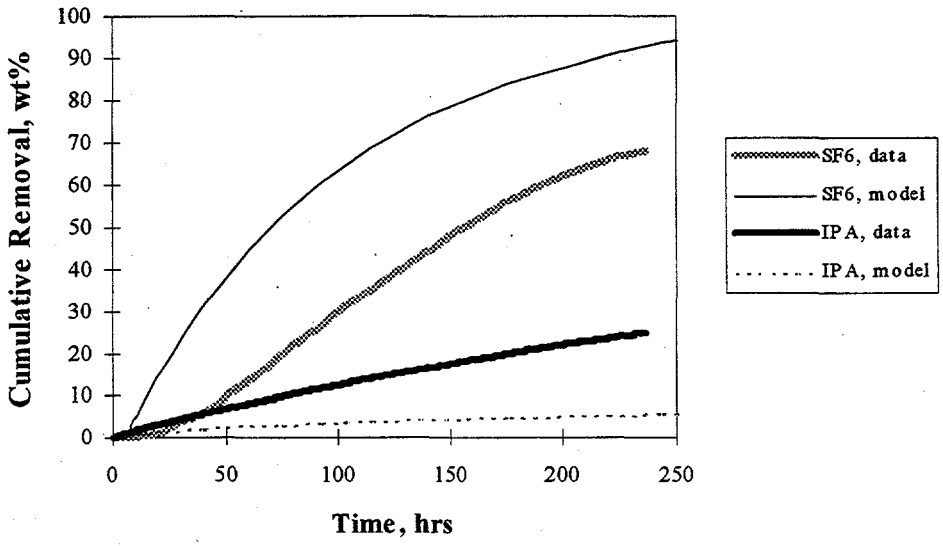


**Figure 4.16.** Experimental and Predicted Cumulative Release, 3-ft Column of 1.0-mm Beads with a Top Layer of 0.2-mm Beads

The 1.2-m (4-ft) column was filled with a mixture of 53-, 105-, 250-, and 420-micron-diameter Ottawa sand to give an overall packing height of about 1 m (3 ft). A complex layering pattern was achieved by slowly pouring the mixtures through the top of the water-filled column and allowing the sand to settle. Because the largest particles settled first, each pouring produced a layer stratified by size from largest to smallest. This procedure was repeated several times to give roughly thirty-six 2.54-cm (1-in) layers. The initial trapped gas saturation was 6.8% (2.1% void). Before draining the IPA solution from the column, the head space was purged for about 100 hours to monitor any IPA flux loss while the medium was still saturated. The IPA solution was then drained at 0.42 mL/min for 4.5 hours until approximately 12 of the initial 138 mL of solution remained in the column.

IPA and $SF_6$ fluxes were measured for approximately 600 hours (500 hours after draining). Figures 4.17 and 4.18 show the measured $SF_6$ and IPA fluxes and the cumulative amounts removed, respectively. While approximately 60% of the IPA was released during this time, no significant amount of $SF_6$ was released, indicating that it was still being retained even though the bubbles had been exposed. (The flux, while not significant compared with the amount present, was measurable. Only a few data points were below the detection limits of the instrument.) To validate this surprising result by confirming that $SF_6$ was still present in the packing, a small flow of nitrogen (0.5 sccm) was introduced at the bottom of the column. Shortly after the nitrogen flush began, the $SF_6$ flux rose, and approximately 20% of the estimated initial amount was removed. During this time (about 40 hours), the nitrogen stripped an additional 5% of the IPA from solution. The nitrogen flow was then increased to 10 sccm to try to release more of the $SF_6$. The fluxes were monitored for another 25 hours; however, no additional $SF_6$ was removed (though an additional 10% of the IPA was recovered).

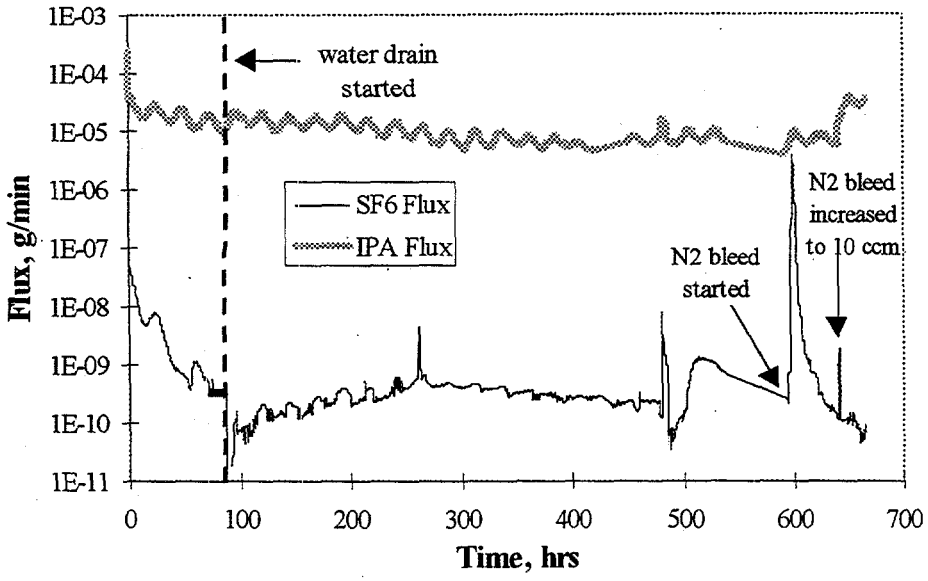


**Figure 4.17**. Experimental Fluxes from Three Feet of Complex Sand Layers

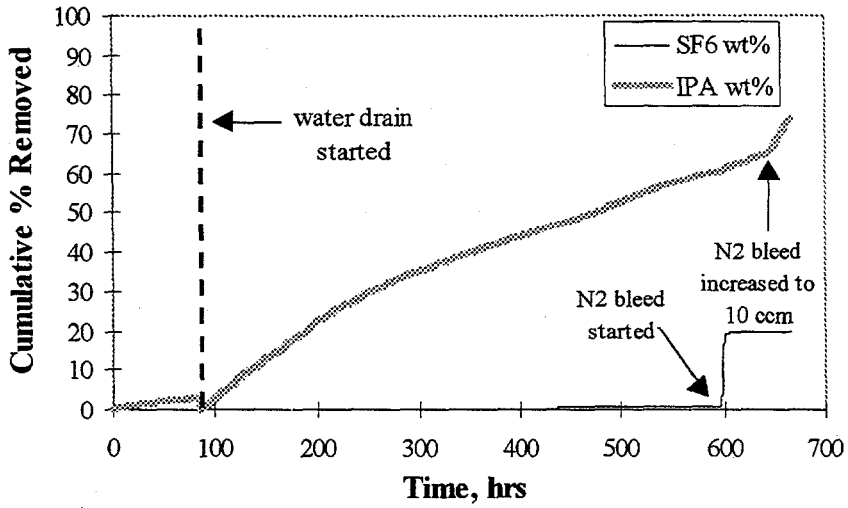


**Figure 4.18**. Cumulative Removals from Three Feet of Complex Sand Layers

Figure 4.17 shows the $SF_6$ concentration decaying exponentially during the 100-hour head-space purge, as expected. No additional $SF_6$ should be released until draining exposes the bubbles. A couple of small peaks appear, possibly from trapped gas released by temperature cycling. The IPA flux remained constant during the purge, with about 3% of the initial IPA present in the column removed during this stage. After the liquid was drained, virtually no $SF_6$ was released, whereas the IPA flux remained fairly constant (except for the daily increases resulting from temperature changes in the laboratory). The failure of the IPA to purge significantly and the absence of a large increase in its release at the beginning of draining are somewhat unexpected. However, for this particular experiment, the liquid level receded into the

packing somewhat while the test was being set up. The small amount of exposed, wet sand is probably responsible for these elevated fluxes.

That only 20% of the $SF_6$ was ever recovered could be attributed to losses during draining (i.e., bubbles accidentally withdrawn from the bottom of the column with the liquid) or from system leaks. Regardless of how much was removed, however, this experiment seems to indicate that insoluble gas release from highly heterogeneous media is very slow to negligible. The ability of such materials to retain gas should be explored more fully in future work.

## 4.2 Model Predictions for Gas Release During Salt-Well Pumping

The primary objective of the 2-D modeling is to predict gas release under conditions as close as possible to actual salt-well pumping. For this reason, we used as many of the physical properties of tank waste as are available (listed in Table 2.1 along with citations). However, the physical properties of the waste vary from tank to tank; moreover, many of the relevant parameters for these studies (e.g., the saturation function parameters) are not well known. Thus, a secondary objective of this work is to study the sensitivity of the gas release predictions to changes in the following key properties:

- permeability
- initial gas saturation (void fraction)
- waste thickness.

In addition, the simulations described below show the effect of including a layer of lower permeability material (as in the 1-D work) and the result of pumping and stopping before the waste is completely drained.

Two gases, nearly insoluble hydrogen and soluble ammonia, are included in the 2-D modeling to show how their behavior differs. For most of these simulations, a volume of 100 standard cubic meters (SCM) of each gas was selected as an initial gas content for the waste because recent retained gas sampling has shown it to be approximately the correct order of magnitude for Tanks AW-101, A-101, AN-103, AN-104, and AN-105 (Shekarriz et al. 1997). Another advantage of using a total initial gas inventory of 100 SCM is that the numerical value can also be interpreted as a volume percent.

At a void fraction of 5%, the resulting initial concentrations of hydrogen and ammonia in the retained gas are 80 and 0.044%, respectively. The balance of the void space is occupied by an inert gas. The initial liquid-phase concentration of ammonia in the waste is $3.9 \times 10^3$ moles/ liter.

The domain in the base-case simulation is a 23-m (75-ft)-diameter tank with a 6-m (20-ft)-thick saltcake layer. Another purpose of the 2-D modeling is to show radial variations in gas saturation during pumping. It is expected that the gas saturation will be higher near the central well and lower near the tank edges during draining, as depicted in Figure 1.1.

The boundary conditions for the 2-D model simulate an open space for the well at the center of the cylindrical domain. (Actual salt-well pumping will likely be from off-center risers,

but locating the well centrally simplifies modeling and interpretation.) The boundary conditions have been set so that the liquid level in the well is held constant at 15 cm (0.5 ft) above the bottom of the tank, in the manner it would be during pumping. Liquid is then allowed to seep into the well along its height by applying hydraulic gradients to both the liquid and gas phases.

This boundary condition does not allow the liquid removal rate to be controlled; it simply depends on the overall seepage rate, which, in turn, depends on the saltcake permeability, the liquid viscosity, and the pressure gradient. The draining rate can therefore be expected to decay as the liquid level slowly falls. Moreover, no fixed drainage time (such as 100 days) can be applied. In practice, however, the draining (pumping) rate will be limited to 19 L (5 gal) per minute. If the liquid level in the well is set initially to a few feet, too large a draining rate results (when using the waste physical properties below). For this reason, the liquid level in the well is lowered from the top of the saltcake to the 73-cm (2.4-ft) level over the first hours or days of the simulation, depending on the waste's permeability. As shown below, this gradual startup prevents the instantaneous draining rate from exceeding 19 L (5 gal)/min at any time.

For the base-case simulation, the initial gas saturation is 10%, corresponding to a void fraction of 5%, a rough average for the nonconvective layers of the five tanks characterized by the retained gas sampler (RGS) (Shekarriz et al. 1997). Finally, the chosen value of the equilibrium constant for the ammonia, $5 \times 10^{-3}$ (moles of solute/$m^3$ of gas)/moles of solute/$m^3$ of aqueous phase), is based on estimates for SY-101 simulants (Norton and Pederson 1994).

### 4.2.1 Base Case

Table 4.1 gives the key physical parameters in the base case, the one reflecting our best estimates of the properties of a typical saltcake tank. The interval for draining the salt well refers to the amount of time over which the liquid level in the salt well was lowered to prevent the maximum pumping rate from exceeding 5 gpm.

Figures 4.19, 4.20, and 4.21 show progressive gas saturation profiles after 50 and 200 days of pumping and the final profile. (The figures are not to scale but are oriented correctly, with the bottom of the tank at the lower edge of the graph. The salt well is located along the left side. The r-axis is highly compressed because, whereas the elements are shown as square, the node spacing in the radial dimension is much larger than that in the vertical dimension.) As seen in Figure 4.19, the saltcake near the well on the left is preferentially drained, with saturation profiles tapering gradually inward. Even after only 50 days of draining, gas saturations near the top of the saltcake approach 90% (45% void), the maximum value attainable at the specified residual liquid saturation of 10%.

**Table 4.1**. Key Physical Properties for the Base Case Simulation

| Parameter | Value |
|---|---|
| Waste thickness, m (ft) | 6.1 (20) |
| Initial gas saturation (void fraction) | 10% (5%) |
| Waste permeability, darcies | 22 |
| van Genuchten saturation function parameters[a] | $\alpha_i = 2.2$ 1/m; $\alpha_d = 3.3$ 1/m; n = 4 |
| Interval for draining salt well, days | 0.5 |

The simulation showed that the tank was essentially drained after about 430 days, defined as the point at which 90% of the pumpable liquid had been removed. For these parameters, the pumpable liquid was 250,000 gallons, or 84% of the original liquid content of 300,000 gallons. Figure 4.22 shows the flow of liquid into the salt well and the flow of invading air into of the top of the waste as a function of time. The flow rates in Figure 4.22 confirm that gradually lowering the liquid level in the well keeps the withdrawal rate below 19 L (5 gal)/min, while the drain rate falls to less than 0.2 L (0.05 gal)/min after about 400 days of continuous pumping. The inflow rate of invading air is somewhat less than the liquid outflow rate because bubble expansion fills some of the growing void volume.

The liquid that remains after draining is complete is trapped in the interstitial pore spaces of the saltcake. Gravity is not sufficient to pull this residual liquid out. The amount of this unpumpable liquid depends strongly on the consistency of the waste, specifically on the particle size distribution. In STOMP, both the permeability and the van Genuchten alpha and n parameters depend on the waste consistency.[b] Data for characterizing the saturation behavior of saltcake are limited, and the values of these parameters are uncertain. The values chosen for the

---

(a) The van Genuchten function (van Genuchten 1980) relates the capillary pressure to the liquid saturation through two correlation parameters, $\alpha$ and $n$, according to the equation:

$$s_l = \left[ 1 + \left( \alpha \left[ \frac{P_g - P_l}{\rho_l g} \right] \right)^n \right]^{\left(\frac{1}{n} - 1\right)}$$

where $s_l$ is the liquid saturation, $P_g$ is the gas-phase pressure, $P_l$ is the liquid-phase pressure, $\rho_l$ is the liquid density, and $g$ is the gravitational constant. Since this version of the model accounts for hysteresis in the saturation function, two values of $\alpha$ are used, $\alpha_i$ for imbibition and $\alpha_d$ for draining. The units of $\alpha$ are an inverse length. Qualitatively, the inverse of alpha is related to the entry pressure for a typical pore in a porous material. The n parameter is a measure of how narrow the particle size distribution is for the material, with larger values of n corresponding to more uniform particle size distributions.

(b) Ibid.

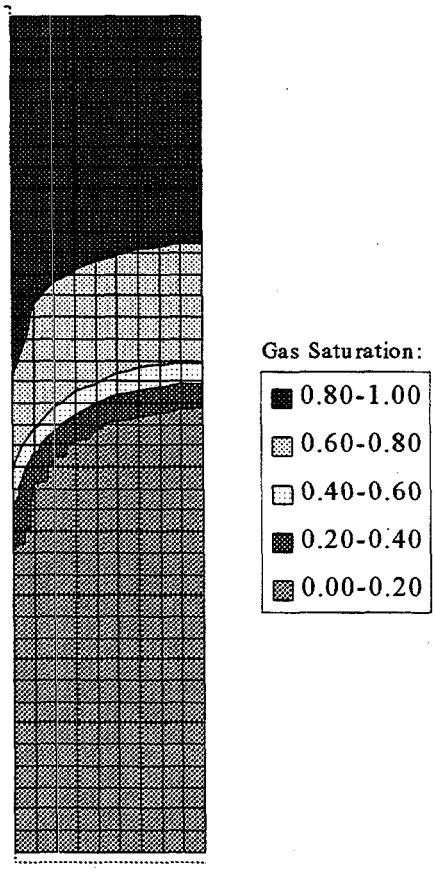


**Figure 4.19.** Gas Saturation Profile after 50 Days, Base Case (note compressed radial scale)

base case typify saltcake as a poorly graded sand (with a large particle size distribution).[a] Subsequent cases, discussed in Section 4.2.2, show the effect of varying the average particle size in the waste by changing the permeability and van Genuchten alpha parameters. Changing these parameters affects not only the amount of pumpable liquid but also the rate of liquid draining and hence the rate of gas release.

Figure 4.23 shows the release rate for both retained gases as a function of time in standard cubic meters per day. (To convert to standard cubic feet [SCF], multiply by 35; to convert to moles, multiply by 45.) The hydrogen flux is noisy at first due to the coarse discretization in the model. Figure 4.24 shows the cumulative gas release. While 99% of the hydrogen has diffused out of the saltcake within the first 500 days, the ammonia gas release

(a) This approach is similar, but not identical, to the approach of Simmons (1996) in his work on the moisture content of saltcake wastes. Simmons uses a Brooks and Corey model of capillarity rather than a van Genuchten model.

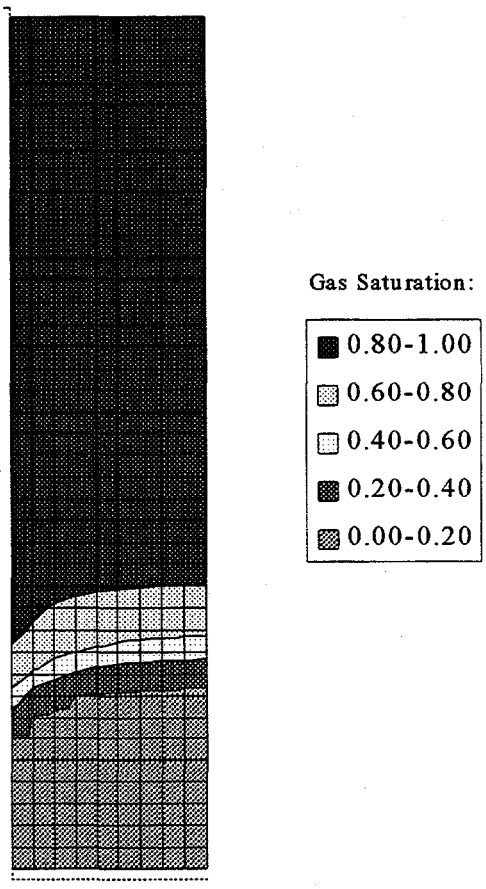


**Figure 4.20.** Gas Saturation Profile after 200 Days, Base Case (note compressed radial scale)

continues for several years. (While actual pumping activity will never extend beyond a few years, the simulations were allowed to continue both to demonstrate the physical response of the waste and to show that eventually all the gas is released.) Ultimately, all of the hydrogen and 22% of the ammonia initially present are released in volatile form through the upper surface of the saltcake. The remaining ammonia is removed in solution in the pumped liquid.

The maximum instantaneous release rate of hydrogen is on the order of 10 SCM/day, or 0.2 scfm. However, this rate decays within a few weeks to a more sustained rate of about 1 SCM/day (0.02 scfm). Likewise, the maximum rate of ammonia gas release is 0.6 SCM/day, which decays to about 0.1 SCM/day within weeks.

To assess whether these release rates could cause the dome space to exceed 25% of the lower flammability limit (LFL), further analysis is needed. Passive ventilation of tanks typically results in flow rates of about 1 to 5 $ft^3$/min (1400 to 7200 $ft^3$/day), while active ventilation raises the flow to 200 scfm. A crude dome space model would be to equate sustained gas releases from

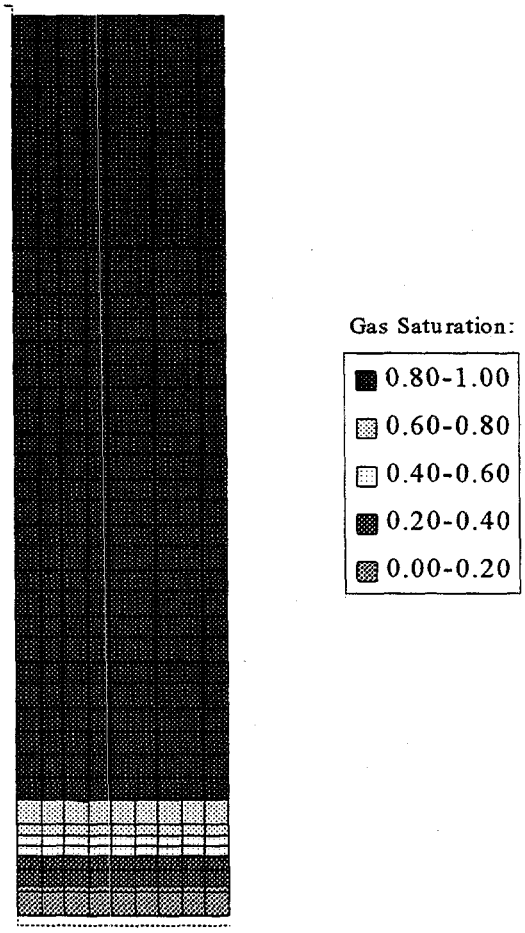


**Figure 4.21.** Final Gas Saturation Profile, Base Case (note compressed radial scale)

the waste into a completely mixed dome space with the gas removed by ventilation. Under base case conditions, the resulting dome space concentration would be about 0.02 scfm/1 scfm = 2% hydrogen for the case of passive ventilation and 0.02 scfm/200 scfm = 0.01% for active ventilation. Therefore, release of hydrogen early in draining could potentially cause the concentration in a passively vented tank to exceed 25% of the LFL, which is about 4% for hydrogen in air. Ammonia would also contribute to the overall concentration of flammable gases in the dome space, though its concentration would be low because of its much lower rate of release.

Active ventilation would reduce the flammable gas concentration below the level of concern, but it would probably be discontinued after pumping ceases. Flammable gas concentrations in the dome space would rise again but only to very low levels. According to the base-case simulation, both the hydrogen and ammonia release rates fall after a few years of pumping to 0.01 SCM/day (0.0002 scfm). The resulting steady-state concentration of each gas, assuming 1 scfm passive ventilation, would then be 0.02%. This value is well below the level of concern.

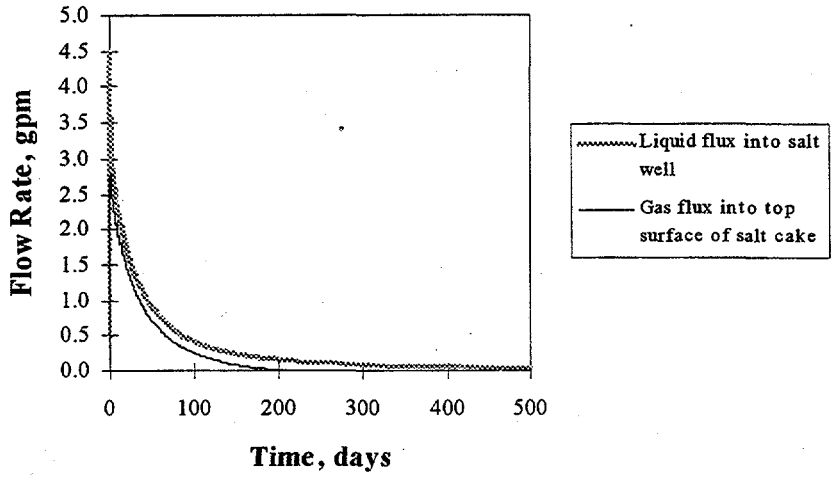


**Figure 4.22.** Liquid Removal Rate and Gas Influx into Surface of Saltcake, Base Case Conditions

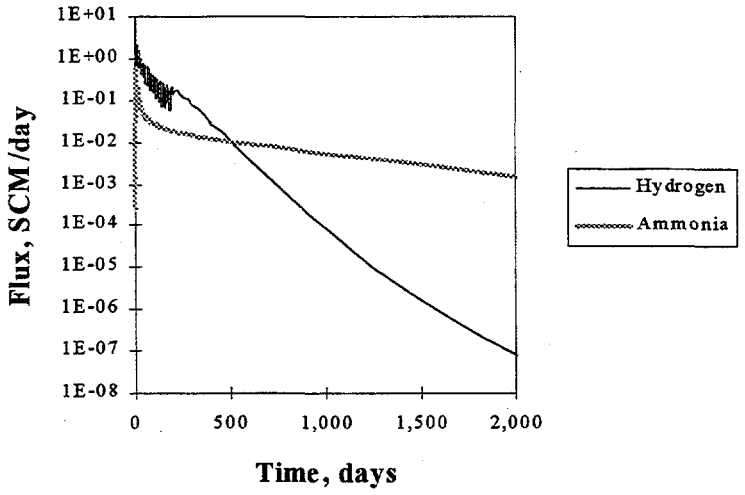


**Figure 4.23.** Hydrogen and Ammonia Gas Release Rates, Base Case Conditions

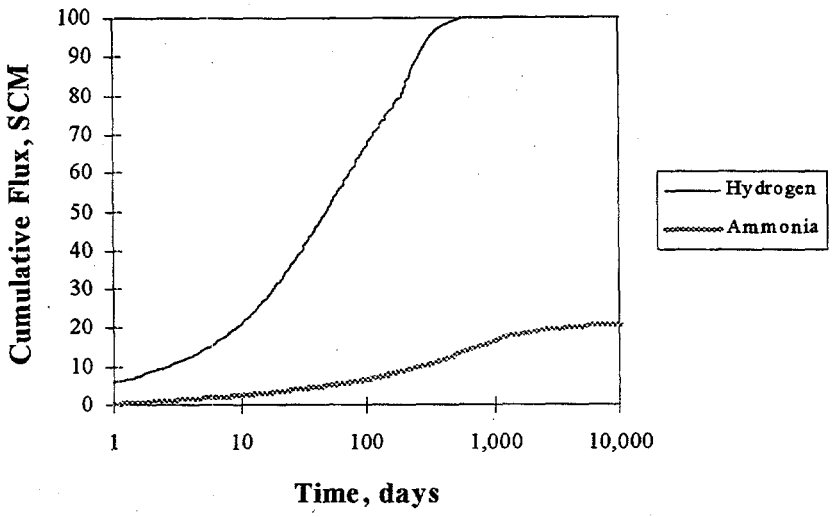


**Figure 4.24.** Cumulative Release of Hydrogen and Ammonia Gas, Base Case Conditions

Active ventilation during the first part of salt-well pumping appears to be sufficient (but probably necessary) to keep the flammable gas concentration in the dome space to a safe level. This dome space model is extremely simple; more detailed dome space calculations would likely be necessary to fully address this issue, which is beyond the scope of this work. The particular retained gas inventory of the tank should also be considered.

Figure 4.25 shows the cumulative release of each gas into the tank dome against the cumulative amount of liquid pumped from the waste. As might be expected, the relationship is approximately linear for hydrogen, indicating that drained waste releases trapped bubbles. The relationship for ammonia is less linear because of the prolonged release of dissolved gas after liquid removal is essentially complete.

### 4.2.2 Effect of Varying Permeability

The distribution of pore sizes and saltcake crystal sizes in the waste varies from tank to tank and is not well characterized. The average particle size in a porous material affects its permeability and saturation function (controlled in STOMP by the van Genuchten alpha parameters). Changing these parameters controls not only the amount of pumpable liquid but also the rate of liquid draining and hence the rate of gas release. For a porous material, the permeability is proportional to the square of the average particle size, while the alpha parameters vary linearly with the average particle size.

Table 4.2 gives the key physical parameters in the four cases with varying particle size, reflecting a range of possible values for saltcake waste. The waste thickness and initial gas saturation have the same values as the base case. The rate at which the waste drains by gravity

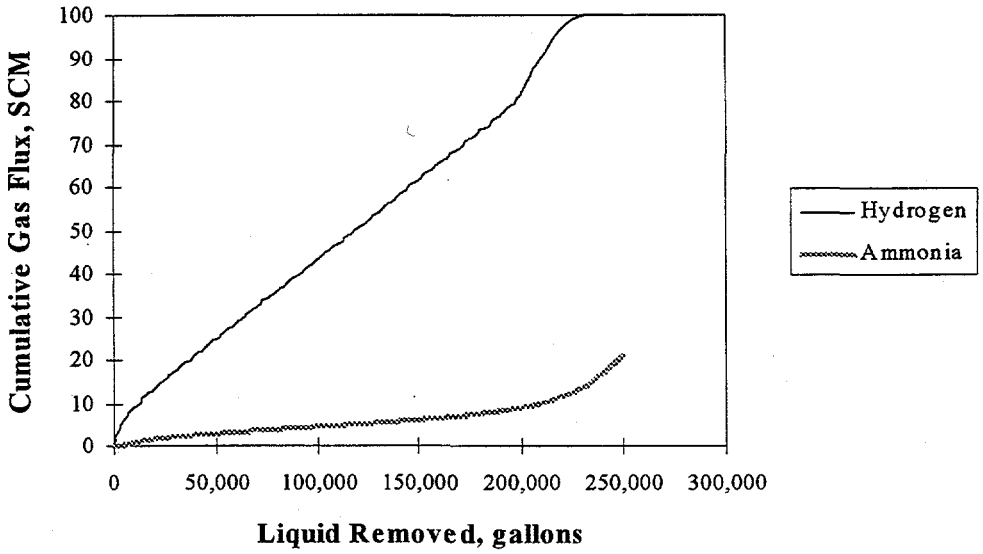


**Figure 4.25.** Cumulative Gas Release Versus Cumulative Amount of Liquid Removed, Base Case Conditions

depends strongly on its permeability. In the 220-darcy case, the liquid level must be lowered very slowly to keep the apparent pump rate below 5 gpm. The draining interval is kept constant for the other cases for simplicity.

Figures 4.26 through 4.29 show the final saturation profiles for these four cases. The smaller the particle size, the more liquid is ultimately retained by the waste.

Figures 4.30 and 4.31 compare the instantaneous hydrogen and ammonia gas fluxes for all five permeability cases, including the base case, and Figures 4.32 and 4.33 show the cumulative fluxes. The gas release rates show similar qualitative behaviors between cases, with the change in parameter values primarily scaling the time for the waste to drain and release its gas. Figure 4.32 shows that in all five cases, all of the hydrogen is eventually released. The difference in the cumulative ammonia gas release in Figure 4.33 is due to the difference in the amount of pumpable liquid. Since less ammonia is removed in the liquid phase for the low-permeability materials, more remains to volatilize into the dome space.

**Table 4.2.** Key Physical Properties for Simulations with Varying Particle Size

| | Case 1 | Case 3 | Case 4 | Case 5 |
|---|---|---|---|---|
| Waste permeability, darcies | 220 | 2.2 | 0.22 | 0.022 |
| van Genuchten saturation function parameters: $\alpha_i$, 1/m | 6.3 | 0.63 | 0.22 | 0.063 |
| $\alpha_d$, 1/m | 9.5 | 0.95 | 0.33 | 0.095 |
| n | 4 | 4 | 4 | 4 |
| Interval for draining salt well, days | 31.5 | 0.5 | 0.5 | 0.5 |

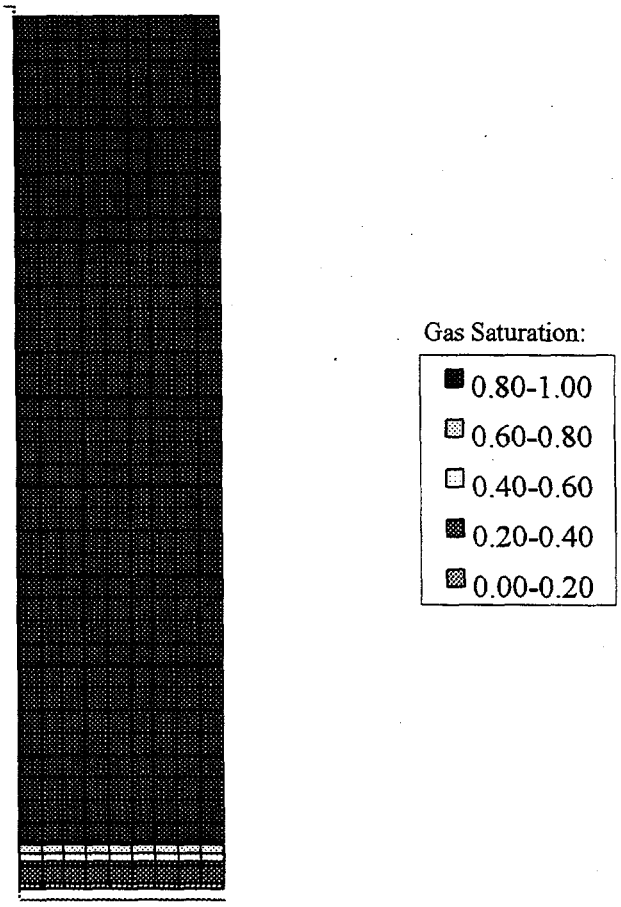


**Figure 4.26.** Final Gas Saturation Profile, 220-Darcy Waste

Figures 4.34 and 4.35 compare the results for cumulative gas release and cumulative drained liquid. The results of the five cases are similar; differences are primarily the total amount of drainable liquid. Table 4.3 compares some of the numerical values of the results for the five simulations with varying permeability.

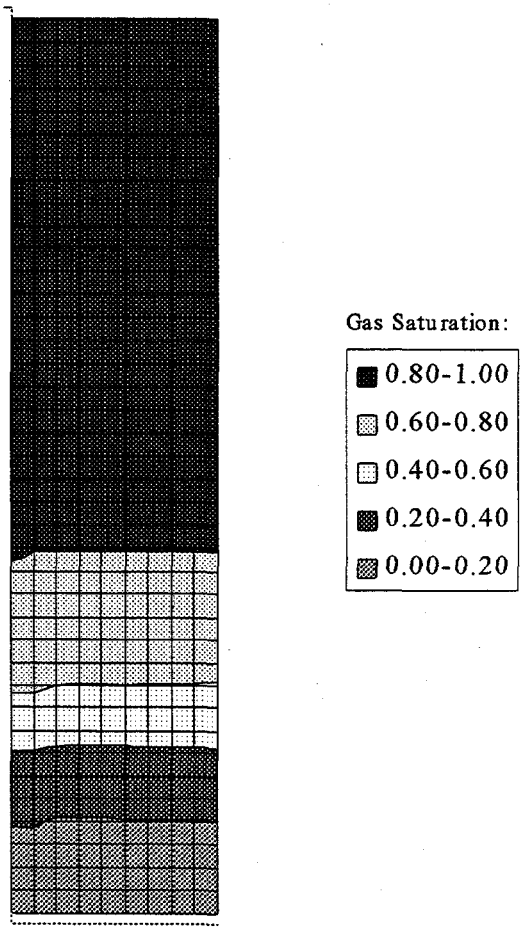


**Figure 4.27.** Final Gas Saturation Profile, 2.2-Darcy Waste

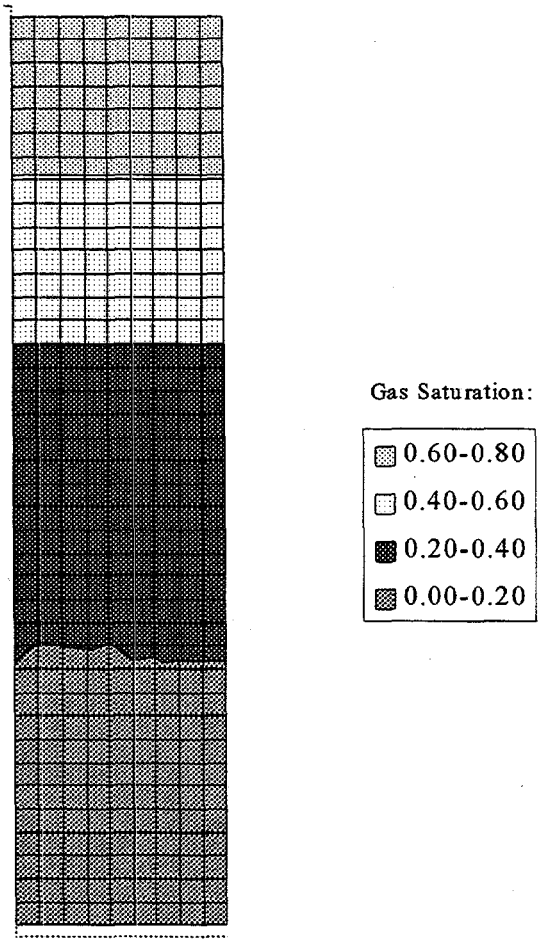


**Figure 4.28.** Final Gas Saturation Profile, 0.22-Darcy Waste

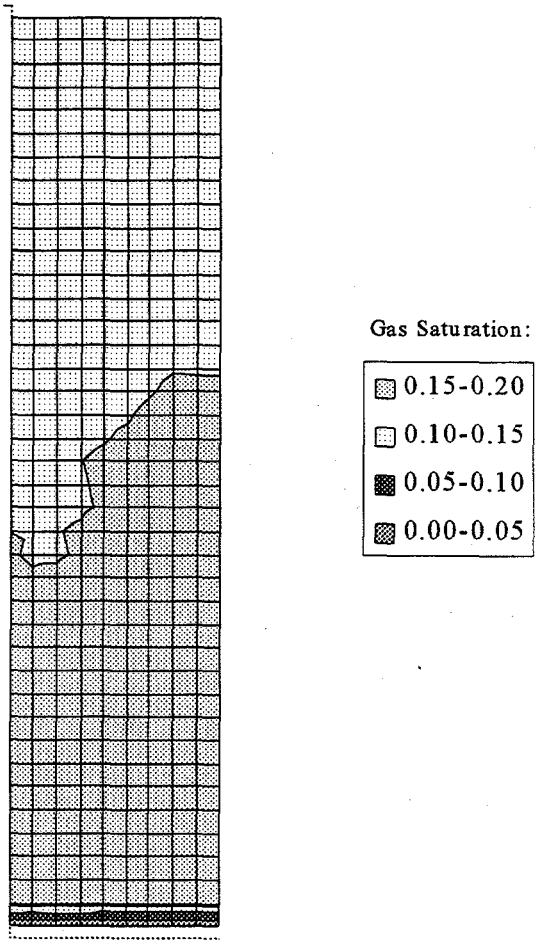


**Figure 4.29.** Final Gas Saturation Profile, 0.022-Darcy Waste

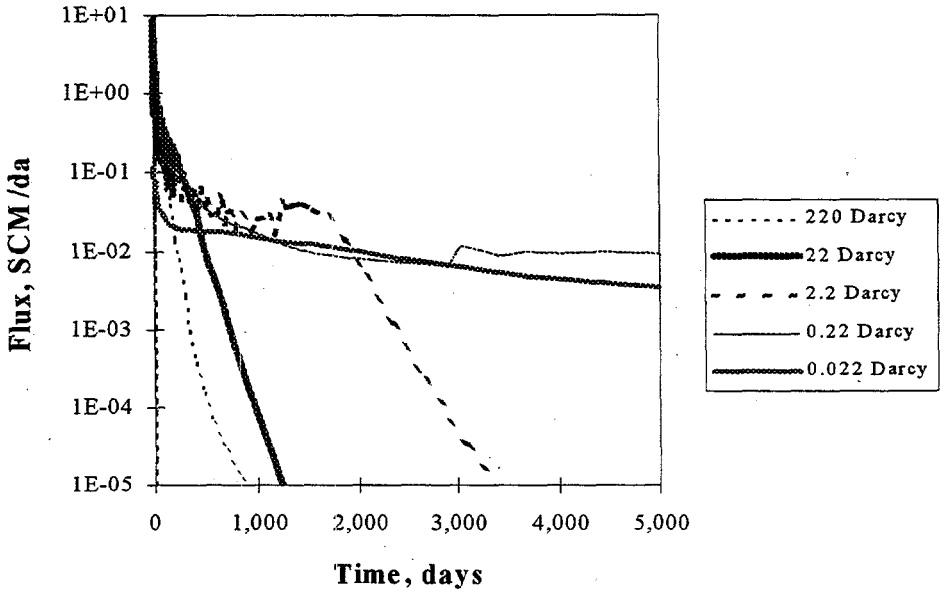


**Figure 4.30.** Comparison of Hydrogen Release Rates for Five Waste Permeability Cases

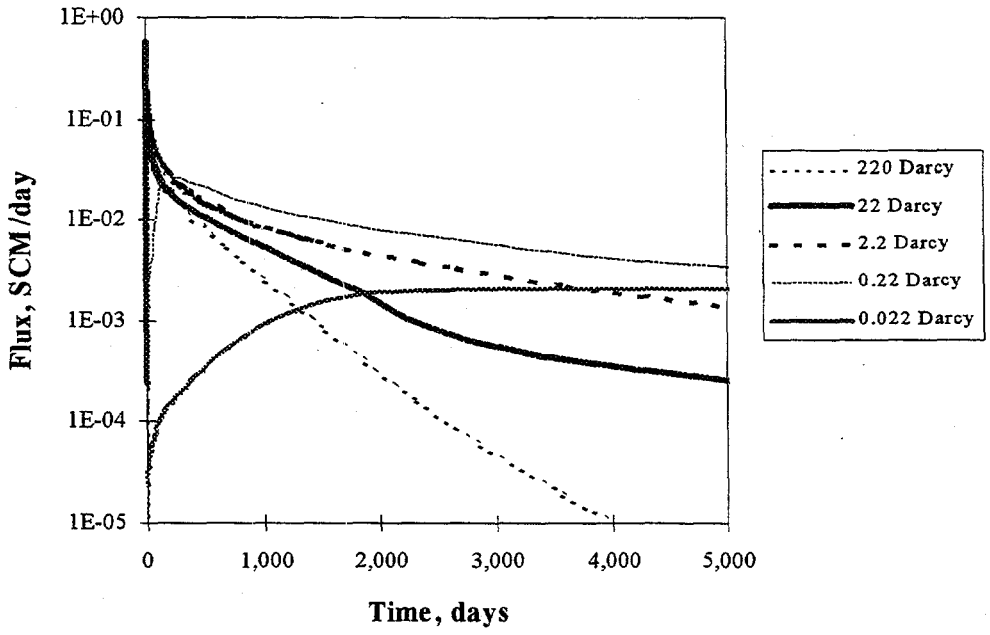


**Figure 4.31.** Comparison of Ammonia Gas Release Rates for Five Waste Permeability Cases

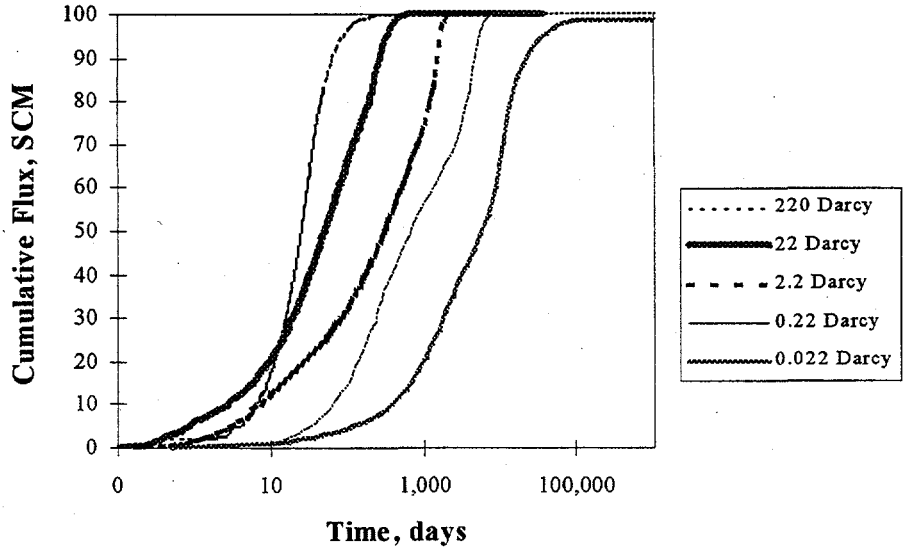


**Figure 4.32.** Comparison of Cumulative Hydrogen Release for Five Waste Permeability Cases

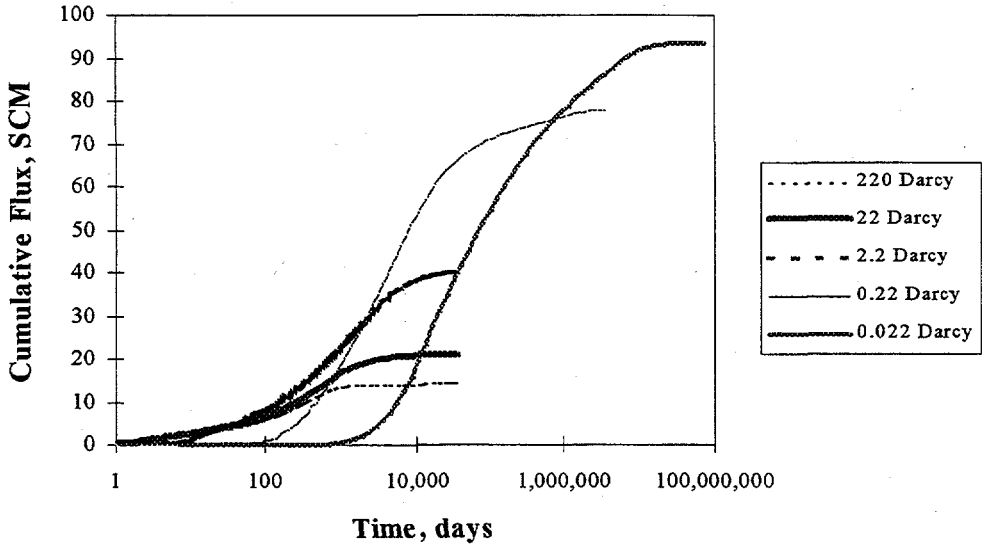


**Figure 4.33.** Comparison of Cumulative Ammonia Gas Release for Five Waste Permeability Cases

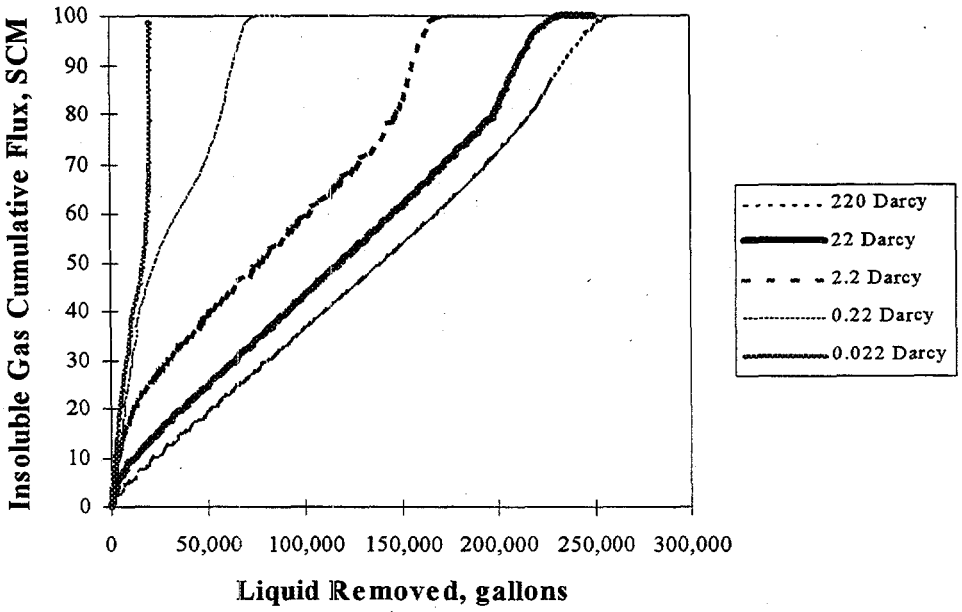


**Figure 4.34.** Cumulative Hydrogen Release Versus Cumulative Liquid Removed for Five Permeability Cases

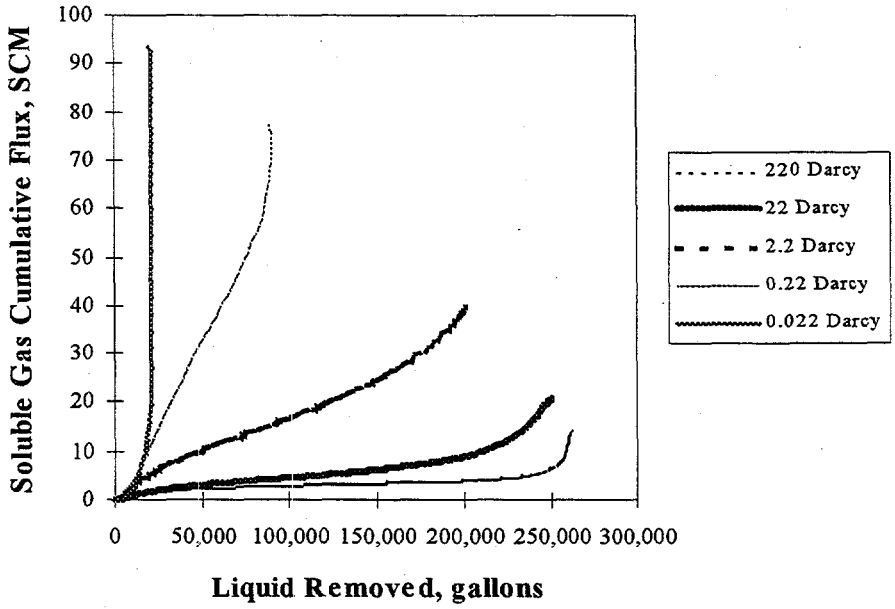


**Figure 4.35.** Cumulative Ammonia Gas Release Versus Cumulative Liquid Removed for Five Permeability Cases

**Table 4.3**. Numerical Results for Simulations with Varying Particle Sizes

| Case | Case 1 220 darcy | Case 2 22 darcy | Case 3 2.2 darcy | Case 4 0.22 darcy | Case 5 0.022 darcy |
|---|---|---|---|---|---|
| Apparent drain time, days[a] | 65 | 430 | 3100 | 11,000 | 8300 |
| % Liquid removed at 2 years | 87.4 | 79.1 | 41.0 | 8.5 | 1.3 |
| % Hydrogen removed at 2 years [b] | 100 | 100 | 67.2 | 51.7 | 15.3 |
| % Ammonia removed at 2 years [b] | 96.3 | 90.0 | 58.2 | 22.7 | 1.5 |
| % Ammonia removed in aqueous phase, 2 years | 84.0 | 75.1 | 38.5 | 7.8 | 1.3 |
| Total time of simulation, years | 100 | 100 | 100 | 10,000 | 200,000 |
| % Liquid removed ultimately | 88.2 | 84.1 | 67.8 | 30.2 | 6.6 |
| % Hydrogen removed ultimately [b] | 100 | 100 | 100 | 100 | 98.9 |
| % Ammonia removed ultimately [b] | 98.7 | 98.5 | 96.8 | 99.9 | 99.97 |
| % Ammonia removed in aqueous phase ultimately | 84.4 | 77.7 | 56.8 | 22.1 | 6.5 |
| Maximum drain rate, gpm | 4.89 | 4.48 | 0.58 | 0.068 | 0.0065 |
| Maximum hydrogen flux to dome, SCM/day | 11.1 | 12.0 | 1.8 | 0.17 | 0.12 |
| Maximum ammonia flux to dome, SCM/day | 0.60 | 0.58 | 0.19 | 0.028 | 0.0021 |

(a) Defined as 90% of pumpable liquid drained.
(b) Includes gas removed in pumped liquid and that volatilized into the dome space.

### 4.2.3 Simplified, Lumped-Parameter Model for Gas Release

Recently, there has been an effort by the Safety Controls Optimization by Performance Evaluation (SCOPE) panel to formulate a set of simple predictive models for estimating the flux of ammonia from tank waste under various scenarios. This set could be used as a tool for defining a safe operating envelope for tank farms. In response to the panel, we developed an equation as a simple, linear fit to our STOMP predictions that captured much of the relevant physics:

$$R_{NH_3} = \alpha (y_{eq} - y_{dome}) e^{-0.67 t / t_{1/2}},$$

where $R_{NH_3}$ is the flux of ammonia into the dome space in scfm, $\alpha$ is a global proportionality constant in scfm $NH_3$/mole fraction $NH_3$, $y_{eq}$ is the mole fraction of ammonia in the gas phase in equilibrium with the dissolved ammonia in the waste, $y_{dome}$ is the dome-space ammonia mole fraction, $t$ is time, and $t_{1/2}$ is a characteristic decay constant (in the form of a half-life) that depends on the physical properties of the waste. The dependence of the flux on the concentration driving force, $y_{eq} - y_{dome}$, is fairly intuitive, and this term accounts for the overall inventory of ammonia in the waste as well as suppression of volatilization by any significant concentration in the dome space. Taking $\alpha$ as a global constant (i.e., one that does not vary from tank to tank) has two implications. First, since the exponential term is unity at t = 0, the initial flux depends only on the ammonia content of the waste. Second, all tank-to-tank variations other than ammonia content can be rolled into the $t_{1/2}$ parameter.

Figure 4.36 shows fits of the ammonia flux data (for the four highest permeability values) from Figure 4.31 to the equation. The fits do not capture the initial rapid flux of ammonia STOMP predicts during the early part of draining, and they break down after several thousand days. However, they do capture well the linearity of the intermediate period (the latter part of draining and the first several years afterward). Moreover, forcing all the fits to intercept the y-axis at a single point seems to work reasonably well, allowing the use of a global $\alpha$. To find $\alpha$, the value of $y_{eq}$ in the simulations was $4.4 \times 10^{-4}$, and the dome space concentration, $y_{dome}$, was assumed to be zero. After converting from SCM/day to scfm, the value of $\alpha$ predicted by STOMP is 1.2 scfm/mole fraction. The values of $t_{1/2}$ for each of the four permeability values are given in Table 4.4.

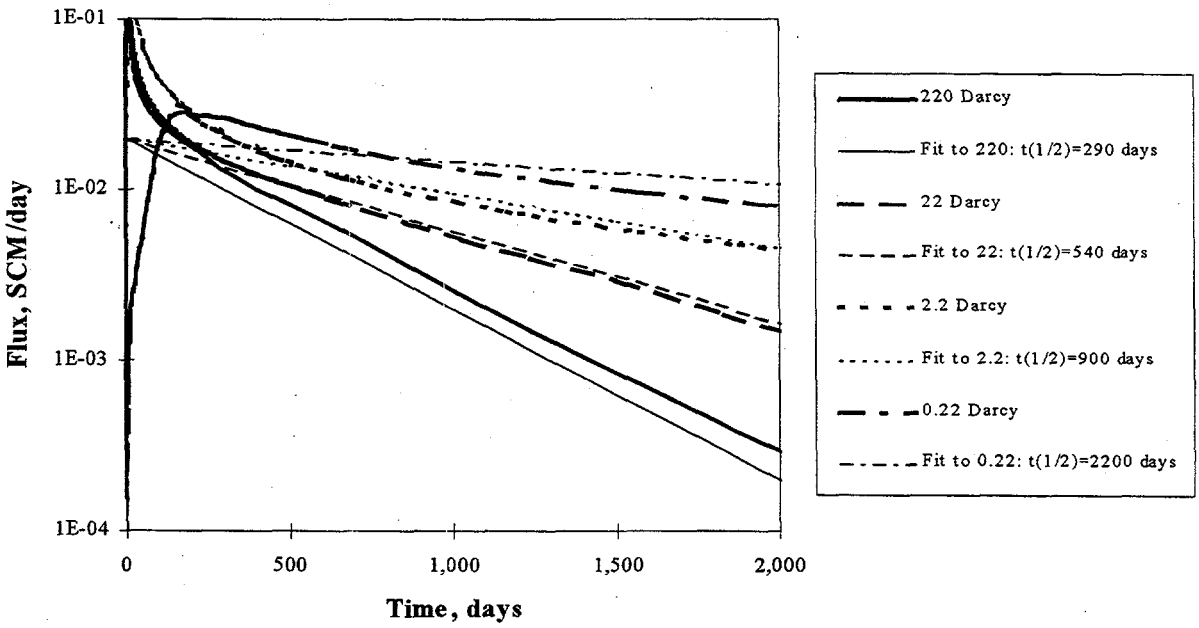


**Figure 4.36.** Fit of STOMP Predictions to Simplified, Lumped-Parameter Model

**Table 4.4**. SCOPE Equation Fitting Parameter for Four Permeability Values

| Permeability, darcies | $t_{1/2}$, days |
|---|---|
| 220 | 290 |
| 22 | 540 |
| 2.2 | 900 |
| 0.22 | 2200 |

While this simple linear model fits the ammonia flux during the intermediate period of draining, STOMP predicts a significantly larger flux at the very beginning of draining. To avoid underpredicting the flux, a simple approach that seems to bound the STOMP results would be to multiply the flux predicted by the equation above by a factor of ten during pumping operations:

$$R_{NH_3} = 10\alpha(y_{eq} - y_{dome})e^{-0.67t/t_{1/2}},$$

Once pumping was complete and no more liquid was being removed from the salt well, the prediction would revert to the previous form.

### 4.2.4 Effect of Varying Initial Void Fraction (gas saturation)

The void fraction in the waste also varies from tank to tank. Obviously, because the retained gases (particularly the insoluble ones) make up the void fraction in the waste, wastes with higher initial void fractions can release more insoluble gas to the tank dome space. However, there is another, more subtle relationship between void fraction and gas release. Draining the waste reduces the pressure on bubbles below the liquid level, causing bubble expansion. The bubbles can grow beyond the value at which they coalesce, at which point the pores become increasingly interconnected, allowing retained gases to diffuse to the top of the saltcake. If the initial void fraction approaches the limit where coalescence begins, gas release may be faster than it was with the low initial void fraction.

To study the degree of this effect with STOMP, this case simulates release from a waste with the same properties as the base case but with an initial gas saturation of 19.5%. (The gas saturation is the fraction of pore space occupied by the gas phase; void fraction refers to the fraction of the waste [including solids] occupied by gas. The two are related by the waste's porosity. The void fraction is equal to the gas saturation times the porosity, which is 50% for the 2-D simulations.) With a maximum trapped gas saturation of 20%, bubbles will interconnect in virtually all regions of the waste well before draining introduces invading air into local pores.

The initial hydrogen and ammonia concentrations have been held constant in the two cases. Thus the overall amount of hydrogen present is a factor of 1.95 times higher for the higher void fraction case, while the amount of ammonia initially present has been reduced slightly (by a factor of 80.5/90).

Figures 4.37 and 4.38 show the predicted hydrogen and ammonia gas fluxes, respectively, with those of the base case. The higher initial void fraction accelerates release of the hydrogen gas during the first several days of draining by about a factor of 2. As a consequence, fluxes later are reduced when there is less remaining to evolve. The flux of ammonia is about the same in the two cases. Figures 4.39 and 4.40 illustrate the cumulative fluxes versus time. Figure 4.39 shows roughly the expected factor of 1.95 between the two cases, the ratio of the amount of hydrogen initially present. In Figure 4.40, the fraction of ammonia ultimately volatilized is 22% versus 21% in the base case. Rather than a ratio of 8/9, which might be expected, the values are about the same. These results illustrate that the total amount of ammonia ultimately released is controlled by how much is left in the residual liquid, which is about the same in each case.

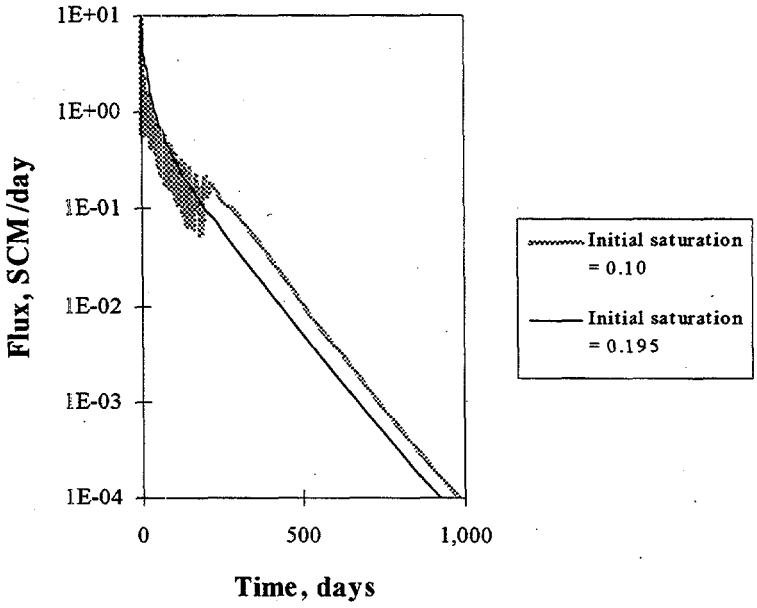


**Figure 4.37.** Comparison of Hydrogen Release for Two Initial Void Fraction (gas saturation) Cases

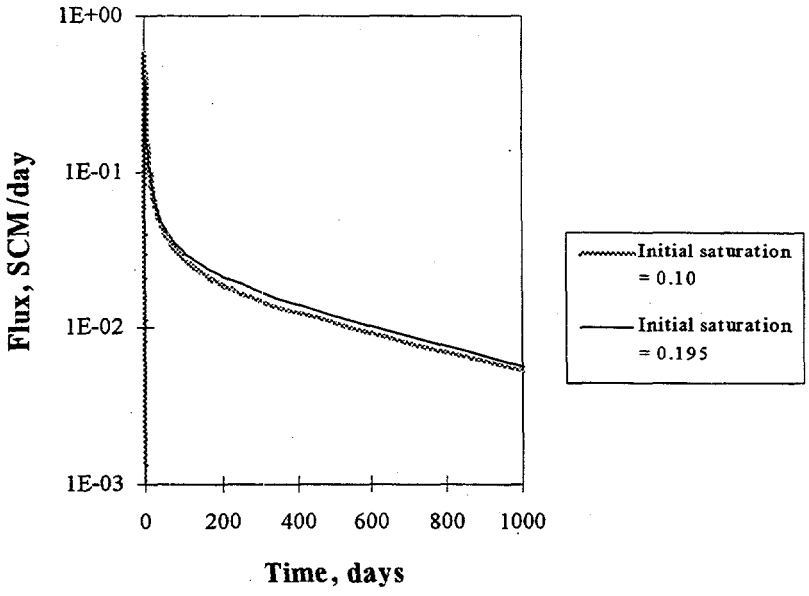


**Figure 4.38.** Comparison of Ammonia Gas Release for Two Initial Void Fraction (gas saturation) Cases

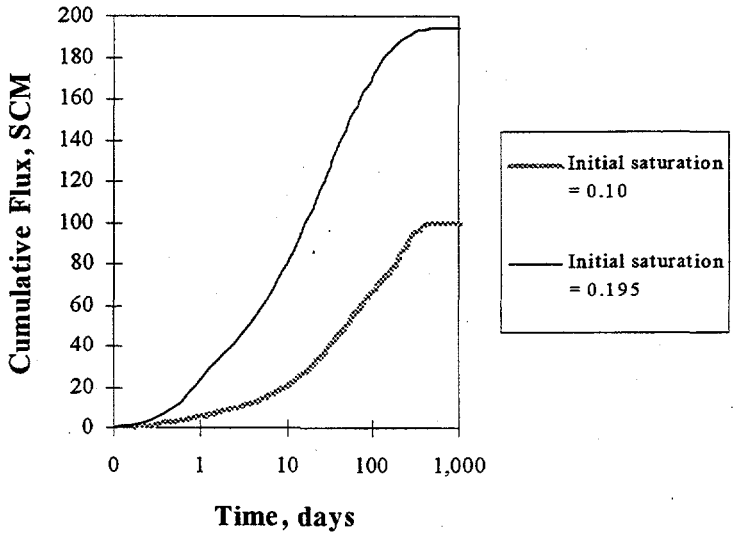


**Figure 4.39.** Comparison of Cumulative Hydrogen Release for Two Initial Void Fraction (Gas Saturation) Cases

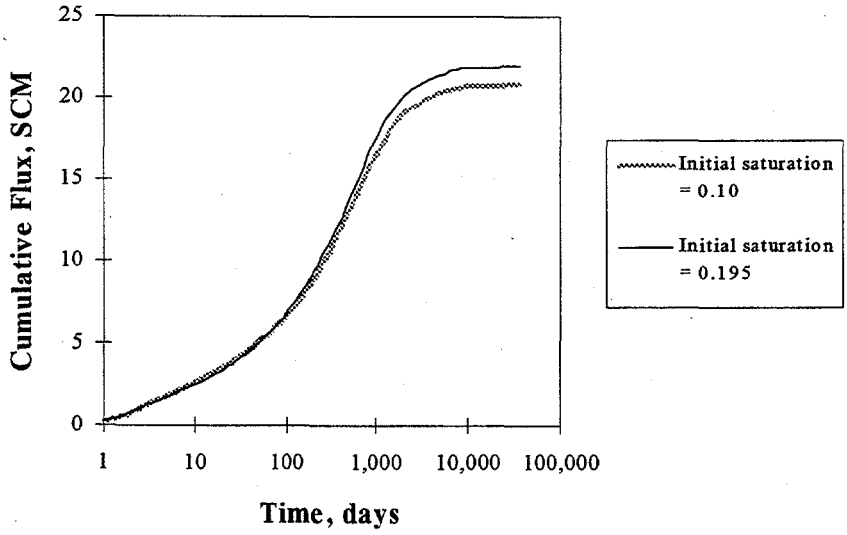


**Figure 4.40.** Comparison of Cumulative Ammonia Gas Release for Two Initial Void Fraction (gas saturation) Cases

### 4.2.5 Effect of Varying Waste Thickness

The thickness of the saltcake waste in the tanks varies but is generally in the range of 10 to 30 feet. Figures 4.41 through 4.44 show the instantaneous and cumulative fluxes for the cases of 10-, 20-, and 30-ft-thick waste. For these simulations, the initial gas concentrations have been kept constant, so the overall amount of gas present in the 10-ft-thick case is half that in the 20-ft-thick case, while the 30-ft case has 50% more.

Increasing the waste thickness from the base-case value of 20 ft to 30 ft increases the pressure on the liquid and hence the initial liquid flow rate considerably, so the liquid level must be lowered over 15 days. However, waste is still exposed more quickly than in the base case, producing elevated flux levels of hydrogen at early times. In contrast, the 10-ft-thick waste drains more slowly, prolonging the release of hydrogen initially. The cumulative hydrogen flux in Figure 4.43 shows the expected 30/20/10 ratio after draining is complete.

While a thicker waste releases more ammonia, the cumulative release in Figure 4.44 does not show an exact 30/20/10 ratio. Because the waste in each of these three cases has the same physical consistency, the height of the capillary fringe (the partially drained region of the waste) is the same in each case. Therefore, while the capillary fringe may occupy only the bottom quarter or so of the 20-ft-thick waste, the fraction is closer to one-half for the 10-ft waste and one-sixth for the 30-ft waste. As a result, the final overall moisture content of the waste is larger for thinner waste, and it retains a larger fraction of the ammonia initially present.

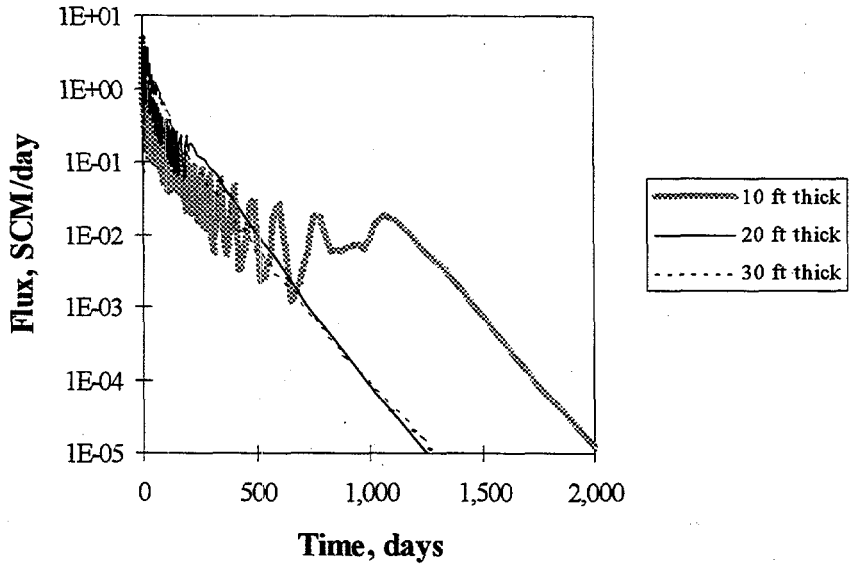


**Figure 4.41.** Comparison of Hydrogen Release Rates for Three Waste Thickness Cases

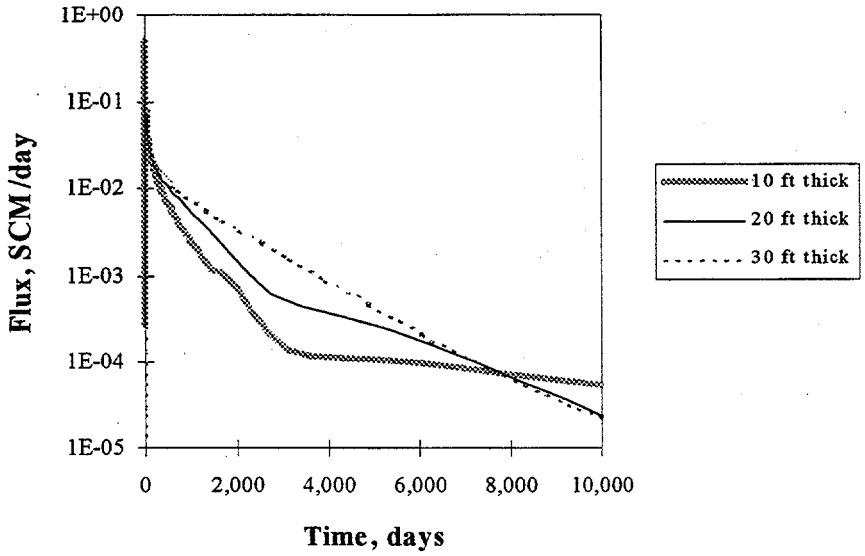


**Figure 4.42.** Comparison of Ammonia Gas Release Rates for Three Waste Thickness Cases

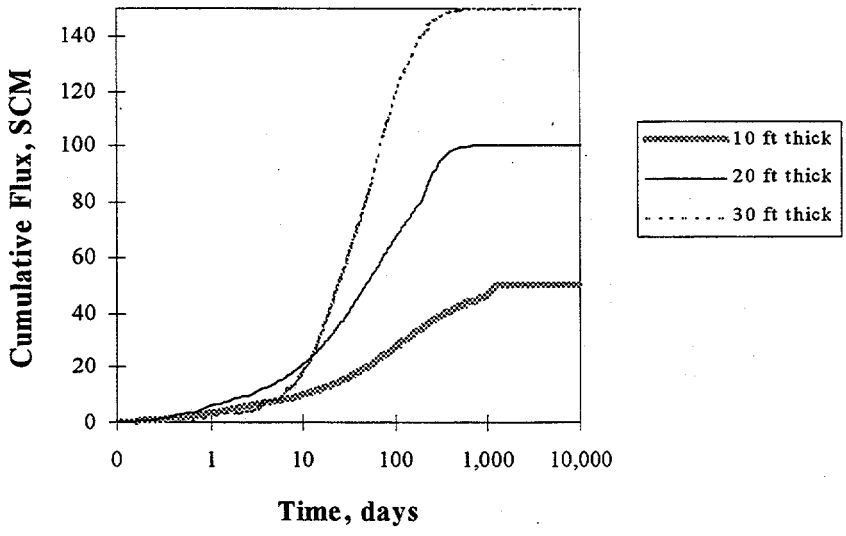


**Figure 4.43.** Comparison of Cumulative Hydrogen Release for Three Waste Thickness Cases

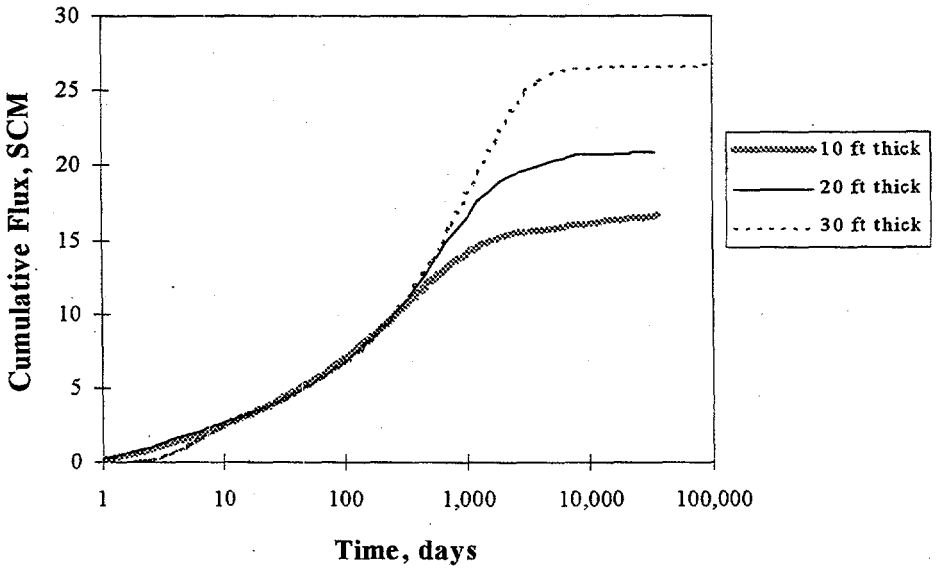


**Figure 4.44.** Comparison of Cumulative Ammonia Gas Release for Three Waste Thickness Cases

### 4.2.6 Effect of Introducing Low-Permeability Layers

As seen in the laboratory experiments and one-dimensional modeling in Section 4.1, layers of lower permeability material can have a strong effect on gas release. The concern in salt-well pumping is that the heterogeneity of the waste may inhibit the release of gas and not allow for the expected reduced flammable gas inventory and associated hazard. To investigate this possibility, two simulations are presented in which a lower permeability layer exists either in the middle (i.e., at an elevation of 3 m [10 ft]) or at the top of the saltcake. The thickness of the layer in both cases is 0.61 m (2 ft). The consistency of the bulk of the waste is the same as the base case (22 darcy), and the normal tortuosity is 0.67. The low permeability layer has the consistency of the 0.22 darcy material and a tortuosity of 0.1.

Figures 4.45 and 4.46 show the predicted gas release rates, and Figures 4.47 and 4.48 show the cumulative release. The base case results are also shown for comparison. The layer on top has the strongest suppression effect on the release of hydrogen, with roughly an order of magnitude reduction in that flux at early times. Consequently, the flux is higher at later times. The layer in the middle has only a modest effect on hydrogen release. Likewise, the flux of ammonia is strongly suppressed initially for the "capped" waste, while the middle layer also retards release but to a lesser degree. Both layered cases result in a larger amount of liquid being retained in the waste and hence a larger cumulative ammonia release to the dome space, as seen in Figure 4.48.

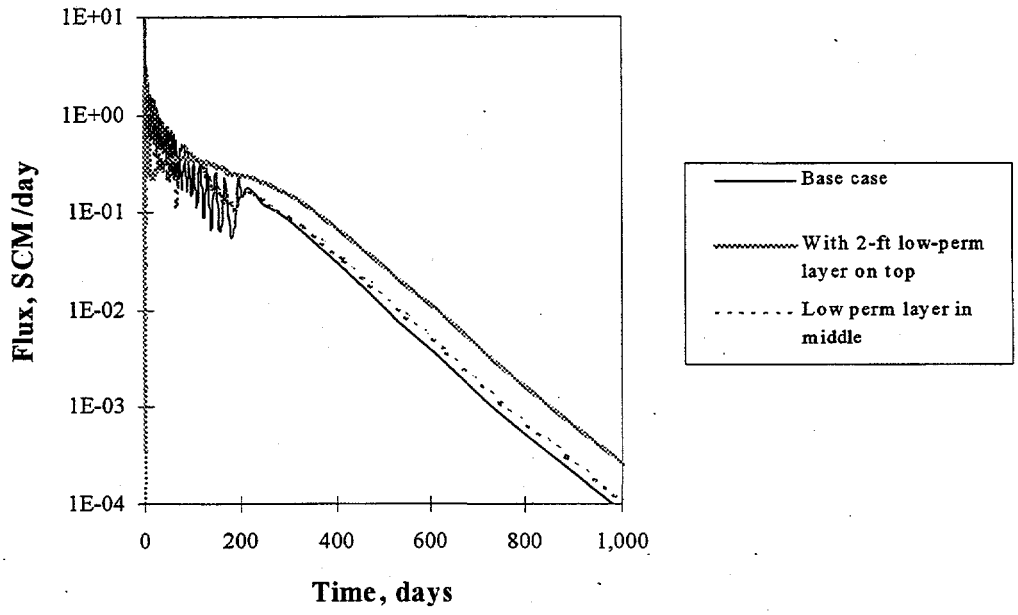


**Figure 4.45.** Comparison of Hydrogen Gas Release Rates Between Base Case and Two Cases with Low Permeability Layers

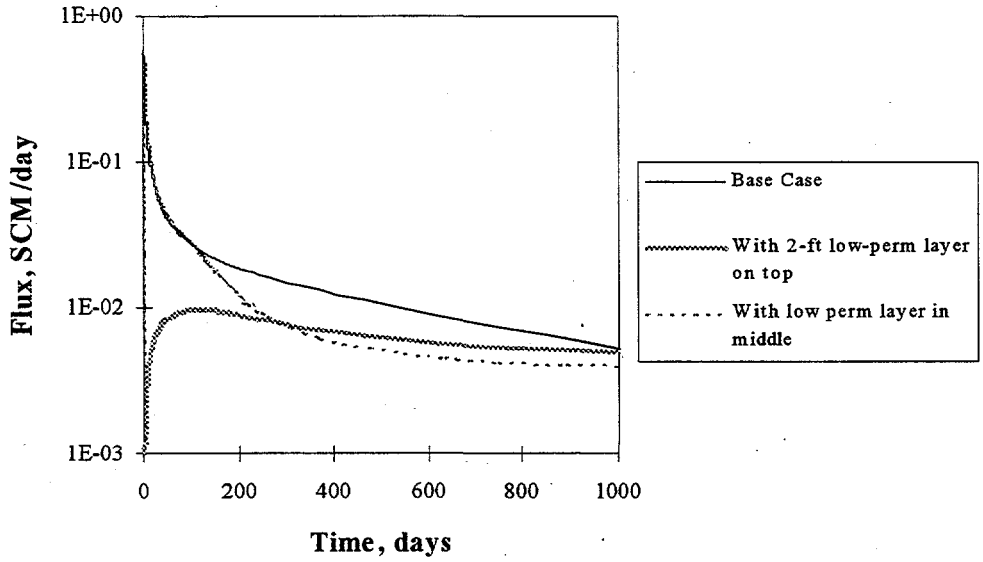


**Figure 4.46.** Comparison of Ammonia Gas Release Rates Between Base Case and Two Cases with Low Permeability Layers

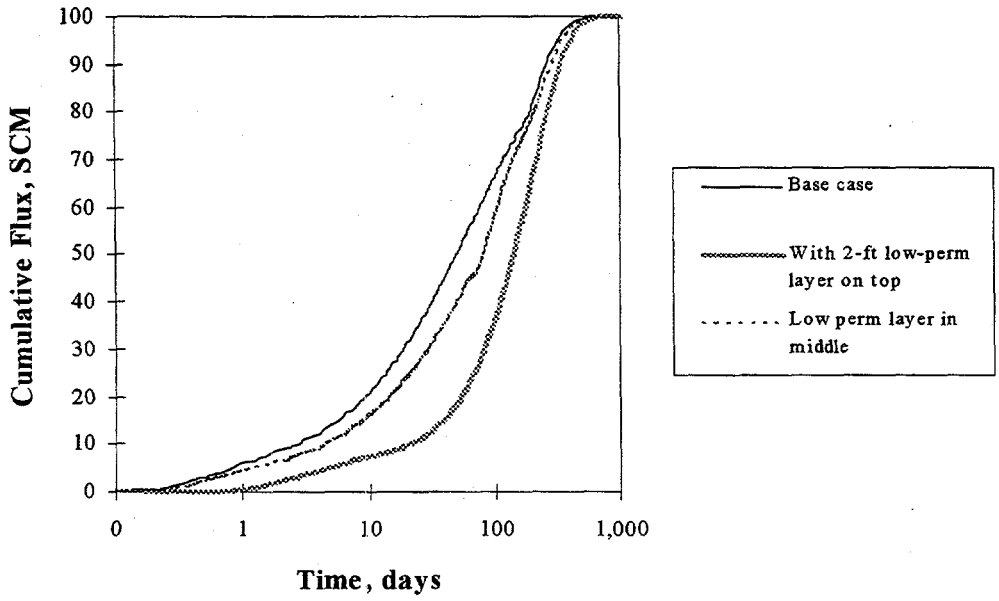


**Figure 4.47.** Comparison of Cumulative Hydrogen Release Between Base Case and Two Cases with Low Permeability Layers

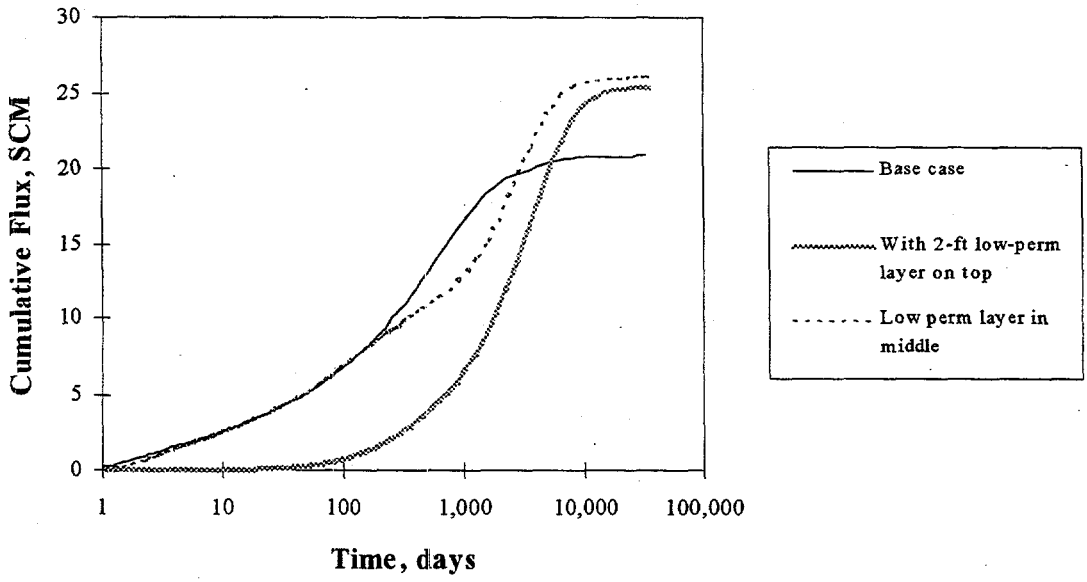


**Figure 4.48.** Comparison of Cumulative Ammonia Gas Release Between Base Case and Two Cases with Low Permeability Layers

### 4.2.7 Start-and-Stop Behavior

This case illustrates that when pumping is turned off the release of hydrogen quickly stops as well, but the ammonia release continues. The reason for this is that insoluble gas chiefly resides in the bubbles, while soluble gas is mostly dissolved in the liquid phase. Once gas bubbles are exposed to invading air by draining, insoluble gas is released, diffuses to the waste surface, and dissipates. When pumping stops, draining and hence exposure of new bubbles (except perhaps for a small amount of waste toward the tank walls that is exposed as the liquid level flattens) also stops. Moreover, for the base-case waste consistency (the 22-darcy material), draining is sufficiently slow that the convective flux of air into the waste does not greatly retard the diffusion of the released gas to the surface. Therefore, there is no holdup of insoluble gas in the drained portion of the waste that is released suddenly by turning off the pump.

However, the soluble gas (ammonia) release mechanism is different because it evolves from residual liquid in the pores, not from bubbles. Draining exposes this residual liquid to air and creates pathways to the surface for soluble gas that are not turned off by turning off the pump. While this gas can also diffuse rapidly to the surface, its inventory is so large that it takes many pore volumes of air to deplete it. Thus the liquid pump rate could be used to control the rate of hydrogen gas release and accumulation in the dome space but not that of ammonia (at least not without reducing the normal pumping rate dramatically to allow ammonia to dissipate).

The simulations in this section illustrate this point. In the two simulations, the waste physical properties are the same as those for the base case (Table 4.1). Pumping is turned off after 10 days in one case and after 50 days in another by changing the hydraulic gradient boundary condition at the salt well to a no-flux condition.

Figures 4.49 and 4.50 show the resulting instantaneous and cumulative fluxes of both gases. (The fluxes are, of course, identical until 10 days.) Notice that the hydrogen flux tails off quickly each time pumping stops. This decay time represents the amount of time required for released gas to diffuse to the surface of the waste. The decay time for the 50-day case is longer than for the 10-day case because the diffusion time becomes longer as the liquid level sinks down into the tank. However, in both cases, the relative amount of hydrogen gas released when pumping stops is small, strikingly illustrated in Figure 4.50 by how quickly the cumulative flux curve flattens.

In contrast, ammonia release continues with no abrupt change in the instantaneous flux at all. The cumulative amount of ammonia released does differ between these cases and the case of a fully drained waste because dissolved gas below the final liquid level remains unexposed to air. The total amount of ammonia gas ultimately released is determined by the amount held in the residual liquid in the drained fraction of the waste. This amount is greater for the 50-day case than the 10-day case because there is more partially drained waste.

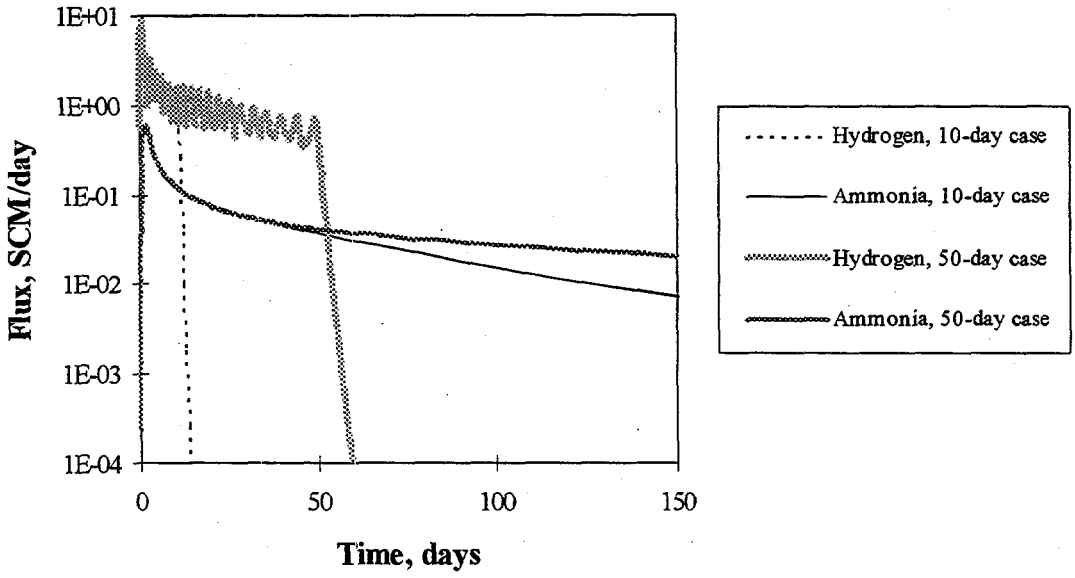


**Figure 4.49.** Hydrogen and Ammonia Gas Release Rates with Pumping Stopped after 10 or 50 Days

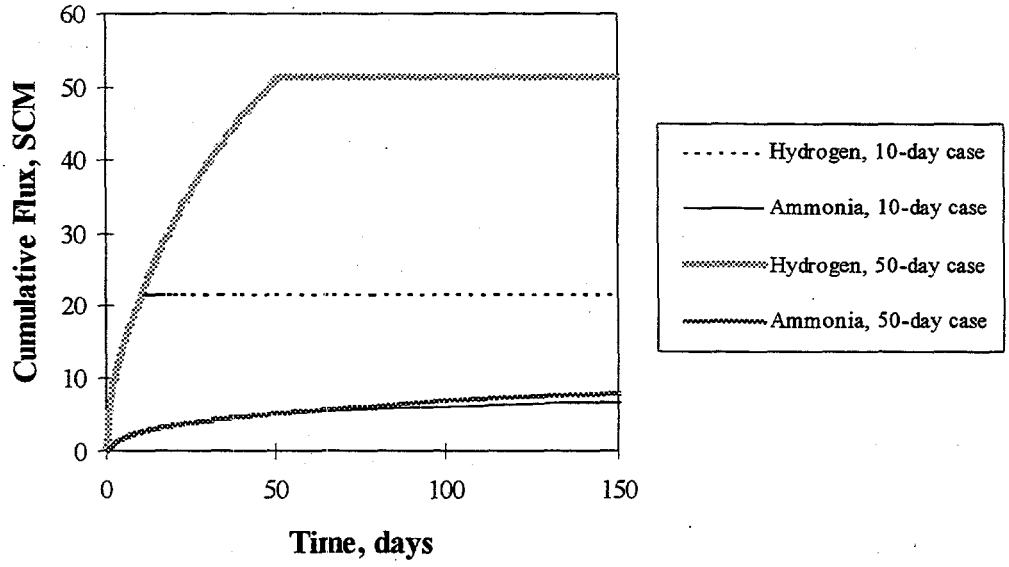


**Figure 4.50.** Cumulative Hydrogen and Ammonia Gas Release with Pumping Stopped after 10 or 50 Days

# 5.0 Summary and Conclusions

The results of these studies clearly show very different gas release mechanisms for the two types of gas. The distinction arises because the insoluble gas chiefly resides in trapped gas bubbles, while the majority of the soluble gas inventory is dissolved in the liquid phase. Insoluble gas is primarily released as the retreating liquid exposes trapped gas bubbles, which then diffuse through connected gas channels to the surface of the saltcake. As expected, essentially all of the insoluble gas in the exposed bubbles is released, although the release rate depends on a number of parameters. Some insoluble gas can also be released as the liquid head is reduced during the draining process, causing the trapped gas bubbles to expand. Depending on the parameter range, these expanded bubbles may connect and allow gas flow or may remain trapped until exposed to the invading gas by the retreating liquid. For either mechanism, if draining ceases, the release of further trapped gas stops and the relatively small amount of released gas in the drained portion of the saltcake quickly dissipates.

The behavior of the soluble gas is quite different. Much of the soluble gas is withdrawn with the pumped liquid; however, capillary forces hold some residual liquid in the pores after draining, which includes a substantial inventory of dissolved gas. This gas volatilizes into adjacent air-filled pores and then diffuses into the dome space like the insoluble gas. Thus, the amount of soluble gas ultimately released to the dome space is roughly equal to the initial concentration of dissolved gas times the amount of nonpumpable liquid. Because of the affinity of the soluble gas for the liquid phase, many pore volumes of air are required to deplete the liquid of dissolved gas. Soluble gas release therefore takes longer than insoluble gas release. Moreover, if draining ceases, soluble gas release continues until the residual liquid is depleted. This implies that while the liquid pump rate could be used to control the rate of hydrogen release and accumulation in the tank dome space, the ammonia release could not be controlled in this manner.

Heterogeneities can have a profound effect on gas release. Low permeability layers, particularly near the top of the saltcake, displayed an ability to retard the release of both soluble and insoluble gases. In one experiment with many complex layers of graded sands, draining did not achieve any release of the insoluble gas. This result challenges the assumption that salt-well pumping will cause retained gases to be released. An assessment of the degree and size of heterogeneities in the tank waste is needed to settle this issue.

These are our specific conclusions from modeling salt-well pumping:

- Given our best estimate of typical waste consistency, 70–90% of the liquid in the saltcake is pumpable (Figure 4.25; Table 4.3). When liquid is pumped from the bottom of the tank, some drains by gravity and part is retained in the interstices of the pores.

- For sufficiently homogeneous media, essentially all the gas in bubbles is released when exposed by invading gas (i.e., when the liquid level falls below that region). Therefore, draining the pumpable liquid from the saltcake releases essentially all of the insoluble gases, which reside primarily in these bubbles (Figure 4.34; Table 4.3).

- For our best estimate of the characteristics of a typical saltcake (20 ft thick with a permeability of 22 darcies), 90% of the drainable liquid can be pumped in 430 days. At that time, 98.6% of the hydrogen has been released to the dome space. The initial release rate is as high as 12 SCM/day (0.3 scfm), but a more typical release rate is 1 to 0.1 SCM/day (Figures 4.23 and 4.24; Table 4.3).

- The release behavior of soluble gases is different from that of the insoluble gas because the majority of their inventory is in the liquid phase rather than in bubbles. Thus much of the soluble gas is withdrawn with the pumped liquid. Some remains in the residual liquid held in the pores after draining, where it volatilizes and is released into the dome space. Thus, the amount of soluble gas released to the dome space is primarily controlled by the fraction of pumpable liquid.

- Assuming the best-estimate, typical saltcake characteristics, 12.3% of the ammonia has been released to the dome space after 430 days. Ultimately, 20.9% of the initial ammonia inventory is released to the dome, but only after several years. The other 79.1% is removed with the liquid phase. The initial release rate is 0.6 SCM (20 $ft^3$)/day, while a more typical rate is 0.1 to 0.01 SCM/day (Figures 4.23 and 4.24; Table 4.3).

- The model suggests that active ventilation of tanks may be necessary to prevent dome space concentrations of flammable gas from exceeding the 25% LFL limit, but only during the early part of draining. Hydrogen is the primary concern. However, this conclusion assumes a relatively homogeneous waste. The model also suggests that passive ventilation will be sufficient to control flammable gas concentrations after pumping ends (Section 4.2.1).

- If the gas saturation is near its percolation threshold, some trapped gas is released from below the liquid level as bubbles expand, but just enough to maintain the material at its percolation threshold. Gas release is slow and steady rather than sudden and dramatic.

- When the rate of liquid withdrawal is small, as in the hundreds of days needed to stabilize a tank, diffusion of gas from exposed bubbles is far faster than convection of invading air into the saltcake. As a result, gases released from trapped bubbles quickly diffuse through the drained portion of the saltcake and into the dome space. In this situation, little bubble gas accumulates in the drained portion of the saltcake. The release rate of hydrogen is proportional to the draining rate, and the cessation of pumping quickly reduces the hydrogen release rate to zero.

- Because soluble gas is released from residual liquid in the drained region of the waste, the cessation of pumping does not immediately slow ammonia release (Figures 4.49 and 4.50). While diffusion of this gas is also rapid, the dissolved inventory is so large that many pore volumes of air are required to deplete it. This implies that the liquid pump rate will not control the rate of ammonia release and accumulation in the dome space, which contrasts with release of hydrogen.

- Decreasing the permeability of the saltcake in the simulations increases the time required to complete draining and decreases the amount of pumpable liquid. These effects combine to slow the release rates of both hydrogen and ammonia but increase the total amount of ammonia ultimately released to the dome space. Increasing the permeability has the opposite effect (Figures 4.30 through 4.35; Table 4.3).

- Increasing the initial gas saturation (void fraction) from 10% (5% void) to nearly 20% (10% void) does not have a strong effect on hydrogen release rates beyond the expected factor of two. The relative amount of ammonia ultimately released is about the same because it depends primarily on the amount of residual liquid, which is roughly equal for the two cases (Figures 4.37 through 4.40).

- The thickness of the saltcake affects its initial drain rate, with thick wastes exerting more pressure on their liquids to drain. The hydrogen release rate in the early part of draining is therefore slightly higher for thick wastes. However, the effect on ammonia release is the opposite, with ammonia fluxes slightly higher for thinner wastes because of the decreased influx of invading air and the larger amount of liquid retained in the waste at the end of draining (Figures 4.41 through 4.44).

- Low permeability layers, particularly near the top of the saltcake, have the ability to retard the release of both insoluble and soluble gases (Figures 4.45 through 4.48).

- A simple model of the ammonia release rate is

$$R_{NH_3} = \alpha (y_{eq} - y_{dome}) e^{-0.67 t / t_{1/2}}$$

where $R_{NH3}$ is the flux of ammonia into the dome space in scfm, $a$ is a global proportionality constant in scfm $NH_3$/mole fraction $NH_3$, $y_{eq}$ is the mole fraction of ammonia in the gas phase in equilibrium with the dissolved ammonia in the waste, $y_{dome}$ is the dome-space ammonia mole fraction, $t$ is time, and $t_{1/2}$ is a characteristic decay constant (in the form of a half-life) that depends on the physical properties of the waste. STOMP predicted that the global constant $\alpha$ was equal to 1.2 scfm/mole fraction. For our best estimate of saltcake consistency, $t_{1/2}$ was equal to 540 days. During the initial period of draining, this estimate underpredicts the ammonia gas flux. To estimate a bounding gas release rate, a simple correction consistent with the STOMP results is multiplying the estimate by a factor of 10 during pumping (Section 4.2.3).

These are our conclusions from the model validation tests:

- The agreement between the experimental results and the model predictions is good, though it is better for the 1.0-mm diameter beads than for the 0.2-mm beads. For homogeneous bead packs, the model reflects the magnitude and qualitative release behavior of both insoluble and soluble gas. The insoluble gas flux was shown to decay exponentially, and the model matched the exponential decay constants well. The soluble gas flux was shown to be prolonged. Decreasing the length of the column had the anticipated effect of reducing the decay constant.

- Heterogeneities in bead packs (in the form of layers of smaller beads) serve to retard the flux of both gases, but particularly the insoluble one. The model was also able to capture this behavior, but the agreement was more qualitative and less quantitative.

- Increasing the initial concentration of soluble gas in an attempt to show a breakdown of the model's assumption of infinite dilution did not show a substantially larger release of the insoluble gas, helping to validate the assumption.

# 6.0 Recommendations

1) The true test of the predictive capability of the model is to compare it with data from actual salt-well pumping operations. Once such data are available (e.g., gas monitoring, pump rate, neutron log, or RGS data), they should be evaluated for consistency with the model.

2) This study has shown that heterogeneity can greatly retard gas release and may even prevent it. The question of whether drained waste can still retain its gas is key to resolving the safety issue. Several activities could help to answer this question:

   a) The heterogeneity of tank waste should be quantified or at least qualitatively assessed, both in terms of the degree of permeability variation and the length scales of these variations. Core studies, neutron logs, and RGS data could be evaluated to reveal information on heterogeneity. Preferably, the waste data evaluated would include tanks before, during, and after salt-well pumping.

   b) STOMP could then be used to predict release, incorporating the estimated degree of heterogeneity. Depending on the actual degree of heterogeneity in the waste, it may be necessary to extend the experimental validation studies to lower permeability materials and packing with larger permeability variations.

   c) A new numerical approach to modeling trapped gas is available and should be implemented in STOMP. This approach would ensure that trapped gas remains trapped in low permeability materials.

   d) Finally, draining actual waste samples (or hydrologically comparable simulants) and measuring their gas retention behavior could resolve the issue more convincingly. However, such work still might not be completely representative of tank-scale draining.

3) The experimental work showed no strong effect of the dissolved gas concentration on insoluble gas release. However, the assumption of no mass transfer limitations between the gas and liquid phases is still somewhat questionable as the dissolved gas concentration increases, as the system becomes more three-dimensional, and as more heterogeneities are introduced. Future model validation experiments could include higher soluble gas concentrations and larger columns. These extensions would permit an assessment of the potential for mass transfer limitations and a need to modify STOMP.

4) Several of the tanks to be salt-well pumped are sludge tanks or contain a significant fraction of sludge. The conceptual model may need to be modified or extended for sludge tanks. Sludge may simply drain by a different physical process at the pore scale. An effort to study alternate concepts may be needed. Moreover, sludge waste is more likely to subside significantly, which is not currently incorporated into STOMP.

# 7.0 References


Agnew SF. 1997. *Hanford Tank Chemical and Radionuclide Inventories: HDW Model Rev. 4.* LA-UR-96-3860, Los Alamos National Laboratory, Los Alamos, New Mexico.

Bredt PR and SM Tingey. 1996. *The Effect of Dilution on the Gas Retention Behavior of Tank 241-SY-103 Waste.* PNL-10893, Pacific Northwest National Laboratory, Richland, Washington.

Bredt PR, SM Tingey, and EH Shade. 1995. *The Effect of Dilution on the Gas-Retention Behavior of Tank 241-SY-101 Waste.* PNL-10781, Pacific Northwest Laboratory, Richland, Washington.

Caley SM, LA Mahoney, and PA Gauglitz. 1996. Summary of Tank Information Relating Salt Well Pumping to Flammable Gas Safety Issues. PNNL-11335, Pacific Northwest National Laboratory, Richland, Washington.

Dullien FAL. 1992. *Porous Media: Fluid Transport and Pore Structure.* Academic Press, San Diego.

Ecology, EPA, and DOE. 1996. *Hanford Federal Facility Agreement and Consent Order.* Washington State Department of Ecology, U.S. Environmental Protection Agency, and U.S. Department of Energy, Olympia, Washington, as amended.

Gauglitz PA, SD Rassat, PR Bredt, JH Konynenbelt, SM Tingey, and DP Mendoza. 1996. *Mechanisms of Gas Bubble Retention and Release: Results for Hanford Waste Tanks 241-S-102 and 241-SY-103 and Single-Shell Tank Simulants.* PNNL-11298, Pacific Northwest National Laboratory, Richland, Washington.

Gauglitz PA, SD Rassat, MR Powell, RR Shah, and LA Mahoney. 1995. *Gas Bubble Retention and its Effect on Waste Properties: Retention Mechanisms, Viscosity, and Tensile and Shear Strengths.* PNL-10740, Pacific Northwest Laboratory, Richland, Washington.

Gauglitz PA, LA Mahoney, DP Mendoza, and MC Miller. 1994. *Mechanisms of Gas Bubble Retention.* PNL-10120, Pacific Northwest Laboratory, Richland, Washington.

Grimes GW. 1978. *Jet Pump Development for Salt Well Application.* RHO-CD-316, Rockwell Hanford Operations, Richland, Washington.

Handy LL. 1975. *Flow Properties of Saltcake for Interstitial Liquid Removal/Immobilization Development Program.* ARH-C-6, Atlantic Richfield Hanford Company, Richland, Washington.

Hanlon BM. 1996. *Waste Tank Summary Report for Month Ending September 26, 1996.* WHC-EP-0182-102, Westinghouse Hanford Company, Richland, Washington.

Herting DL, DB Bechtold, BA Crawford, TL Welsh, and L Jensen. 1992. *Laboratory Characterization of Samples Taken in May 1991 from Hanford Waste Tank 241-SY-101.* WHC-SD-WM-DTR-024 Rev. 0, Westinghouse Hanford Company, Richland, Washington.

Hodgson KM, RP Anantatmula, SA Barker, KD Fowler, JD Hopkins, JA Lechelt, DA Reynolds, DC Hedengren, RE Stout, RT Winward, and JD Bingham. 1997. *Evaluation of Hanford Tanks for Trapped Gas.* WHC-SD-WM-ER-526 Rev. 1b, Lockheed Martin Hanford Company, Richland, Washington.

Hopkins JD. 1995. *Methodology for Flammable Gas Evaluations.* WHC-SD-WM-TI-724, Westinghouse Hanford Company, Richland, Washington.

Kubic WL Jr. 1995. *Summary, Review, and Analysis of Data for Tank 241-A-101.* TSA10-CN-WT-SA-DA-001, Los Alamos National Laboratory, Los Alamos, New Mexico.

Lenhard RJ and JC Parker. 1987. "A Model for Hysteretic Constitutive Relations Governing Multiphase Flow 2. Permeability-Saturation Relations." *Water Resources Research,* 23:2197-2206.

Metz WP. 1976. *A Topical Report on Interstitial Liquid Removal from Hanford Saltcakes.* ARH-CD-545, Atlantic Richfield Hanford Company, Richland, Washington.

Millington RJ and JP Quirk. 1959. "Permeability of Porous Media." *Nature,* 183:387-388.

Norton JD, and LR Pederson. 1994. *Ammonia in Simulated Hanford Double-Shell Tank Wastes: Solubility and Effects on Surface Tension.* PNL-10173, Pacific Northwest National Laboratory, Richland, Washington.

Parker JC and RJ Lenhard. 1987. "A Model for Hysteretic Constitutive Relations Governing Multiphase Flow 1. Saturation Pressure Relations." *Water Resources Research,* 23:2187-2196.

Peurrung LM, SM Caley, EY Bian, and PA Gauglitz. 1996. *Gas Release During Salt-Well Pumping: Model Predictions and Comparisons to Laboratory Experiments.* PNNL-11310, Pacific Northwest National Laboratory, Richland, Washington.

Rassat SD and PA Gauglitz. 1995. *Bubble Retention in Synthetic Sludge: Testing of Alternative Gas Retention Apparatus.* PNL-10661, Pacific Northwest Laboratory, Richland, Washington.

Reid RC, JM Prausnitz, and TK Sherwood. 1977. *The Properties of Gases and Liquids,* 3rd Edition. McGraw Hill, New York.

Reynolds DA. 1992. *Tank 101-SY Window C Core Sample Results and Interpretation.* WHC-EP-0589, Westinghouse Hanford Company, Richland, Washington.

Sandia. 1997. *Safety Controls Optimization by Performance Evaluation (SCOPE) Analysis Framework.* HNF-SD-WM-ES-410, Sandia National Laboratory, Albuquerque, New Mexico (to be released).

Shekarriz A, DR Rector, LA Mahoney, MA Chieda, JM Bates, RE Bauer, NS Cannon, BE Hey, CG Linschooten, FJ Reitz, and ER Siciliano. 1997. *Composition and Quantities of Retained Gas Measured in Hanford Waste Tanks 241-AW-101, A-101, AN-105, AN-104, and AN-103.* PNNL-11450 Rev. 1, Pacific Northwest National Laboratory, Richland, Washington.

Simmons CS. 1996. *Modeling Water Retention of Simulant Sludge and Actual Saltcake Tank Wastes.* PNL-10831, Pacific Northwest Laboratory, Richland, Washington.

Stewart CW, ME Brewster, PA Gauglitz, LA Mahoney, PA Meyer, KP Recknagle, and HC Reid. 1996. *Gas Retention and Release Behavior in Hanford Single-Shell Tanks.* PNNL-11391, Pacific Northwest National Laboratory, Richland, Washington.

van Genuchten MTh. 1980. "A Closed-Form Equation for Predicting the Hydraulic Conductivity of Unsaturated Soils." *Soil Sci. Soc. Am. J.,* 44:892-898.

Welty JR, CE Wicks, and RE Wilson. 1984. *Fundamentals of Momentum, Heat, and Mass Transfer, 3rd Edition.* John Wiley and Sons, New York.

Westinghouse Hanford Company. 1996. *A Safety Assessment for Salt Well Jet Pumping Operations in Tank 241-A-101.* WHC-SD-WM-SAD-036 Rev. 0, Westinghouse Hanford Company, Richland, Washington.

White MD and M Oostrom. 1996. *STOMP Subsurface Transport Over Multiple Phases, Theory Guide.* PNNL-11217, Pacific Northwest Laboratory, Richland, Washington.

Whitney P. 1995. *Screening the Hanford Tanks for Trapped Gas.* PNL-10821, Pacific Northwest National Laboratory, Richland, Washington.

# Distribution

No. of
Copies

**Offsite**

2 Office of Scientific and Technical Information

H. Babad
2540 Cordoba Ct
Richland, WA 99352

C. W. Forsberg
Oak Ridge National Laboratory
P.O. Box 2008 MS 6495
Oak Ridge, TN 37831

B. C. Hudson
P.O. Box 271
Lindsborg, KA 67456

T. E. Larson
2711 Walnut St.
Los Alamos, NM 87544

6 Los Alamos National Laboratory
P.O. Box 1663
Los Alamos, NM 87545

| | | |
|---|---|---|
| Attn: | D. R. Bennett | K575 |
| | W. Kubic | K575 |
| | K. Pasamehmetlogu | K575 |
| | J. Spore | K575 |
| | C. Unal | K575 |
| | J. R. White | K575 |

J. L. Kovach
Nuclear Consulting Services, Inc.
P.O. Box 29151
Columbus, OH 43229-0151

No. of
Copies

D. A. Powers
Sandia National Laboratories
MS-0744
Albuquerque, NM 87185-0744

S. E. Slezak
Sandia National Laboratory
P.O. Box 5800 MS 1004
Albuquerque, NM 87110

A. B. Stone
Washington Department of Ecology
1315 W. 4th, B5-18
Kennewick, WA 00336

**Onsite**

5 DOE Richland Operations Office

| | |
|---|---|
| K. Chen | S7-54 |
| C. A. Groendyke | S7-54 |
| G. W. Rosenwald | S7-54 |
| J. M. Gray | S7-54 |
| G. M. Neath | S7-51 |

17 Project Hanford Management Contract Team

| | |
|---|---|
| S. A. Barker | R2-11 |
| W. B. Barton | R2-11 |
| R. E. Bauer | S7-14 |
| D. R. Bratzel | S7-14 |
| R. J. Cash | S7-14 |
| K. M. Hodgson | R2-11 |
| G. D. Johnson (3) | S7-15 |
| N. W. Kirch | R2-11 |
| M. A. Lane | S8-05 |
| J. W. Lentsch | S7-15 |
| W. H. Meader | S8-05 |

No. of Copies

| | | |
|---|---|---|
| | D. A. Reynolds | R2-11 |
| | E. R. Siciliano | H0-31 |
| | L. M. Stock | S7-14 |
| | R. J. Van Vleet | R3-27 |
| 53 | Pacific Northwest National Laboratory | |
| | Z. I. Antoniak | K7-15 |
| | S. Q. Bennett | K7-90 |
| | M. E. Brewster | K9-62 |
| | J. W. Brothers (5) | K9-20 |
| | P. R. Bredt | P7-41 |

No. of Copies

| | | |
|---|---|---|
| | S. M. Caley | P7-41 |
| | P. A. Gauglitz (15) | P7-41 |
| | B. J. Palmer | K7-15 |
| | L. R. Pederson | K2-44 |
| | L. M. Peurrung (15) | P7-41 |
| | S. D. Rassat | P7-41 |
| | A. Shekarriz | K7-15 |
| | C. S. Simmons | K9-33 |
| | C. W. Stewart | K7-15 |
| | G. Terrones | K7-15 |
| | M. D. White | K9-36 |
| | Information Release (5) | K1-06 |